

## **Response to comments by editor and anonymous reviewers**

We appreciate the editor and anonymous reviewers' comments and helpful suggestions. We have revised the manuscript according to their comments and suggestions. We hope the revised manuscript can meet the quality requirements of *Atmospheric Chemistry and Physics*.

## **Response to Reviewer #1's comments**

### **Anonymous Reviewer #1**

**Received and published: 5 July 2017**

#### **Overview**

**This paper as the other reviewer has pointed out potentially has an amazing dataset which is really needed for greater understanding of air pollution and its impacts in agricultural regions. The paper could be hugely improved by moving away from the gas-particle ratio analysis to more detailed atmospheric chemistry and physics which would allow insight into the processes occurring and whether current understanding of emission, transformation and deposition can explain the observations. There is an overuse of “the data suggests...” and “this indicates...” without backup of information.**

**Answer:** Thank you for your comments and suggestions, which are valuable in improving the quality of our manuscript. We have made additional data analysis and revised the manuscript according to the comments and suggestions by both reviewers. To gain more insight into the role of ammonia in the formation of secondary inorganic aerosol, simulations were made using the thermodynamic equilibrium model ISORROPIA II. The measurements were used as input of model to simulate the variations of the components in gas, liquid and solid phases, which are useful in the investigation of the gas-aerosol equilibrium characteristics.

#### **Major comments:**

##### **Introduction:**

**I think the ambition of the paper (as described in the last paragraph) needs to be more detailed and then the critical analysis done in the paper.**

**P3 More details of instrumentation is needed, in particular the calibration and response time of the NH<sub>3</sub> instrument is required. Did the authors see an influence on the response time from PM deposition on the inlet and instrument filters (see Bobrutski et al 2009 and other papers for details of this issue). Some raw data and calibrations would be useful – ACP is not figure limited. Though rainfall is mentioned as a key meteorological driver, the method of measurement and the data are not shown at all.**

**Answer:** We have added some more details about the instrumentation and issues regarding quality control. We paid attention to the influences on NH<sub>3</sub> measurements from the inlet and PM deposition on it and tried to reduce such influences. Although we do not exclude some unperceivable influences from adsorption and desorption, these influences should be much smaller than the high NH<sub>3</sub> values we observed and cause mainly slightly slower response or a lag in the recorded NH<sub>3</sub> concentration, which may not impact our analysis based on hourly average data. Some figures are added in the revised

manuscript and supplementary materials to provide information about calibration, meteorological condition, etc. Section 2.2 “Sampling and analysis” has been rewritten as follows:

“Ambient  $\text{NH}_3$  was measured using an ammonia analyser (DLT-100, Los Gatos Research, USA), which utilize a unique laser absorption technology called Off-Axis Integrated Cavity Output Spectroscopy (OA-ICOS). The analyzer has a precision of 0.2 ppb at 100 sec average and a maximum drift of 0.2 ppb over 24 hrs. The response time of the analyzer is less than 2 s (with optional external N920 vacuum pump). During the campaign,  $\text{NH}_3$  data were recorded as 100-s average. In principle, the  $\text{NH}_3$  analyzer does not need external calibration, because the measured fractional absorption of light at an ammonia resonant wavelength is an absolute measurement of the ammonia density in the cell (Manual of Economical Ammonia Analyzer - Benchtop Model 908-0016, Los Gatos Research). However, we confirmed the good performance of the  $\text{NH}_3$  analyzer using a reference gas mixture  $\text{NH}_3/\text{N}_2$  (Scottgas, USA) traceable to US National Institute for Standards and Technology (NIST). The reference gas of  $\text{NH}_3$  (25.92 ppm with an accuracy of  $\pm 2\%$ ) was diluted to different concentrations using zero air and supplied to the analyzer and a sequence with 5 points of different  $\text{NH}_3$  concentrations (including zero) were repeated for several times to check the performance of the analyzer. As shown in Fig. S1, the analyzer followed rapidly to changes of the  $\text{NH}_3$  concentration, produced stable response under stabilized  $\text{NH}_3$  concentrations, and repeated accurately (within the uncertainty) the supplied  $\text{NH}_3$  concentrations. The  $\text{NH}_3$  analyzer contains an internal inlet aerosol filter, which was cleaned before our campaign. Nevertheless, some very fine particles can deposit on the mirrors of the ICOS cell, leading to gradual decline in reflectivity. However, slight mirror contamination does not cause errors in  $\text{NH}_3$  measurements because the mirror reflectivity is continually monitored and the measurement is compensated using the mirror ringdown time. Interferences to  $\text{NH}_3$  measurements can be from the sample inlets, for example, due to water condensation or adsorption/desorption effects (e.g., Schwab, 2008; Norman et al., 2009). Such interferences were not quantified but reduced as possibly as we could. PTFE tubing (4.8 mm ID), which is one of the well suited materials for  $\text{NH}_3$  measurement (Norman et al., 2009), was used to induced ambient air. The length of the tubing was kept as short as possible (about 5 m) to limit the residue time to less than 3 s. The aerosol filter at the inlet was changed every two weeks. Water condensation was avoided. Nevertheless, we cannot exclude the influence from the adsorption and desorption, which can also occur on dry surfaces. However, this influence should be small at our site, where the  $\text{NH}_3$  concentration

is very high, and cause mainly a lag in the recorded  $\text{NH}_3$  concentration.

A set of commercial instruments from Thermo Environmental Instruments, Inc. were used to measure  $\text{O}_3$  (TE 49C),  $\text{NO}/\text{NO}_2/\text{NO}_x$  (TE 42CTL),  $\text{CO}$  (TE 48C), and  $\text{SO}_2$  (TE 43CTL). All instruments were housed in an air-conditioned room in the observation building at the site. Two parallel inlet tubes (Teflon, 4.8 mm ID $\times$ 8 m length) were shared by the analyzers. The height of the inlets was 1.8 m above the roof of the building and about 8m above the ground. The inlet residence time was estimated to be less than 5 s (Lin et al., 2009). Zero and span checks were performed weekly on the analyzers of these trace gases to identify possible analyzer malfunctions and zero drifts. Multipoint calibrations of  $\text{SO}_2$ ,  $\text{NO}_x$ ,  $\text{CO}$  and  $\text{O}_3$  analyzers were performed on the instruments at approximately 1-month intervals. Measurement records were saved as 1-min averages. After the correction of data on the basis of the multipoint calibrations, hourly average data were calculated and used for the analysis.

An Ambient Ion Monitor (AIM) (URG 9000D Series, USA) was deployed at the site to measure hourly concentrations of water-soluble inorganic components in  $\text{PM}_{2.5}$  during 15 June–11 August, 2013. A detailed description of performance evaluation of AIM-IC system is reported by Han et al., (2016). Briefly, ambient air was introduced in to the AIM with a 2 meter Teflon coated aluminum pipe and particles larger than 2.5  $\mu\text{m}$  were removed by a cyclone at a flow rate of 3 L/min. A liquid diffusion denuder was used to remove the interfering acidic and basic gases, in combination with a Steam-Jet Aerosol Collector followed by an Aerosol Sample Collector, until the particles can be injected into the ion chromatograph (Hu et al., 2014). The detection limit of  $\text{NH}_4^+$ ,  $\text{SO}_4^{2-}$  and  $\text{NO}_3^-$  were 0.05  $\mu\text{g m}^{-3}$ , 0.04  $\mu\text{g m}^{-3}$  and 0.05  $\mu\text{g m}^{-3}$ , respectively. For the AIM, multipoint calibrations were performed weekly by using calibration standard solutions. Acceptable linearity of ions was obtained with an  $R^2$  of  $\geq 0.999$ . The flow rate of the AIM was checked weekly at the sample inlet with a certified flow meter. The flow rate of the AIM was kept at 3 L/min with standard derivation of  $<1\%$ . Hourly data were obtained for the concentrations of water-soluble inorganic ions in summer 2013.

Meteorological parameters were measured at the site. Air temperature and relative humidity were monitored using a humidity and temperature probe (HMP155, Vaisala, Finland); wind speed and direction were measured using an anemometer (ZQZ-TFD12, Jiangsu Radio Scientific Institute Co., Ltd, China); rainfall was measured using a tilting rain gauge (SL2-1, Tianjin Meteorological Instrument Factory, China). Global radiation observation was made at the site but showed a drift by the end of July,

2013. Instead we use the photolysis rate  $j\text{NO}_2$  observed using a 2-pi-actinic-flux spectrograph (CCD type, Meteorologie Consult GmbH, Germany) to indicate radiation condition for photochemistry. Hourly meteorological data were calculated from the in-situ measurements and used in this paper. Planetary boundary layer height values at 14:00 were derived from the ERA-Interim data using the Bulk Ricardson number method (Guo et al., 2016; Miao et al., 2017).”

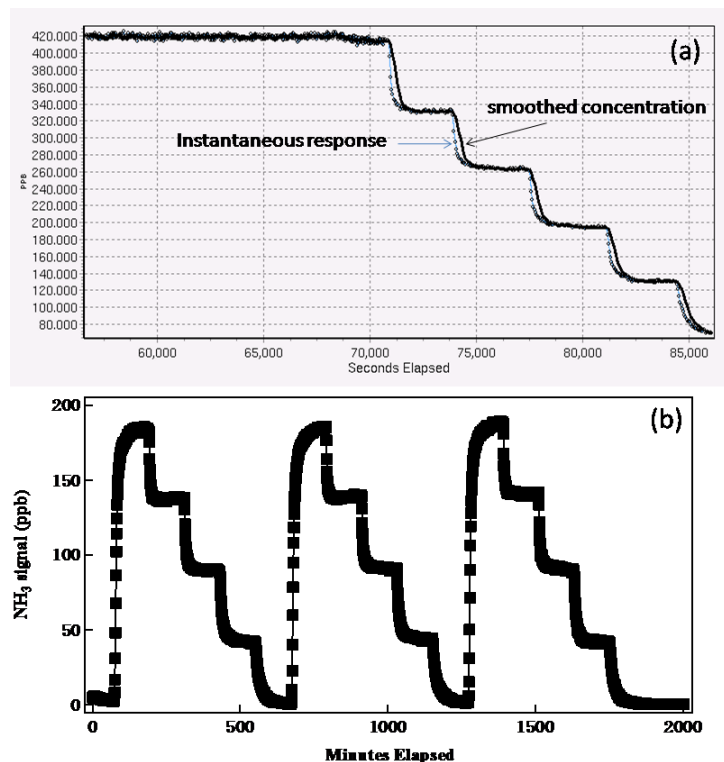


Figure S1 Confirmation of the performance of  $\text{NH}_3$  analyzer using diluted standard gas (mixture  $\text{NH}_3/\text{N}_2$ ). (a) Instrument response to changed  $\text{NH}_3$  concentration and stability; (b) repeated multipoint calibrations.

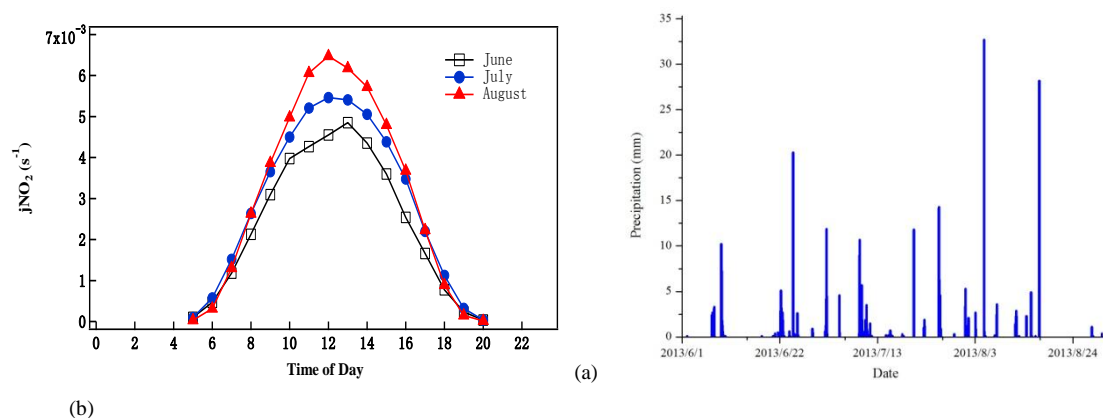


Figure S2. Monthly average diurnal variations of the  $\text{NO}_2$  photolysis frequency ( $j\text{NO}_2$ ) (a) and hourly rainfall (b) observed at Gucheng during June-August 2013.

- Han, B., Zhang, R., Yang, W., Bai, Z., Ma, Z., and Zhang, W.: Heavy haze episodes in Beijing during January 2013: inorganic ion chemistry and source analysis using highly time-resolved measurements from an urban site, *Sci. Total Environ.*, *544*, 319-329, 2016.
- Lin, W., Xu, X., and Zhang, X.: Characteristics of gaseous pollutants at Gucheng, a rural site southwest of Beijing, *J. Geophys. Res.*, *114*, 10339, 2009.
- Norman, M., Spirig, C., Wolff, V., Trebs, I., Flechard, C., Wisthaler, A., Schnitzhofer, R., Hansel, A., and Neftel, A.: Intercomparison of ammonia measurement techniques at an intensively managed grassland site (Oensingen, Switzerland), *Atmos. Chem. Phys.*, *9*, 2635–2645, 2009.
- Schwab, J.J.: Ambient Gaseous Ammonia: Evaluation of Continuous Measurement Methods Suitable for Routine Deployment, Final Report Prepared for the New York State Energy Research and Development Authority (NYSERDA), Final Report 08-15, New York, October 2008.
- Wu, W. S. and Wang, T.: On the performance of a semi-continuous PM<sub>2.5</sub> sulphate and nitrate instrument under high loadings of particulate and sulphur dioxide. *Atmos. Environ.* *41*, 5442-5451, 2007.

**P 11 section 3.4: Relationship between ammonium and ammonia: This discussion is very brief and limited. In particular after noting previously (and probably correctly) that local ammonia emissions dominate the chemical speciation observed, the authors then infer “NH<sub>3</sub> dominates NH<sub>x</sub> deposition”. With the dataset they have they could have performed calculations of deposition vs emission over the 4 month period would have given much more insight, i.e. the process is bidirectional therefore it is uncertain whether any net deposition would occur under the ambient conditions. This is a missed opportunity to explore the atmospheric chemistry and physics of the system.**

**Answer:** Thank you for your valuable comments. Indeed it would be great if we could use our measurements to systematically explore the atmospheric chemistry and physics over the our site and to gain more insight, including the emission and deposition of NH<sub>3</sub> and NH<sub>4</sub><sup>+</sup>. However, we did not observe the emission and deposition of NH<sub>3</sub> and NH<sub>4</sub><sup>+</sup>. The air/surface exchange of NH<sub>3</sub> is very complex, bidirectional and highly variable, and is influenced by many factors (e.g., Schrader et al., 2016). Given the parameters we observed, it is hardly possible to obtain robust and quantitative results about the emission vs deposition purely based on available measurements. To well understand the processes of emission, conversion and deposition of NH<sub>x</sub> species in the polluted NCP region, it is highly needed to design observational and 3D modeling studies. Our in-situ measurements present in this paper can be used as supporting data in future modeling studies.

Schrader, F., Brümmer, C., Flechard, C.R., Wichink Kruit, R.J., van Zanten, M.C., Zöll, U., Hensen, A., and Erisman, J.W.: Non-stomatal exchange in ammonia dry deposition models: comparison of two state-of-the-art approaches, *Atmos. Chem. Phys.*, *16*, 13417–13430, 2016.

**Given that there are several thermodynamic models freely available, it would have been useful to explore the dataset against what is predicted by models. What is the ion balance – are**

**dicarboxylic acids needed to explain aerosol neutralisation? (is it neutral?). Is the atmospheric chemistry at the site dominated by thermodynamic equilibrium or is there kinetic limitations on the processes? The authors have missed an opportunity with the dataset to fully understand the chemistry and rely in the results and discussions to discuss the ratios between gas and aerosol partitioning to explain scientific concepts which are known and therefore not surprising.**

**Answer:** Thank you for your suggestions. We have used the thermodynamic equilibrium model (ISORROPIA II) to investigate gas-aerosol partitioning characteristics and compared the modeling results with our measurements. The pH values of aerosol, estimated based on the simulated results, are mostly in the range of 2.5-4.5, with an average of 3.5. While simulated sulfate and nitrate are well comparable with the measurements, simulated ammonium substantially underestimates the observed one, indicating the importance of organic acids in the formation of ammonium. Although we did not measure organic acids in aerosol, the presence of oxalic acid and other low molecular weight dicarboxylic acids in aerosols is often reported (e.g., Hsieh et al., 2007; Kawamura et al., 2010, 2013; Sauerwein and Chan, 2017). There is no doubt about the presence of significant amount of dicarboxylic acids over the North China Plain particularly during summer (Kawamura et al., 2013). Therefore, it is highly possible that neutralizing dicarboxylic acids in aerosol particles contributed significantly to the conversion of ammonia to ammonium. Our results also suggest that the gas-aerosol partitioning at the Gucheng site is dominated by thermodynamic equilibrium. We have added a section about the ISORROPIA II model in the revised manuscript and more text about the simulation results and related discussions as follows:

### **“2.3.2 ISORROPIA II model**

Thermodynamic gas-aerosol equilibrium characteristics during summer 2013 were examined using ISORROPIA II model (Fountoukis and Nenes, 2007). ISORROPIA II is a thermodynamic equilibrium model for inorganic gases and aerosols in the atmosphere (available at <http://isorro피아.eas.gatech.edu>). To obtain the best available predictions of aerosol pH, ISORROPIA II, was run in the forward mode with metastable aerosol state salts precipitate once the aqueous phase becomes saturated with respect to salts, which often showed better performance than the stable state solution (solid + liquid) and was commonly applied in previous pH predictions (Liu et al., 2017). The concentrations of the measured NH<sub>3</sub> and water-soluble ions in PM<sub>2.5</sub> were input into the model as total (gas + aerosol) concentrations, along with simultaneously measured relative humidity and temperature data. The bulk particle pH was calculated using the following equation:

$$pH = -\log_{10} \frac{1000H_{air}^{+}}{AWC} \quad (4)$$

where  $H_{air}^{+}$  ( $\mu\text{g m}^{-3}$ ) and AWC ( $\mu\text{g m}^{-3}$ ) are the ISORROPIA-II predicted equilibrium particle hydronium ion concentration per volume air and aerosol water content, respectively. Evaluation of the

AWC prediction have been reported in previous studies and shows a good performance compared with particle water measurements (Bian et al., 2014; Guo et al., 2015). ”

We have added a new section (Section 3.3 Results from thermodynamic equilibrium simulation) to present our main modeling results and discussed them also other section.

### **"3.4 Results from thermodynamic equilibrium simulation**

We have used the thermodynamic equilibrium model ISORROPIA II to investigate gas-aerosol partitioning characteristics.  $\text{NO}_3^-$ ,  $\text{SO}_4^{2-}$  and  $\text{NH}_4^+$ . The model outputs include equilibrium  $\text{NO}_3^-$ ,  $\text{SO}_4^{2-}$ ,  $\text{NH}_4^+$ ,  $\text{H}^+_{\text{air}}$ ,  $\text{HNO}_3$ ,  $\text{NH}_3$ , AWC, etc. As shown in Fig. 5, the modelled  $\text{NO}_3^-$ ,  $\text{SO}_4^{2-}$ ,  $\text{NH}_3$  show excellent correlations with the corresponding measurements, but modelled  $\text{NH}_4^+$  is much worse correlated with the measured one. Modelled  $\text{NO}_3^-$ ,  $\text{SO}_4^{2-}$ , and  $\text{NH}_3$  values agree well with the measurements, while the modelled  $\text{NH}_4^+$  largely underestimate the measurements. Considering the unbalance between observed  $\text{NH}_4^+$  and the sum of observed  $\text{SO}_4^{2-} + \text{NO}_3^- + \text{Cl}^-$ , we can confirm that other acids in aerosol particles are important in the conversion of  $\text{NH}_3$  to  $\text{NH}_4^+$ . These other acids may be oxalic acid and other dicarboxylic acids. Although we did not measure organic acids in aerosol, the presence of oxalic acid and other low molecular weight dicarboxylic acids in aerosols is often reported (e.g., Hsieh et al., 2007; Kawamura et al., 2010, 2013; Sauerwein and Chan, 2017). There is no doubt about the presence of significant amount of dicarboxylic acids over the North China Plain particularly during summer (Kawamura et al., 2013). Therefore, it is highly possible that neutralizing dicarboxylic acids in aerosol particles contributed significantly to the conversion of ammonia to ammonium.

The simulated  $\text{HNO}_3$  concentrations was  $0.9 \pm 1.1 \mu\text{g m}^{-3}$ , showing a maximum value of  $7.41 \mu\text{g m}^{-3}$  at 11:00 on 19 June 2013. The average diurnal variations of  $\text{HNO}_3$  and  $\text{H}^+_{\text{air}}$  are shown in Fig. S4. The fine particles were moderately acidic in summer, with an average pH values of 3.5. The pH values of aerosol water, estimated based on the simulated results using equation (4), are mostly in the range of 2.5-4.5, with an average of 3.5. On average, pH is over 3.5 during nighttime and below 3.5 during daytime (Fig. 6). Under the medium acidic conditions and high  $\text{NH}_3$  concentrations, organic acid like diacids are able to reaction with ammonia to for ammonium. Because we used ISORROPIA-II for inorganic aerosol composition and no organic acids measurements are available, we cannot analyze in detail the role of organic acids though the model performed quite well (Fig. S5). "

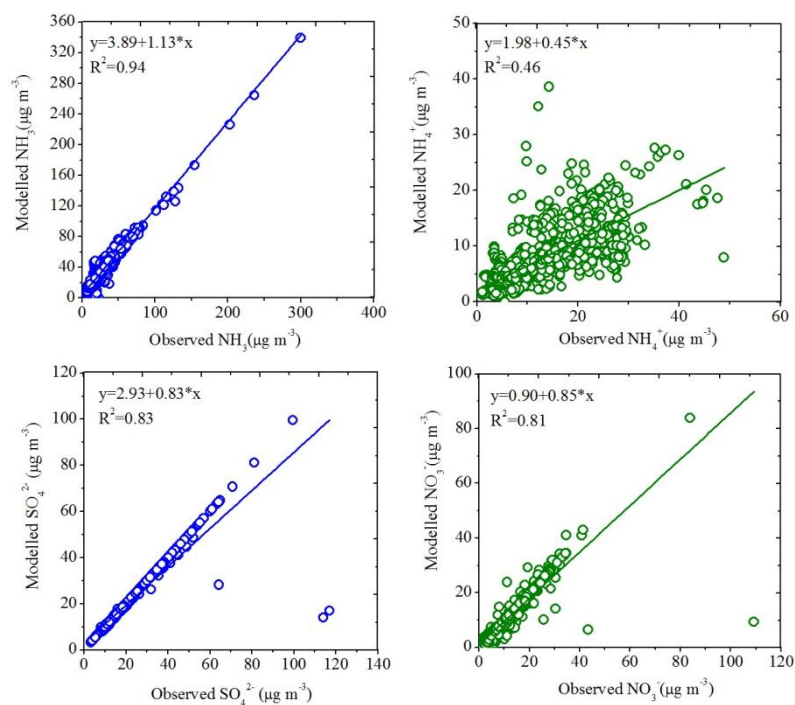


Figure 5. Observed and modelled concentrations of  $\text{NH}_3$ ,  $\text{NH}_4^+$ ,  $\text{SO}_4^{2-}$  and  $\text{NO}_3^-$  in summer 2013.

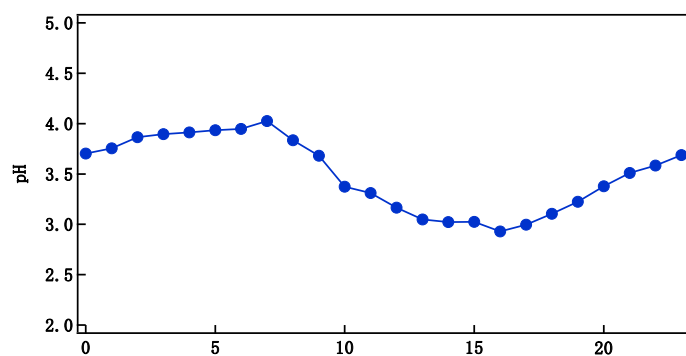


Figure 6. Calculated diurnal variation of pH value of aerosol water.



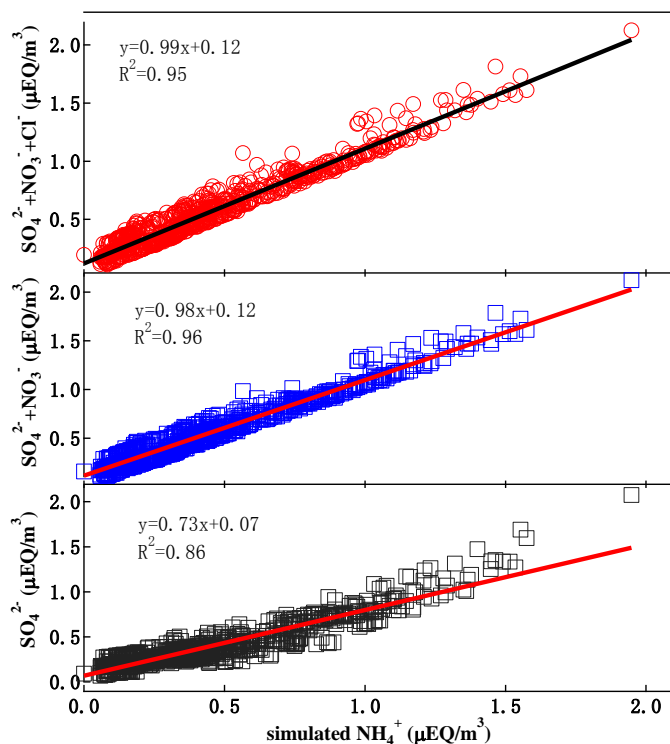


Figure S5 Correlation of modelled  $\text{NH}_4^+$  with modelled  $\text{SO}_4^{2-}$ ,  $\text{SO}_4^{2-}+\text{NO}_3^-$  and  $\text{SO}_4^{2-}+\text{NO}_3^-+\text{Cl}^-$ .

We have made another new section (3.6 A case study of a pollution period) to present and discuss the 7-11 August measurement with additional analysis.

### "3.6 A case study of a pollution period

On several days during the study period, very high  $\text{NH}_3$  and inorganic  $\text{PM}_{2.5}$  concentrations were observed. Here make a case study of a pollution period during 7-11 August 2013. Data of gases, major aerosol ions and some key meteorological parameters are presented in Fig. 9. Some other measure and calculated parameters during this period are given in Fig. S6. As shown in Figs. 9 and S6, there was a sharp increase of  $\text{NO}_x$  during the night and early morning of 10 August, followed by that of  $\text{NH}_3$  (peak value 64 ppb at 03:00. In the meantime, a large peak of AWC occurred and gaseous  $\text{HNO}_3$  decreased to nearly zero (Fig. S6), suggesting rapid uptake of wet aerosol. This event caused the first largest peak of  $[\text{SO}_4^{2-}]+[\text{NO}_3^-]+[\text{NH}_4^+]$ . After this event  $\text{NH}_3$  rose again and reached a even higher peak (76.3) shortly before noon of 10 August. This peak of  $\text{NH}_3$  coincided with a valley of  $\text{NO}_x$ , but the  $\text{HNO}_3$  level increased and pH value decreased was observed in parallel. A few hours later  $\text{SO}_2$  showed a large peak and the second largest peak of  $[\text{SO}_4^{2-}]+[\text{NO}_3^-]+[\text{NH}_4^+]$  occurred. These data show that high  $\text{NH}_3$  concentration was accompanied by the large increase in concentrations of  $\text{SO}_4^{2-}$ ,  $\text{NO}_3^-$  and  $\text{NH}_4^+$ , confirming that  $\text{NH}_3$  play an important role in PM mass formation and that gas-particle

conversion occurred when  $\text{NH}_3$  was available, though  $\text{SO}_4^{2-}$  partitions to the aerosol phase regard less of  $\text{NH}_3$  level (Gong et al., 2013). The secondary ions concentrations had similar temporal distributions with slow accumulation and relatively rapid clearing under favourable meteorological conditions. There were good correlation between  $\text{NH}_3$  with  $\text{NH}_4^+$ ,  $\text{SO}_4^{2-}$  and  $\text{NO}_3^-$  ( $R=0.33$ ,  $0.27$  and  $0.49$ , respectively, with  $P < 0.01$ ). However, there was also situation when high  $\text{NH}_3$  did not associate with high  $[\text{SO}_4^{2-}] + [\text{NO}_3^-] + [\text{NH}_4^+]$ , as indicated by the data around noon of 8 August (Fig. 9). During this case, AWC was extremely low and RH was around 40%. These conditions do not favor heterogeneous reactions.

During 7-11 August 2013, the relationships of the observed  $\text{NH}_4^+$  versus those of  $\text{SO}_4^{2-}$ , the sum of  $\text{SO}_4^{2-}$  and  $\text{NO}_3^-$  and the sum of  $\text{SO}_4^{2-}$ ,  $\text{NO}_3^-$  and  $\text{Cl}^-$  are presented in Fig. 10. It is known that  $(\text{NH}_4)_2\text{SO}_4$  is preferentially formed and the least volatile,  $\text{NH}_4\text{NO}_3$  is relatively volatile, while  $\text{NH}_4\text{Cl}$  is the most volatile.  $\text{NH}_4^+$  is thought to be first associated with  $\text{SO}_4^{2-}$ , afterwards, the excess of  $\text{NH}_4^+$  is with nitrate and chloride (Meng et al., 2015). It is noted that the correlation of  $\text{NH}_4^+$  with the sum of  $\text{SO}_4^{2-}$  and  $\text{NO}_3^-$  ( $R=0.91$ , slope=1.23, with  $P < 0.01$ ) was better than that of  $\text{NH}_4^+$  with  $\text{SO}_4^{2-}$  ( $R=0.80$ , slope=1.65, with  $P < 0.01$ ), suggesting that both  $\text{SO}_4^{2-}$  and  $\text{NO}_3^-$  were associated with  $\text{NH}_4^+$ . As shown in Fig.10, sulfate and nitrate were almost completely neutralized with most of the data above the 1:1 line. A few scattered data below the 1:1 line may be caused by uncertainties in measurements. Little different was found between the regression slopes of  $\text{NH}_4^+$  with the sum of  $\text{SO}_4^{2-}$  and  $\text{NO}_3^-$  and the sum of  $\text{SO}_4^{2-}$ ,  $\text{NO}_3^-$  and  $\text{Cl}^-$  due to the very low amount of  $\text{NH}_4\text{Cl}$ . In this study, the level of  $\text{NH}_3$  was high enough to neutralize both  $\text{SO}_4^{2-}$  and  $\text{NO}_3^-$ , and likely to be form  $(\text{NH}_4)_2\text{SO}_4$  and  $\text{NH}_4\text{NO}_3$ . In addition to these substances, it is likely that  $\text{NH}_3$  also reacted with oxalic acid and other dicarboxylic acid to form ammonium oxalate and other organic ammonium aerosols, as discussed above."

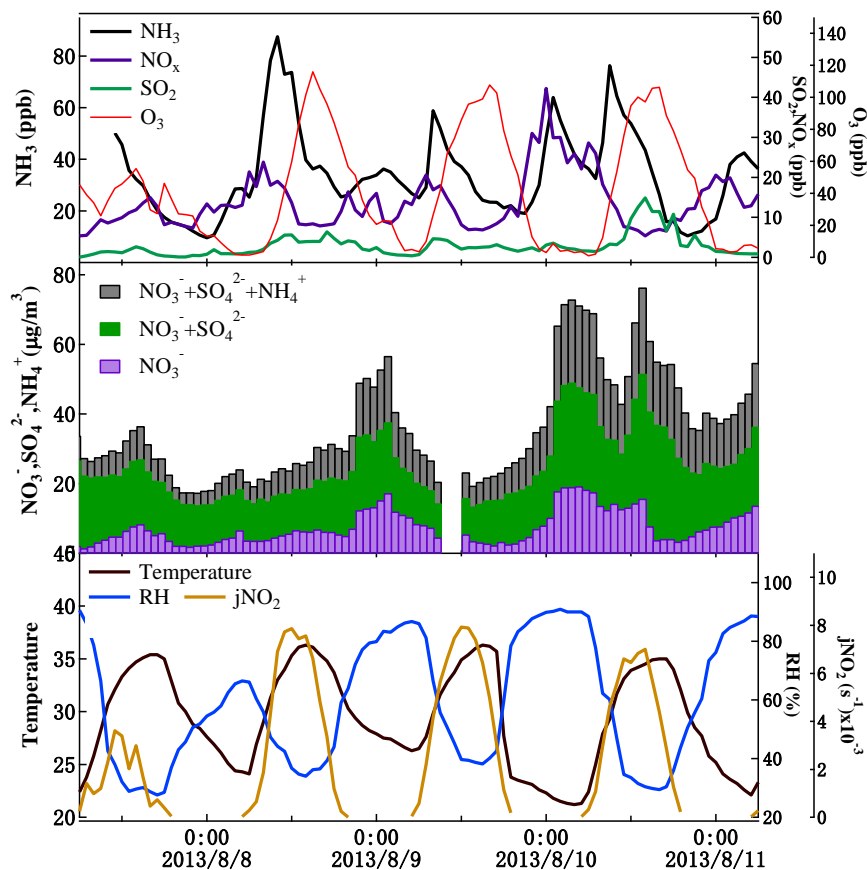


Figure 9. Hourly concentrations of precursor gas and ionic species measured in the pollution episode (a) temporal variations and (b) correlations of  $[\text{NH}_4^+]$  versus  $[\text{SO}_4^{2-}]$ ,  $[\text{SO}_4^{2-}] + [\text{NO}_3^-]$  and  $[\text{SO}_4^{2-}] + [\text{NO}_3^-] + [\text{Cl}^-]$  during 7–11 August 2013.

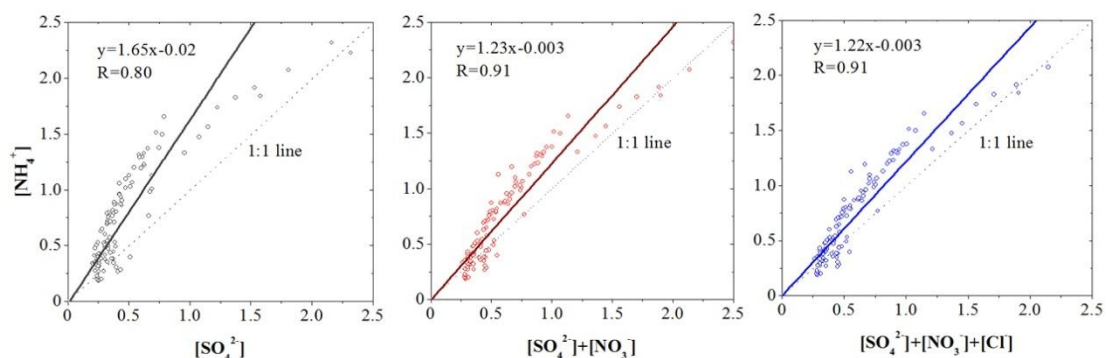


Figure 10. Correlations between  $[\text{NH}_4^+]$  and  $[\text{SO}_4^{2-}]$  (left),  $[\text{NH}_4^+]$  and  $[\text{SO}_4^{2-}] + [\text{NO}_3^-]$  (middle) and  $[\text{NH}_4^+]$  and  $[\text{SO}_4^{2-}] + [\text{NO}_3^-] + [\text{Cl}^-]$  (right) during 7–11 August 2013.

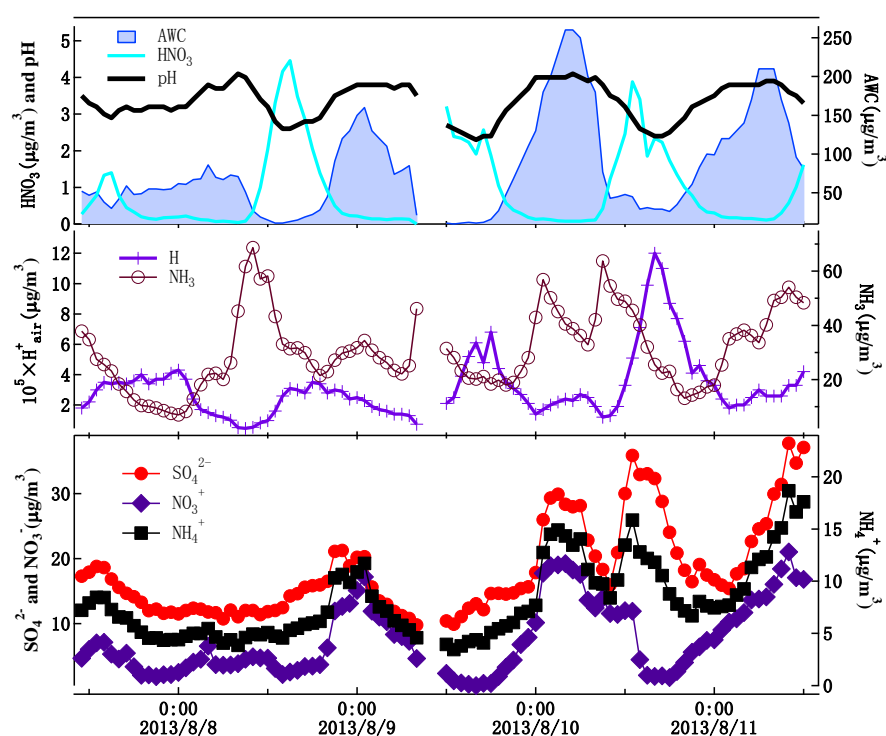


Figure S6. Time series of predicted fine particle pH, predicted particle water mass, predicted  $H_{\text{air}}^+$  and measured  $\text{NH}_3$  and measured inorganic ions during 7-11 August 2013

Hsieh, L.Y., Kuo, S.C., Chen, C.L., Tsai, Y.I.: Origin of low-molecular-weight dicarboxylic acids and their concentration and size distribution variation in suburban aerosol, *Atmos. Environ.*, 41, 6648-6661, 2007.

Kawamura, K., Tachibana, E., Okuzawa, K., Aggarwal, S.G., Kanaya, Y., and Wang, Z. F.: High abundances of water-soluble dicarboxylic acids, ketocarboxylic acids and  $\alpha$ -dicarbonyls in the mountaintop aerosols over the North China Plain during wheat burning season, *Atmos. Chem. Phys.*, 13, 8285–8302, 2013.

Kawamura, K., Barrie, L.A., and Desiree, T.-S.: Intercomparison of the measurements of oxalic acid in aerosols by gas chromatography and ion chromatography, *Atmos. Environ.*, 44, 5316-5319, 2010.

Sauerwein, M. and Chan, C. K.: Heterogeneous uptake of ammonia and dimethylamine into sulfuric and oxalic acid particles, *Atmos. Chem. Phys.*, 17, 6323–6339, 2017

The references are added in the revised manuscript.

Bian, Y. X., Zhao, C. S., Ma, N., Chen, J., and Xu, W. Y.: A study of aerosol liquid water content based on hygroscopicity measurements at high relative humidity in the North China Plain, *Atmos. Chem. Phys.*, 14, 6417-6426, <https://doi.org/10.5194/acp-14-6417-2014>, 2014.

Bougiatioti, A., Nikolaou, P., Stavroulas, I., Kouvarakis, G., Weber, R., Nenes, A., Kanakidou, M., and Mihalopoulos, N.: Particle water and pH in the eastern Mediterranean: Source variability and implications for nutrient availability, *Atmos. Chem. Phys.*, 16, 4579–4591, 2016.

Fountoukis, C. and Nenes, A.: ISORROPIA II: a computationally efficient thermodynamic equilibrium model for  $\text{K}^+$ - $\text{Ca}^{2+}$ - $\text{Mg}^{2+}$ - $\text{NH}_4^+$ - $\text{Na}^+$ - $\text{SO}_4^{2-}$ - $\text{NO}_3^-$ - $\text{Cl}^-$ - $\text{H}_2\text{O}$  aerosols, *Atmos. Chem. Phys.*, 7,

4639–4659, doi:10.5194/acp-7-4639-2007, 2007.

Fountoukis, C., Nenes, A., Sullivan, A., Weber, R., Van Reken, T., Fischer, M., Matias, E., Moya, M., Farmer, D., and Cohen, R. C.: Thermodynamic characterization of Mexico City aerosol during MILAGRO 2006, *Atmos. Chem. Phys.*, 9, 2141–2156, doi:10.5194/acp-9-2141-2009, 2009.

Liu, M., Song, Y., Zhou, T., Xu, Z., Yan, C., Zheng, M., Wu, Z., Hu, M., Wu, Y., and Zhu, T.: Fine particle pH during severe haze episodes in northern China, *Geophys. Res. Lett.*, 44, doi:10.1002/2017GL073210, 2017.

**In the places in the manuscript which use atmospheric chemistry to explain data (e.g. 3.4.2), there are no calculations to check if what is observed is what would be expected under the conditions. Is ozone being lost to the surface or is there a haze which allows aqueous processing in the atmosphere, what might be the role of organics...), what is the surface area of PM (given composition and RH) and hence can N<sub>2</sub>O<sub>5</sub> hydrolysis explain the observations completely? There are lots of questions which are not touched upon, though they are key to understanding the role of NH<sub>3</sub>.**

**Answer:** It is true we did not calculate the O<sub>3</sub> loss, aerosol surface, N<sub>2</sub>O<sub>5</sub> hydrolysis, etc. Having these results would be very helpful in understanding the role of NH<sub>3</sub> in ammonium formation and other aspects of atmospheric chemistry at the site. However, our project was not designed for a “closure study” of gas-aerosol chemistry over the site. Many key parameters were not observed, such as deposition of O<sub>3</sub>, NH<sub>3</sub>, etc., concentrations of radical species, organic aerosols, aerosol surface and size distribution, changes in boundary layer, etc. In the absence of these parameters, many assumptions have to be made, which will lead to large uncertainties in the results. We think a comprehensive modeling study is needed to obtain quantitative assessments of all the chemical and physical processes. Such a modeling is beyond the scope of this observation-based study. Nevertheless, we have made some calculations and obtained some semi-quantitative results as answer to the reviewer’s questions (Fig. R1). According to Verbeke et al. (2015), the annual mean O<sub>3</sub> dry deposition velocity in the NCP region is about 0.3 cm/s. Assuming a doubled deposition velocity (0.6 cm/s) in summer and a constant PBLH of 200 m (this may cause an overestimate during daytime), dry deposition of O<sub>3</sub> is estimated to be in the range of 1.5–9 ppb/hr, which is much smaller than the estimated NO titration (37–117 ppb/hr). If reaction of O<sub>3</sub> with other gases and uptake by aerosol are neglected, a production rate in the range of 35–127 ppb/hr is required to balance the titration and deposition losses and cause the observed net change from -10 ppb/hr to 12 ppb/hr. Note that photochemical production during nighttime should be zero. Therefore the “production” during nighttime can be considered as source aloft the surface layer. We have added “Nighttime formation, aerosol uptake and hydrolysis of N<sub>2</sub>O<sub>5</sub> are highly uncertain as has been pointed out (e.g., Xue et al. 2014). The NO<sub>x</sub> concentration during nighttime was higher than during daytime, while the NO<sub>3</sub><sup>-</sup> level during nighttime was only slightly higher than that during daytime (Fig. R2). By assuming high aerosol surface to mass ratio (33.7 m<sup>2</sup>/g, Okuda, 2013) and a high uptake coefficient (0.1, Seinfeld and Pandis, 2006), we estimate the nighttime N<sub>2</sub>O<sub>5</sub> under the conditions over our site to be in the range of about 3–10 ppb, corresponding to a HNO<sub>3</sub> production rate of about 1–3 ppb/hr (or 2.6–7.7 µg/m<sup>3</sup>). This rate of HNO<sub>3</sub> production would cause an obvious night

production of  $\text{NH}_4^+$ . Indeed we can see increases in the  $\text{NH}_4^+$  concentration and NHR during night (Fig. R3). However, a more or less accurate estimate of the relative contribution of the night  $\text{N}_2\text{O}_5$  chemistry to  $\text{NH}_3$  conversion needs to be made in the future."

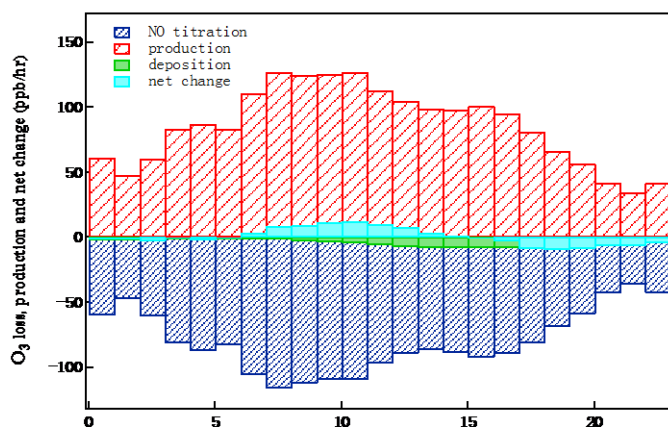


Figure R1 Estimated budget of surface  $\text{O}_3$  at Gucheng during summer 2013.

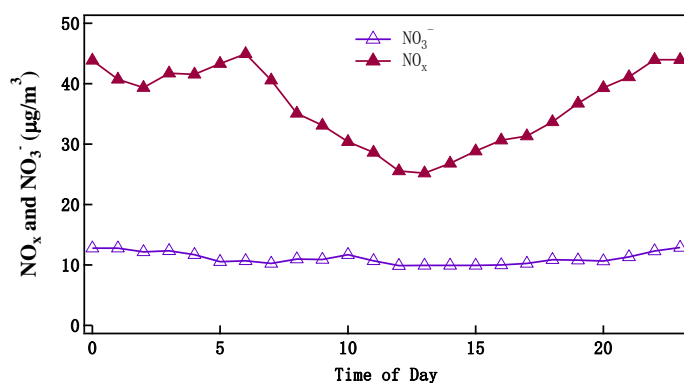


Figure R2 Diurnal variations of  $\text{NO}_x$  and aerosol  $\text{NO}_3^-$  at Gucheng during summer 2013.

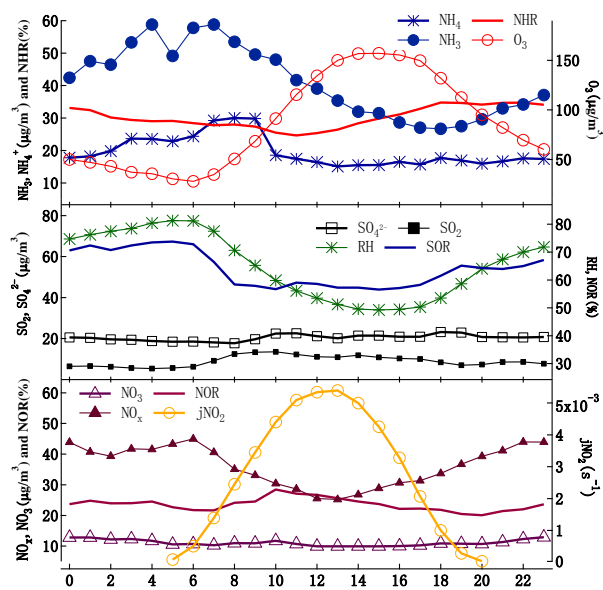


Figure R3 Average diurnal cycles of NHR, SOR, NOR, gaseous precursors, major water soluble ions, and meteorological factors in summer 2013.

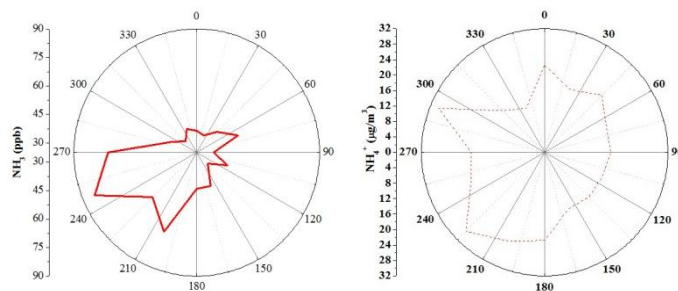
- Okuda, T.: Measurement of the specific surface area and particle size distribution of atmospheric aerosol reference materials, *Atmos. Environ.*, 75, 1-5, 2013.
- Seinfeld, J. H. and Pandis, S. N.: *Atmospheric chemistry and physics: from air pollution to climate change* (2nd ed.), Wiley Interscience, New Jersey, 2006.
- Verbeke, T., Lathi ère, J., Szopa, S., and de Noblet-Ducoudr é N.: Impact of future land-cover changes on HNO<sub>3</sub> and O<sub>3</sub> surface dry deposition, *Atmos. Chem. Phys.*, 15, 13555-13568, 2015.
- Xue, L. K., Wang, T., Gao, J., Ding, A. J., Zhou, X. H., Blake, D. R., Wang, X. F., Saunders, S. M., Fan, S. J., Zuo, H. C., Zhang, Q. Z., and Wang, W. X.: Ground-level ozone in four Chinese cities: precursors, regional transport and heterogeneous processes, *Atmos. Chem. Phys.*, 14, 13175–13188, doi:10.5194/acp-14-13175-2014, 2014.

**Having read the paper I am still not sure what the authors want a reader to learn from the gas-particle ratios. I would suggest the authors revise to include pollution/wind rose diagrams to look at the pollution footprint (e.g. ones are available on Open air and other packages), use current thermodynamics and kinetics of the system to see if current models would accurately represent the observations, if not what may be missing?**

**Answer:** We have drawn the Figure of NH<sub>3</sub> rose and added the analysis of local source in Section 3.5 (now section 3.7) as follows:

“3.5 Local and long-rang transport source of ammonia and ammonium aerosol

Dependence of the concentrations of NH<sub>3</sub> on wind direction at Gucheng is studied to get insight into the distribution of local emission sources around the monitoring site. As shown in Fig. 11, during the sampling period, the prevailing surface winds at Gucheng were northeasterly and southwesterly. High NH<sub>3</sub> originated from the southwest sector of the measurement site, which may be due to a local unidentified agricultural or industrial source or transport from the Xushui township, which is approximately 15 km away from Gucheng. Lower NH<sub>3</sub> concentrations were observed under winds from other sectors. Since NH<sub>3</sub> is either readily converted to NH<sub>4</sub><sup>+</sup> or subjected to dry deposition, high concentrations are found only close to the surface and near the emission sources. Previous studies have reported an inverse relationship between ground-level concentrations of trace gases, such as ammonia, and wind speed (Robarge et al., 2002; Lin et al., 2011). Thus, NH<sub>3</sub> concentrations might be generally lower at higher wind speeds because of turbulent diffusion.



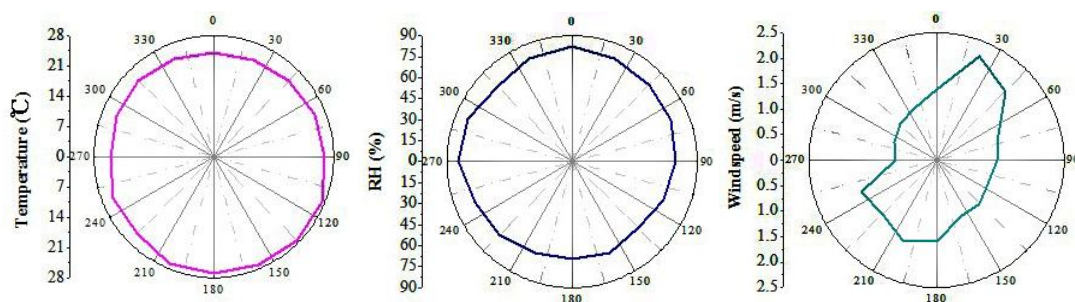


Figure 11. The average  $\text{NH}_3$ ,  $\text{NH}_4^+$  concentrations and meteorological data roses in different wind sectors during summer 2013.”

Oxidised nitrogen chemistry and the gas-aerosol partitioning dynamic are mentioned in passing but are key to understanding whether  $\text{NH}_3$  is driving the PM formation or it is a reservoir gas which grows PM when the presence of the other pollutants is there. Biomass burning is mentioned and K and CO as the indicators. With the dataset they could estimate the fraction of PM due to biomass burning, how much of the PM is explained by biomass burning, and does the biomass burning “seed” larger PM events. Finally the discussion and conclusion would be enhanced if some discussion about the impacts and potential solutions to the impacts. What is the evidence that limiting the  $\text{NH}_3$  emission would improve the air quality - it may well achieve this, but to make the case, evidence or hypothesis is needed to back the statements up.

**Answer:** We have made simulations using the thermodynamic equilibrium model ISORROPIA II. The simulated results indicate that the strong acids ( $\text{H}_2\text{SO}_4$ ,  $\text{HNO}_3$  and  $\text{HCl}$ ) are well balanced by  $\text{NH}_3$  (Fig. R4). However, the correlation between observed  $\text{NH}_4^+$  and the sum of observed  $\text{SO}_4^{2-}$ ,  $\text{NO}_3^-$  and  $\text{Cl}^-$  (Fig. R5) suggests that the neutralization of the strong acids explain 56% of the observed  $\text{NH}_4^+$ . In other words, nearly 44% of the observed  $\text{NH}_4^+$  was due to the presence of other acids in aerosol particles. As mentioned above these acids may be oxalic acid and other dicarboxylic acids. The level of  $\text{NH}_3$  at Gucheng in summer 2013 was very high. Under the  $\text{NH}_3$ -rich condition acid neutralization was easily achieved. As shown in Fig. R3, the average NHR values were around 30%, indicating  $\text{NH}_3$  was not a factor limiting the PM formation. Some recent studies suggest that the formation of sulfate in aerosol can be largely enhanced by  $\text{NO}_2$  oxidation under higher pH values (e.g., Xie et al., 2015; Cheng et al., 2016). Higher pH in aerosol water can be caused by high dust aerosol or  $\text{NH}_3$ . The pH values in aerosol water at Gucheng during our observations was estimated to mostly range from 2.5 to 4.5, based on the ISORROPIA modeling results. Our data do not indicate any increase in sulfate content with the increased  $\text{NO}_2$ . Therefore, high  $\text{NH}_3$  at our site was not driving more PM formation and it served as a reservoir gas to neutralize acids present in aerosol and gas phases.

Open biomass burning occurred occasionally in the NCP region during our campaign though open burning of agricultural wastes had been prohibited. We observed no significant open fires nearby Gucheng. However, fires in the surrounding areas may impact the measurements at the site. The fire maps show that open burning occurred mainly in June and July, which is usually the period of burning wheat straw. During a few days around middle and end June, we observed relatively higher



concentrations of CO and aerosol  $K^+$ , which may be resulted from biomass burning. The  $K^+$  concentration is fairly well correlated with the  $PM_{2.5}$  concentration (Fig. R7), suggesting an impact of biomass burning on particle pollution. The concentration of  $K^+$  is not correlated with those of Na and Ca. Therefore, the observed  $K^+$  in aerosol should be mainly from biomass burning. Although the slope of the  $K$ - $PM_{2.5}$  regression line is small (0.026), the total contribution of biomass burning to  $PM_{2.5}$  may be much larger than a few percentages considering carbonaceous aerosols and other species emitted by biomass burning (Cheng et al., 2013).

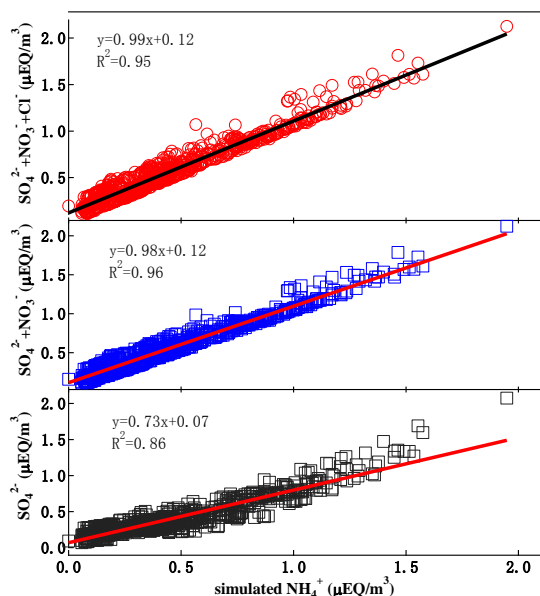


Figure R4 Correlation of simulated  $NH_4^+$  with simulated  $SO_4^{2-}$ ,  $NO_3^-$  and  $Cl^-$ .

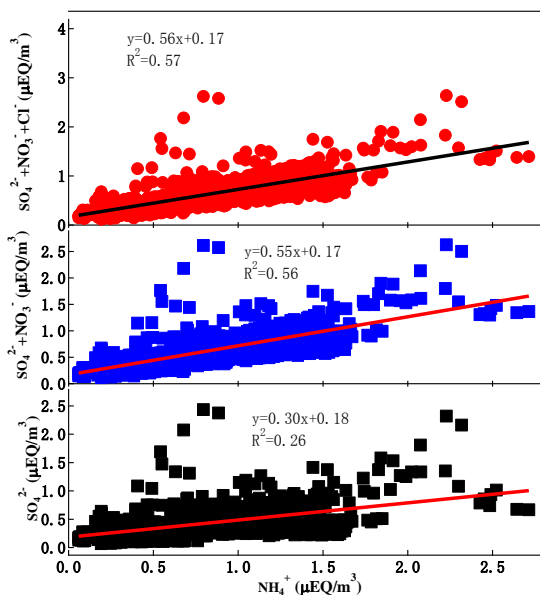


Figure R5 Correlation of observed  $NH_4^+$  with observed  $SO_4^{2-}$ ,  $SO_4^{2-} + NO_3^-$  and  $SO_4^{2-} + NO_3^- + Cl^-$ .

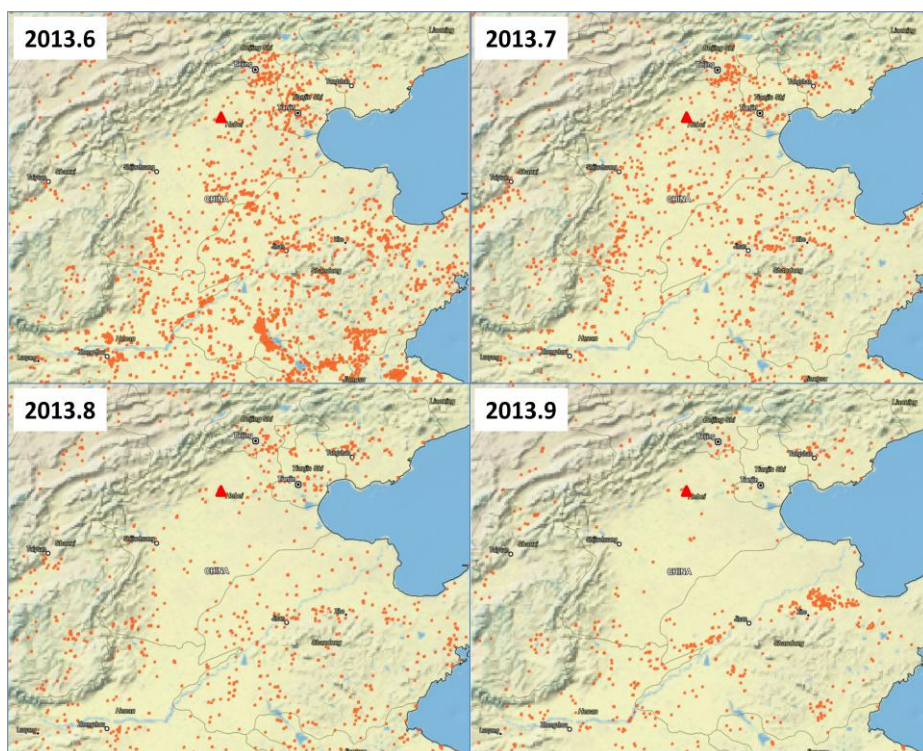


Figure R6 Open fires in the NCP region during June-September, 2013. The red triangelns indicate the position of the Gucheng site. Data source: <https://firms.modaps.eosdis.nasa.gov/firemap/>.

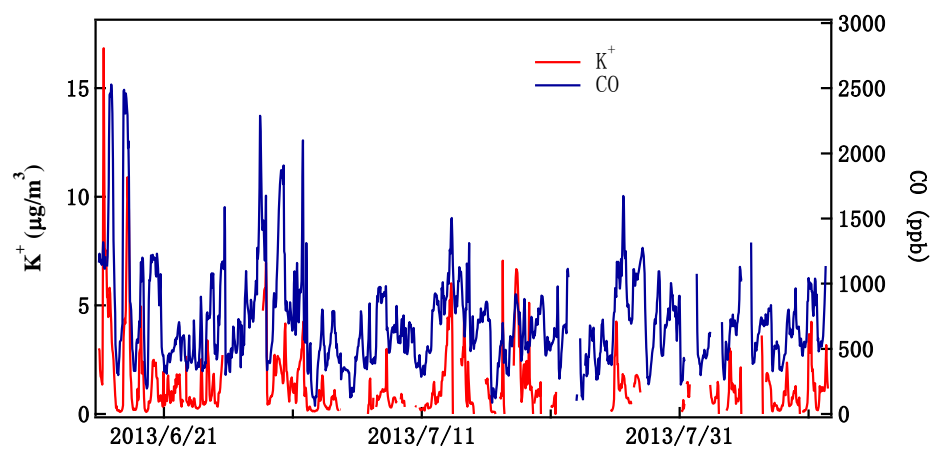


Figure R7  $K^+$  in aerosol and CO concentrations observed at Gucheng during summer 2013.

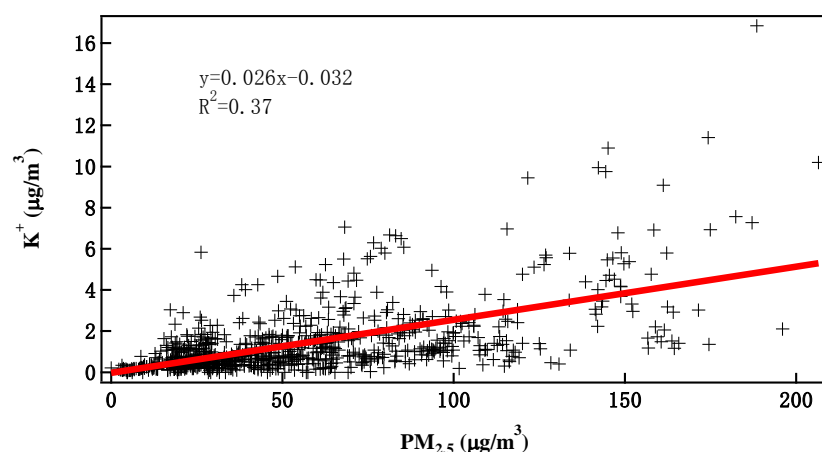


Figure R8 Correlation between  $K^+$  and  $PM_{2.5}$  concentrations.

Cheng, Y., Engling, G., He, K.-B., Duan, F.-K., Ma, Y.-L., Du, Z.-Y., Liu, J.-M., Zheng, M., and Weber, R. J.: Biomass burning contribution to Beijing aerosol, *Atmos. Chem. Phys.*, 13, 7765–7781, 2013

Cheng, Y., Zheng, G., Wei, C., Mu, Q., Zheng, B., Wang, Z., Gao, M., Zhang, Q., He, K., Carmichael, G., Pöschl, U., Su, H.: Reactive nitrogen chemistry in aerosol water as a source of sulfate during haze events in China. *Sci. Adv.* 2, e1601530, 2016.

Xie, Y., Ding, A., Nie, W., Mao, H., Qi, X., Huang, X., Xu, Z., Kerminen, V.-M., Petäjä T., Chi, X., Virkula, A., Boy, M., Xue, L., Guo, J., Sun, J., Yang, X., Kulmala, M., Fu, C.: Enhanced sulfate formation by nitrogen dioxide: Implications from in-situ observations at the SORPES Station, *J. Geophys. Res.* 120, 12679-12694, 2015.

#### Minor corrections:

**P1 Line 22 The observation that  $NH_3$  drives  $NH_4$  content of PM is not new, so I do not think the word “ suggesting” is appropriate**

**Answer:** We have changed the word "suggesting" to "reflecting".

**1 P1 Line 24: This is a percentage not a ratio.**

**Answer:** We have revised the percentage to the ratio according to the reviewer's comments.

**P1 Line 25: use previous NCP abbreviation**

**Answer:** We have added “in the NCP” in Line 25 according to the reviewer's comments.

**P2 line 15: Actually most atmospheric chemistry text books discuss this, would cite them rather than research papers.**

**Answer:** We have revised the sentence. "Some studies have suggested that reducing  $NH_3$  concentrations could be an effective method for alleviating secondary inorganic  $PM_{2.5}$  pollution."

**P5, line 19: asymmetric errors would be more appropriate given that one cannot have negative**

**concentrations.**

**Answer:** We have decided to use the range instead of standard deviation. The sentence reads now "During 15 May–25 September 2013, the average concentrations (ranges) of NH<sub>3</sub>, SO<sub>2</sub> and NO<sub>x</sub> were 36.2 (0-862.9), 5.0 (0-86.8) and 15.4 (2.7-67.7) ppb, respectively."

**P25 Figure 2: given that it rained during the 4 months, why does the RH never go above 90%?**

**Answer:** To accurately measure high RH is still difficult so that the absolute errors associated the high RH values may be large. The measured RH does include some values over 90%, with the maximum of 93%. There might be negative bias. On the other hand, raining does not necessarily mean the surface air is saturated with water.

**P27: for the PM composition it would be useful to have them as stacked so that one can see the variation of composition through time** References: There are not many references from 2015 and 2016 despite many papers being published on this subject area. I would suggest the authors review the recent literature.

**Answer:** The figure on this page has been redrawn. The PM compositions are shown as stacked. Global radiation and wind speed data are removed from the figure. Instead measurements of O<sub>3</sub> and jNO<sub>2</sub> are shown to provide information about photochemistry. We have reviewed the some recent papers (Guo et al., 2015; Han et al., 2016; Sudheer and Rengarajan, 2015; Tang et al., 2016; Wen et al., 2015; Xu et al., 2017; Zhao et al., 2016) and cited them in the revised manuscript.

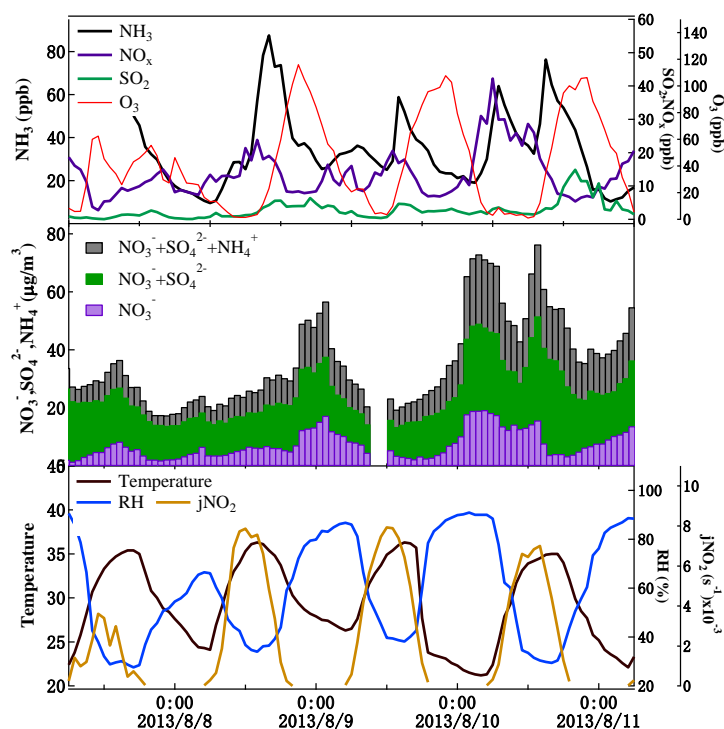


Figure R9 Hourly concentrations of gaseous and ionic species and measurements of air temperature,

RH and jNO<sub>2</sub> observed during the pollution episode 7-11 August 2013.

- Guo, H., Xu, L., Bougiatioti, A., Cerully, K. M., Capps, S. L., Hite Jr., J. R., Carlton, A. G., Lee, S.-H., Bergin, M. H., Ng, N. L., Nenes, A., and Weber, R. J.: Fine-particle water and pH in the southeastern United States, *Atmos. Chem. Phys.*, 15, 5211-5228, <https://doi.org/10.5194/acp-15-5211-2015>, 2015.
- Han, B., Zhang, R., Yang, W., Bai, Z., Ma, Z., and Zhang, W.: Heavy haze episodes in Beijing during January 2013: inorganic ion chemistry and source analysis using highly time-resolved measurements from an urban site, *Sci. Total Environ.*, 544, 319-329, 2016.
- Sudheer, A. K., and Rengarajan, R.: Time-resolved inorganic chemical composition of fine aerosol and associated precursor gases over an urban environment in western India: Gas-aerosol equilibrium characteristics[J]. *Atmospheric Environment*, 109:217-227, 2015.
- Tang, X., Zhang, X.S., Ci, Z.J., Guo, J and Wang, J. Q.: Speciation of the major inorganic salts in atmospheric aerosols of Beijing, China: Measurements and comparison with model. *Atmos. Environ.*, 133:123-134, 2016.
- Wen, L., Chen, J., Yang, L., Wang, X., Xu, C., & Sui, X., et al.: Enhanced formation of fine particulate nitrate at a rural site on the north china plain in summer: the important roles of ammonia and ozone. *Atmos. Environ.*, 101, 294-302, 2015.
- Xu, W., Song, W., Zhang, Y., Liu, X., Zhang, L., Zhao, Y., Liu, D., Tang, A., Yang, D., Wang, D., Wen, Z., Pan, Y., Fowler, D., Collett Jr., J. L., Erisman, J. W., Goulding, K., Li, Y., and Zhang, F.: Air quality improvement in a megacity: implications from 2015 Beijing Parade Blue pollution control actions, *Atmos. Chem. Phys.*, 17, 31-46, <https://doi.org/10.5194/acp-17-31-2017>, 2017.
- Zhao, M., Wang, S., Tan, J., Hua, Y., Wu, D., and Hao, J.: Variation of Urban Atmospheric Ammonia Pollution and its Relation with PM<sub>2.5</sub> Chemical Property in Winter of Beijing, China. *Sci. Total Environ.*, 16(6) , 1378-1389, 2016.

## **Response to Reviewer #2's comments**

**Anonymous Reviewer #2**

**Received and published: 31 May 2017**

**This manuscript presents a comprehensive ambient measurement dataset, including various trace gases and particulate species, for over four months at a rural site in the North China Plain (NCP). Ammonia (NH<sub>3</sub>) is the focus of this study for its role in the formation of secondary inorganic aerosols, which accounts for a major fraction of PM<sub>2.5</sub> in NCP. The hourly resolution, higher than many of the previous ambient ammonia measurements, enables detailed studies on individual pollution events and the diurnal variations. However, I hope the authors can take better advantage of this dataset, and go deeper into Atmospheric Chemistry and Atmospheric Physics, as indicated by the journal name. For example, this work aims to understand the impact of ammonia on secondary ammonium aerosols (page 1, line 20), facilitate developing future ammonia emission control policies (page 1, line 32), and examine the sources of ammonia and ammonium and their chemical conversion mechanism (page 3, line 8). These are all important issues, but I am not convinced that this article has advanced our current knowledge and understanding about these issues after reading it.**

**Answer:** We thank your comments and suggestions. We have made additional data analysis and revised the manuscript according to the comments and suggestions by both reviewers. To gain more insight into the role of ammonia in the formation of secondary inorganic aerosol, simulations were made using the thermodynamic equilibrium model ISORROPIA II. The measurements were used as input of model to simulate the variations of the components in gas, liquid and solid phases, which are useful in the investigation of the gas-aerosol equilibrium characteristics.

## **Major comments**

**1. It takes a significant part of this manuscript to explain the observed concentrations. However many of the explanations are qualitative and even speculative. Further quantitative evidences are needed. To name a few:**

**Page 8, lines 5-6, “the monthly concentration of SO<sub>2</sub>, NO<sub>x</sub>, and CO in July and August decreased because of rapid photochemical reduction, additional removal by rainfall, and excellent vertical mixing.” What are the evidences of photochemistry, wet scavenging, and vertical mixing?**

**Answer:** We have added the analysis of some related meteorological conditions and show figures with measurements of rainfall and the NO<sub>2</sub> photolysis frequency (*j*NO<sub>2</sub>) during June-August 2013 as supplementary materials. Changes are made to text as follows:

"The monthly concentrations of SO<sub>2</sub>, NO<sub>x</sub>, and CO in July and August decreased compared to those in June. In addition to less influences from biomass burning, meteorological conditions were also in favor of lowering the concentrations of these gases. Figure S2 shows the monthly average diurnal variations of *j*NO<sub>2</sub> and the time-series of hourly rainfall during June-August 2013. As can be seen, the average *j*NO<sub>2</sub> increased from June to August, indicating better conditions for photochemical reduction in July and August. There was also a slight increase in rainfall from June to August, which may promote removal of the pollutants."

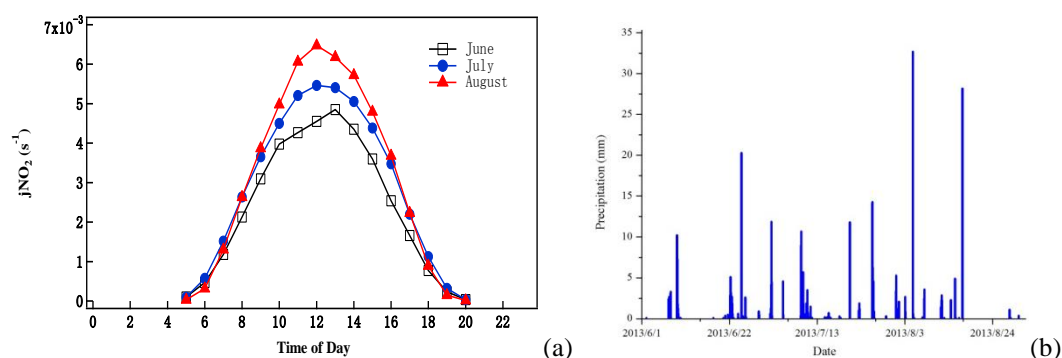


Figure S2. Monthly average diurnal variations of the NO<sub>2</sub> photolysis frequency ( $j\text{NO}_2$ ) (a) and hourly rainfall (b) observed at Gucheng during June-August 2013.

**Page 8, lines 8-9, the ozone was highest in June because of “photochemical production, intense burning of biomass, and transport of regional pollution”. What are the evidences of more photochemistry, biomass burning, and regional transport in June? Shouldn’t July have larger photochemical rates?**

**Answer:** After careful consideration we think the statement should be revised. The sentence is changed to "For the secondary pollutant O<sub>3</sub>, the highest concentration was observed in June. This is consistent with previous results from Gucheng (Lin et al., 2009) and should be related with the annual maximum of background O<sub>3</sub> in the NCP, which occurs in June (Lin et al., 2008; Ding et al., 2008). "

Ding, A. J., Wang, T., Thouret, V., Cammas, J.-P., and Nédélec, P.: Tropospheric ozone climatology over Beijing: analysis of aircraft data from the MOZAIC program, *Atmos. Chem. Phys.*, 8, 1-13, 2008.

Lin, W., Xu, X., Zhang, X., and Tang, J.: Contributions of pollutants from North China Plain to surface ozone at the Shangdianzi GAW Station, *Atmos. Chem. Phys.*, 8, 5889–5898, 2008.

Lin, W., Xu, X., and Zhang, X.: Characteristics of gaseous pollutants at Gucheng, a rural site southwest of Beijing, *J. Geophys. Res.*, 114, 10339, 2009.

**Page 8, lines 26-27, the downward mixing of the residual layer containing higher ammonia concentration could lead to an increase of ammonia in the morning. This would require a very large pool of ammonia in the residual layer. Why did it not happen in other months?**

**Answer:** Indeed, the interpretation about the morning peak is mainly based on the opinions in cited references, which are mostly speculations. We think more investigations are necessary to be able to clearly and quantitatively explain the morning peak phenomenon. We have revised the 2nd and 3rd paragraphs in section 3.2.2 as follows:

"The morning peak of NH<sub>3</sub> was also observed elsewhere and could be resulted from emissions from fertilized soils and plant stomata, evaporation of dew, and human sources, as well as mixing down of

ammonia from the residual layer (Trebs et al., 2004; Norman et al., 2009; Bash et al., 2010; Ellis et al., 2011). Figure 3b reveals that the relative humidity (90%-89%) and temperature (21.5-22.1 °C) remained relatively constant before 06:00, but increased later in the morning. The increasing temperature can heat the earth's surface and vegetation leaves and reduce the RH, potentially leading to evaporation of NH<sub>3</sub> from soil and plants and volatilization of ammonium aerosol (Trebs et al., 2004; Norman et al., 2009; Ellis et al., 2011), which may increase NH<sub>3</sub> concentrations in the morning. When the emission was occurring into a shallow boundary layer, NH<sub>3</sub> increase would be more prominent. In addition, the morning rise might also be due to the breakup of the nocturnal boundary layer. During the sampling period, the majority of peaks of ammonia over 50 ppb occurred at night, which were attribute to local emissions, such as from agricultural activity, into a shallow nocturnal boundary layer. It was supposed by Ellis et al. (2011) that the downward mixing of air containing higher NH<sub>3</sub> from the residual layer could lead to an increase of surface NH<sub>3</sub> after the breakup of the nocturnal boundary layer. "



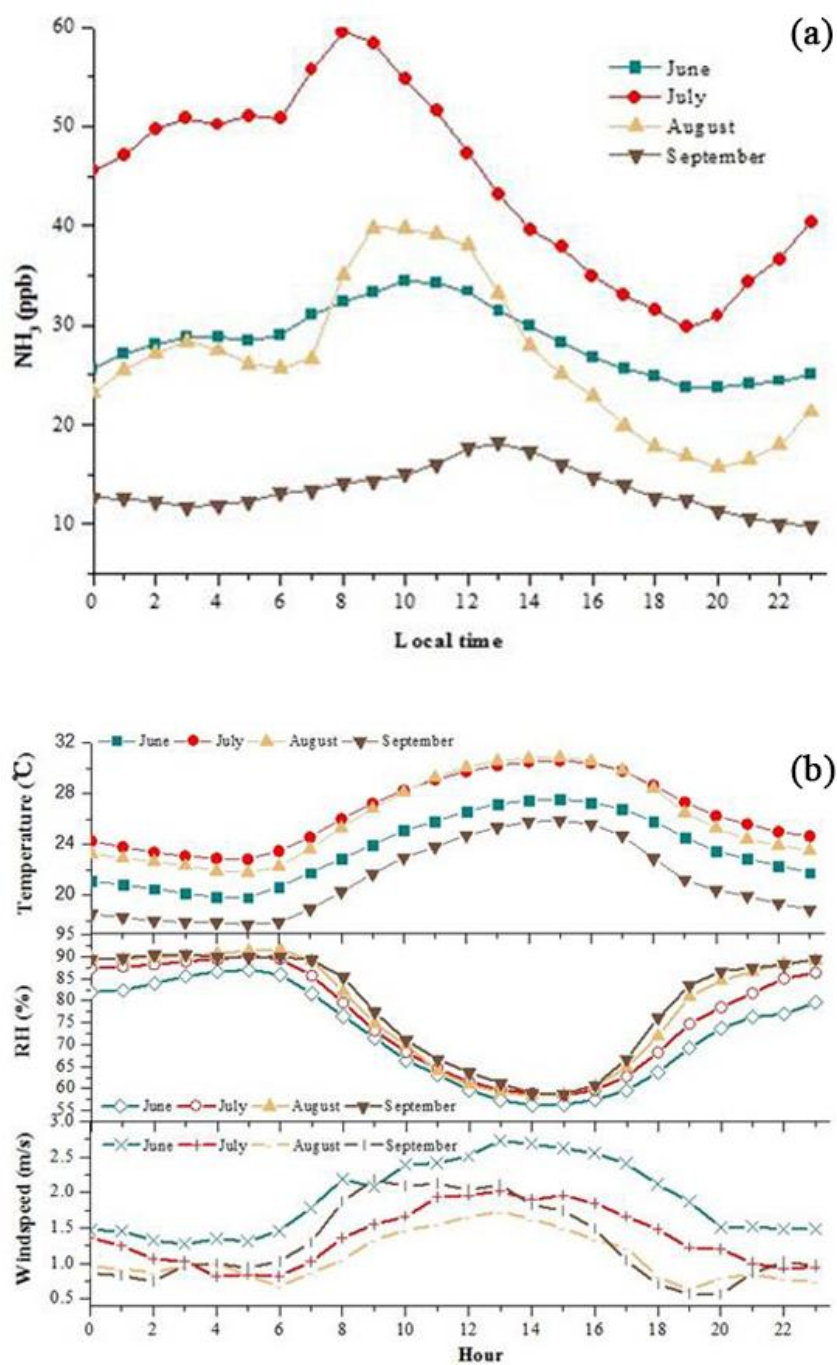


Figure 3. Diurnal variation (a)  $\text{NH}_3$  and (b) meteorological parameters during the sampling period.

Bash, J. O., Walker, J. T., Katul, G. G., Jones, M. R., Nemitz, E., and Robarg, W. P.: Estimation of In-Canopy Ammonia Sources and Sinks in a Fertilized Zea mays Field, *Environ. Sci. Tech.*, 44, 1683-1689, 2010.

Ellis, R. A., Murphy, J. G., Markovic, M. Z., VandenBoer, T. C., Makar, P. A., Brook, J., and Mihele, C.: The influence of gas-particle partitioning and surface-atmosphere exchange on ammonia during BAQS-Met, *Atmos. Chem. Phys.*, 11, 133-145, 2011.

Norman, M., Spirig, C., Wolff, V., Trebs, I., Flechard, C., Wisthaler, A., Schnitzhofer, R., Hansel, A.,

- and Neftel, A.: Intercomparison of ammonia measurement techniques at an intensively managed grassland site (Oensingen, Switzerland), *Atmos. Chem. Phys.*, 9, 2635–2645, 2009.
- Schwab, J.J.: Ambient Gaseous Ammonia: Evaluation of Continuous Measurement Methods Suitable for Routine Deployment, Final Report Prepared for the New York State Energy Research and Development Authority (NYSERDA), Final Report 08-15, New York, October 2008.
- Trebs, I., Meixner, F. X., Slanina J., Otjes, R. P., and Andreae, M. O.: Real-time measurements of ammonia, acidic trace gases and water-soluble inorganic aerosol species at a rural site in the Amazon Basin, *Atmos. Chem. Phys.*, 4, 967–987, 2004.

**Page 9, line 5, the author explains the earlier ammonia morning peak in July by increased emissions. Further evidence?**

**Answer:** We have no direct evidence of emissions. However, the Gucheng site is an experiment station for agrometeorological studies. Corn is the main crop in the station area and nearly all the agricultural areas in the surrounding. According the climate in the NCP, corn is planted around the middle of June and grows rapidly in July. Therefore, July is the key period for the application of nitrogen fertilizers like urea. For example, during last ten days of July 2013, 225-300 kg of urea were applied per hectare of station area (Meng et al., 2015), causing huge NH<sub>3</sub> spikes during the end of July (Fig. 2). In addition, the highest nighttime temperature in July (Fig. 3b) could promote the soil emission of NH<sub>3</sub> and the relatively lower wind speed (Fig. 3b) and lowest PBLH (Fig. S3) in July was in favor of the accumulation of NH<sub>3</sub> in surface air. We have revised the 4th and 5th paragraphs in section 3.2.2 as follows:

"From Fig. 3a, it can be seen that in July the NH<sub>3</sub> level was the highest and peaked earliest. One reason for this might be the increased emissions of local agricultural NH<sub>3</sub> sources in July compared with those in June, August, and September. On the average, the level NH<sub>3</sub> in July had a maximum nighttime increase (20.0 ppb from 20:00 to 06:00), which is much large than those in June (5.2 ppb), August (9.9 ppb) and September (1.8 ppb). The early morning increase of NH<sub>3</sub> in July started from a much higher level than in other months, resulting a earliest NH<sub>3</sub> peak in July.

There is no direct evidence of increased agricultural NH<sub>3</sub> emission in July. However, the Gucheng site is an experiment station for agrometeorological studies. Corn is the main crop in the station area and nearly all the agricultural areas in the surrounding. According the climate in the NCP, corn is planted around the middle of June and grows rapidly in July. Therefore, July is the key period for the application of nitrogen fertilizers like urea. As mentioned above, the urea application in the station on 20 July 2013 and a precipitation process afterwards caused huge NH<sub>3</sub> spikes during the end of July (Fig. 2b). In addition, the highest nighttime temperature in July (Fig. 3b) could promote the soil emission of NH<sub>3</sub>, and the relatively lower wind speed (Fig. 3b) and lowest PBLH (Fig. S3) in July was in favor of the accumulation of NH<sub>3</sub> in surface air.

In summary, ambient NH<sub>3</sub> at Gucheng showed interesting diurnal cycles, which look significantly different in different summer months. We believe the interplay of some processes, such as emissions from agricultural sources, meteorological conditions (temperature, relativity humidity, wind speed, and BHL height, etc.) as well as chemical conversion are important in the determination of levels and

diurnal patterns of  $\text{NH}_3$  at the site. Whether or not these processes are all important in the morning variation of  $\text{NH}_3$ ? How important are they? And what makes the difference in the peaking time and concentration of  $\text{NH}_3$  in different months? These are questions to be answered in the future."

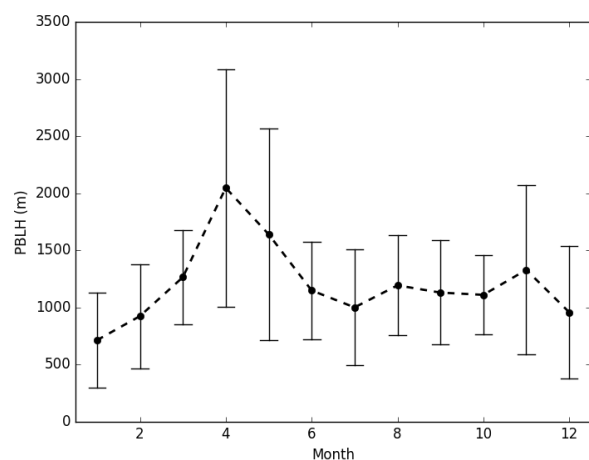


Figure S3. The monthly planetary boundary layer heights at 14:00 during 2013 at Gucheng.

Guo, J., Miao, Y., Zhang, Y., Liu, H., Li, Z., Zhang, W., He, J., Lou, M., Yan, Y., Bian, L., and Zhai, P.: The climatology of planetary boundary layer height in China derived from radiosonde and reanalysis data, *Atmos. Chem. Phys.*, 16, 13309-13319, 2016.

Miao, Y., Guo, J., Liu, S., Liu, H., Li, Z., Zhang, W., and Zhai, P.: Classification of summertime synoptic patterns in Beijing and their associations with boundary layer structure affecting aerosol pollution, *Atmos. Chem. Phys.*, 17, 3097-3110, 2017.

**2. A high observed concentration can always be explained by more emission, less mixing, or less removal. I think a publication in ACP should go beyond reporting the concentrations of these short-lived species, as the concentrations are highly variable. This study used the ratio between ammonium and  $\text{NH}_x$  to infer the gas-particle conversion of ammonia. However the ammonium and ammonia may be from different sources, where ammonium is formed in the city with  $\text{NO}_x$  and  $\text{SO}_2$ , and ammonia is emitted locally. In other words, what if  $\text{NH}_x$  and  $\text{NH}_3$  are decoupled?**

**Answer:** We have made simulations using the ISORROPIA II model and analyzed the model results together measurements. We think we have gained more insight than before but also acknowledge that there are limitations in our observation, modeling and data analysis. Some open issues remain to be addressed in future studies.

The ratios  $\text{NHR}$  ( $\text{NH}_4^+/\text{NH}_x$ ),  $\text{SOR}$  ( $\text{SO}_4^{2-}/(\text{SO}_4^{2-}+\text{SO}_2)$ ) and  $\text{NOR}$  ( $\text{NO}_3^-/(\text{NO}_3^-+\text{NO}_x)$ ) were calculated as measures of chemical conversion of  $\text{NH}_3$ ,  $\text{SO}_2$  and  $\text{NO}_x$ . You are right that  $\text{NH}_x$  and  $\text{NH}_3$  may be decoupled. Sources of  $\text{NH}_3$ ,  $\text{SO}_2$  and  $\text{NO}_x$  may be dislocated. The lifetimes of these gases are different and hence the dispersion areas. Fine aerosol particles may travel much longer than the precursor gases. In the real situation we always observe gases and aerosols originating both from cities and from rural areas, emitted by different sources, and chemically produced. Wherever we measure, we measure is a mixture impacted by different sources from locations and processes. In this sense, we should not attribute our results only to local impacts or local situation. When our observation at a site

covers a longer period, our results should be applicable to areas in varying size.

At page 10, line 13, it is summarized that “This observation emphasizes the important role of NH<sub>3</sub> in the formation of secondary SO<sub>4</sub>, NO<sub>3</sub> and NH<sub>4</sub> aerosols, which should be further explored...”. The title of this manuscript is about the role of ammonia on secondary inorganic aerosols, but what exactly is this role? It is not satisfying to only know it is important and needs further exploration.

**Answer:** We have deleted this sentence. New results from model simulation and data analysis are added and discussed in the revised manuscript. In particular, we have added two new sections:

### **"3.4 Results from thermodynamic equilibrium simulation**

We have used the thermodynamic equilibrium model ISORROPIA II to investigate gas-aerosol partitioning characteristics. NO<sub>3</sub><sup>-</sup>, SO<sub>4</sub><sup>2-</sup> and NH<sub>4</sub><sup>+</sup>. The model outputs include equilibrium NO<sub>3</sub><sup>-</sup>, SO<sub>4</sub><sup>2-</sup>, NH<sub>4</sub><sup>+</sup>, H<sup>+</sup><sub>air</sub>, HNO<sub>3</sub>, NH<sub>3</sub>, AWC, etc. As shown in Fig. 5, the modelled NO<sub>3</sub><sup>-</sup>, SO<sub>4</sub><sup>2-</sup>, NH<sub>3</sub> show excellent correlations with the corresponding measurements, but modelled NH<sub>4</sub><sup>+</sup> is much worse correlated with the measured one. Modelled NO<sub>3</sub><sup>-</sup>, SO<sub>4</sub><sup>2-</sup>, and NH<sub>3</sub> values agree well with the measurements, while the modelled NH<sub>4</sub><sup>+</sup> largely underestimate the measurements. Considering the unbalance between observed NH<sub>4</sub><sup>+</sup> and the sum of observed SO<sub>4</sub><sup>2-</sup>+NO<sub>3</sub><sup>-</sup>+Cl<sup>-</sup>, we can confirm that other acids in aerosol particles are important in the conversion of NH<sub>3</sub> to NH<sub>4</sub><sup>+</sup>. These other acids may be oxalic acid and other dicarboxylic acids. Although we did not measure organic acids in aerosol, the presence of oxalic acid and other low molecular weight dicarboxylic acids in aerosols is often reported (e.g., Hsieh et al., 2007; Kawamura et al., 2010, 2013; Sauerwein and Chan, 2017). There is no doubt about the presence of significant amount of dicarboxylic acids over the North China Plain particularly during summer (Kawamura et al., 2013). Therefore, it is highly possible that neutralizing dicarboxylic acids in aerosol particles contributed significantly to the conversion of ammonia to ammonium.

The simulated HNO<sub>3</sub> concentrations was  $0.9 \pm 1.1 \mu\text{g m}^{-3}$ , showing a maximum value of  $7.41 \mu\text{g m}^{-3}$  at 11:00 on 19 June 2013. The average diurnal variations of HNO<sub>3</sub> and H<sup>+</sup><sub>air</sub> are shown in Fig. S4. The fine particles were moderately acidic in summer, with an average pH values of 3.5. The pH values of aerosol water, estimated based on the simulated results using equation (4), are mostly in the range of 2.5-4.5, with an average of 3.5. On average, pH is over 3.5 during nighttime and below 3.5 during daytime (Fig. 6). Under the medium acidic conditions and high NH<sub>3</sub> concentrations, organic acid like diacids are able to reaction with ammonia to form ammonium. Because we used ISORROPIA-II for inorganic aerosol composition and no organic acids measurements are available, we cannot analyze in detail the role of organic acids though the model performed quite well (Fig. S5). "

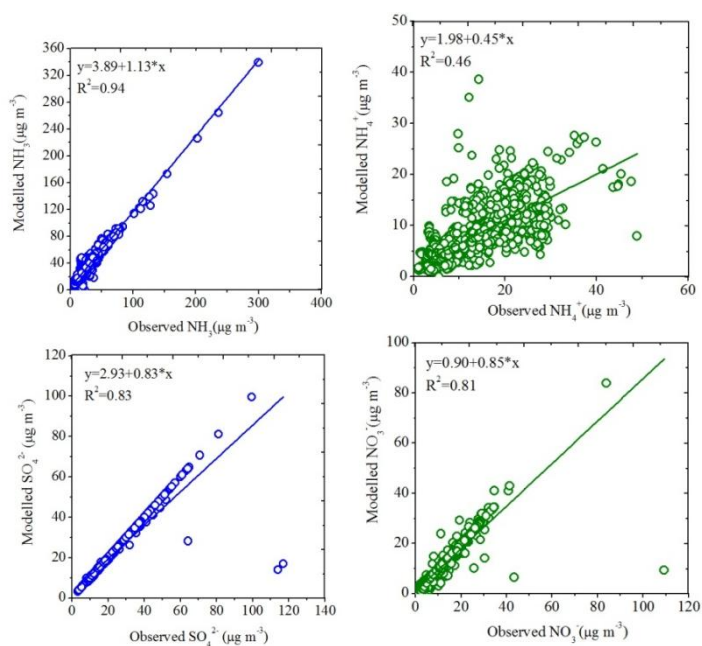


Figure 5. Observed and modelled concentrations of  $\text{NH}_3$ ,  $\text{NH}_4^+$ ,  $\text{SO}_4^{2-}$  and  $\text{NO}_3^-$  in summer 2013.

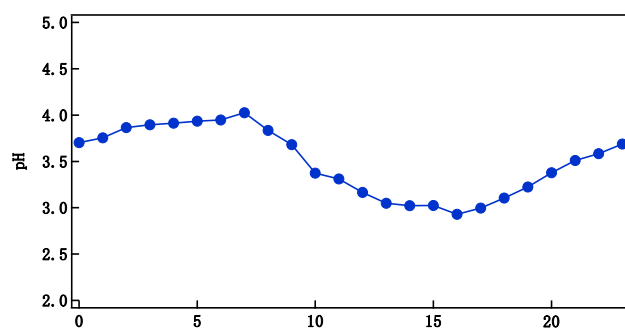


Figure 6. Calculated diurnal variation of pH value of aerosol water.

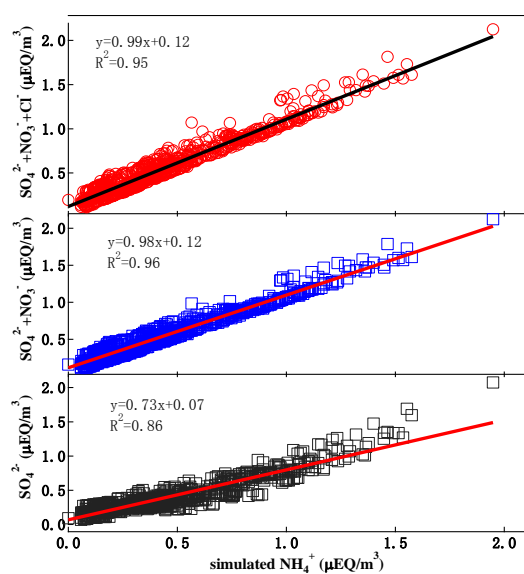


Figure S5 Correlation of modelled  $\text{NH}_4^+$  with modelled  $\text{SO}_4^{2-}$ ,  $\text{SO}_4^{2-} + \text{NO}_3^-$  and  $\text{SO}_4^{2-} + \text{NO}_3^- + \text{Cl}^-$ .

### "3.6 A case study of a pollution period

On several days during the study period, very high  $\text{NH}_3$  and inorganic  $\text{PM}_{2.5}$  concentrations were observed. Here make a case study of a pollution period during 7-11 August 2013. Data of gases, major aerosol ions and some key meteorological parameters are presented in Fig. 9. Some other measure and calculated parameters during this period are given in Fig. S6. As shown in Figs. 9 and S6, there was a sharp increase of  $\text{NO}_x$  during the night and early morning of 10 August, followed by that of  $\text{NH}_3$  (peak value 64 ppb at 03:00. In the meantime, a large peak of AWC occurred and gaseous  $\text{HNO}_3$  decreased to nearly zero (Fig. S6), suggesting rapid uptake of wet aerosol. This event caused the first largest peak of  $[\text{SO}_4^{2-}] + [\text{NO}_3^-] + [\text{NH}_4^+]$ . After this event  $\text{NH}_3$  rose again and reached a even higher peak (76.3) shortly before noon of 10 August. This peak of  $\text{NH}_3$  coincided with a valley of  $\text{NO}_x$ , but the  $\text{HNO}_3$  level increased and pH value decreased was observed in parallel. A few hours later  $\text{SO}_2$  showed a large peak and the second largest peak of  $[\text{SO}_4^{2-}] + [\text{NO}_3^-] + [\text{NH}_4^+]$  occurred. These data show that high  $\text{NH}_3$  concentration was accompanied by the large increase in concentrations of  $\text{SO}_4^{2-}$ ,  $\text{NO}_3^-$  and  $\text{NH}_4^+$ , confirming that  $\text{NH}_3$  play an important role in PM mass formation and that gas-particle conversion occurred when  $\text{NH}_3$  was available, though  $\text{SO}_4^{2-}$  partitions to the aerosol phase regard less of  $\text{NH}_3$  level (Gong et al., 2013). The secondary ions concentrations had similar temporal distributions with slow accumulation and relatively rapid clearing under favourable meteorological conditions. There were good correlation between  $\text{NH}_3$  with  $\text{NH}_4^+$ ,  $\text{SO}_4^{2-}$  and  $\text{NO}_3^-$  ( $R=0.33$ ,  $0.27$  and  $0.49$ , respectively, with  $P < 0.01$ ). However, there was also situation when high  $\text{NH}_3$  did not associate with high  $[\text{SO}_4^{2-}] + [\text{NO}_3^-] + [\text{NH}_4^+]$ , as indicated by the data around noon of 8 August (Fig. 9). During this case, AWC was extremely low and RH was around 40%. These conditions do not favor heterogeneous reactions.

During 7-11 August 2013, the relationships of the observed  $\text{NH}_4^+$  versus those of  $\text{SO}_4^{2-}$ , the sum of  $\text{SO}_4^{2-}$  and  $\text{NO}_3^-$  and the sum of  $\text{SO}_4^{2-}$ ,  $\text{NO}_3^-$  and  $\text{Cl}^-$  are presented in Fig. 10. It is known that  $(\text{NH}_4)_2\text{SO}_4$  is preferentially formed and the least volatile,  $\text{NH}_4\text{NO}_3$  is relatively volatile, while  $\text{NH}_4\text{Cl}$  is the most volatile.  $\text{NH}_4^+$  is thought to be first associated with  $\text{SO}_4^{2-}$ , afterwards, the excess of  $\text{NH}_4^+$  is with nitrate and chloride (Meng et al., 2015). It is noted that the correlation of  $\text{NH}_4^+$  with the sum of  $\text{SO}_4^{2-}$  and  $\text{NO}_3^-$  ( $R=0.91$ , slope=1.23, with  $P < 0.01$ ) was better than that of  $\text{NH}_4^+$  with  $\text{SO}_4^{2-}$  ( $R=0.80$ , slope=1.65, with  $P < 0.01$ ), suggesting that both  $\text{SO}_4^{2-}$  and  $\text{NO}_3^-$  were associated with  $\text{NH}_4^+$ . As shown in Fig.10, sulfate and nitrate were almost completely neutralized with most of the data above the 1:1 line. A few scattered

data below the 1:1 line may be caused by uncertainties in measurements. Little different was found between the regression slopes of  $\text{NH}_4^+$  with the sum of  $\text{SO}_4^{2-}$  and  $\text{NO}_3^-$  and the sum of  $\text{SO}_4^{2-}$ ,  $\text{NO}_3^-$  and  $\text{Cl}^-$  due to the very low amount of  $\text{NH}_4\text{Cl}$ . In this study, the level of  $\text{NH}_3$  was high enough to neutralize both  $\text{SO}_4^{2-}$  and  $\text{NO}_3^-$ , and likely to be form  $(\text{NH}_4)_2\text{SO}_4$  and  $\text{NH}_4\text{NO}_3$ . In addition to these substances, it is likely that  $\text{NH}_3$  also reacted with oxalic acid and other dicarboxylic acid to form ammonium oxalate and other organic ammonium aerosols, as discussed above."

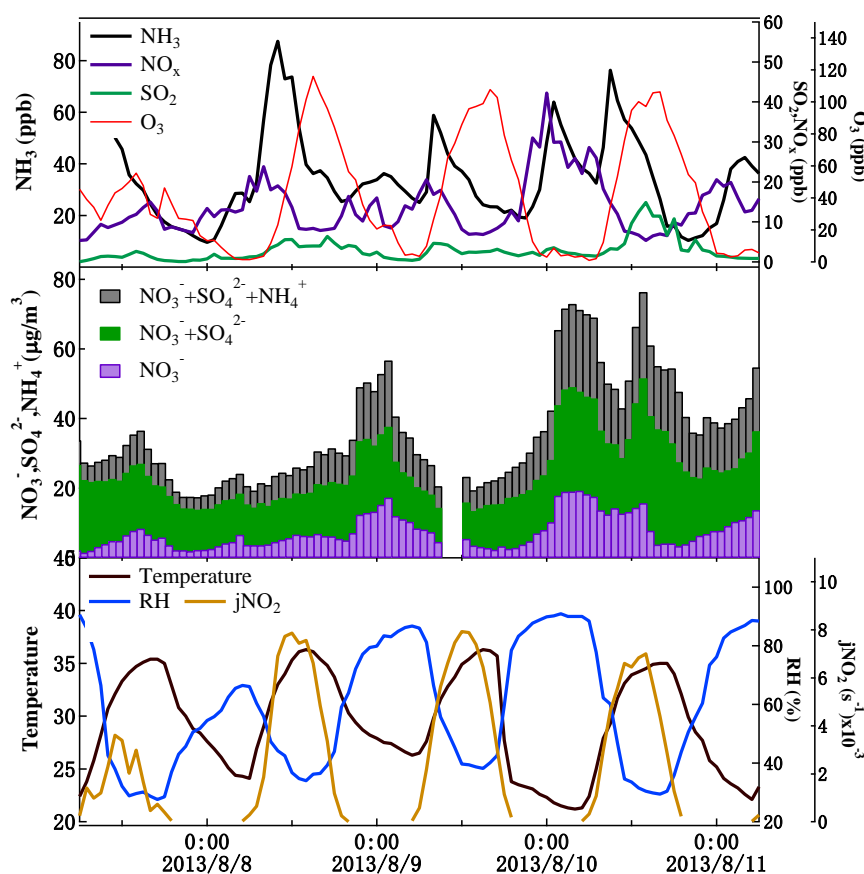


Figure 9. Hourly concentrations of precursor gas and ionic species measured in the pollution episode (a) temporal variations and (b) correlations of  $[\text{NH}_4^+]$  versus  $[\text{SO}_4^{2-}]$ ,  $[\text{SO}_4^{2-}] + [\text{NO}_3^-]$  and  $[\text{SO}_4^{2-}] + [\text{NO}_3^-] + [\text{Cl}^-]$  during 7 –11 August 2013.

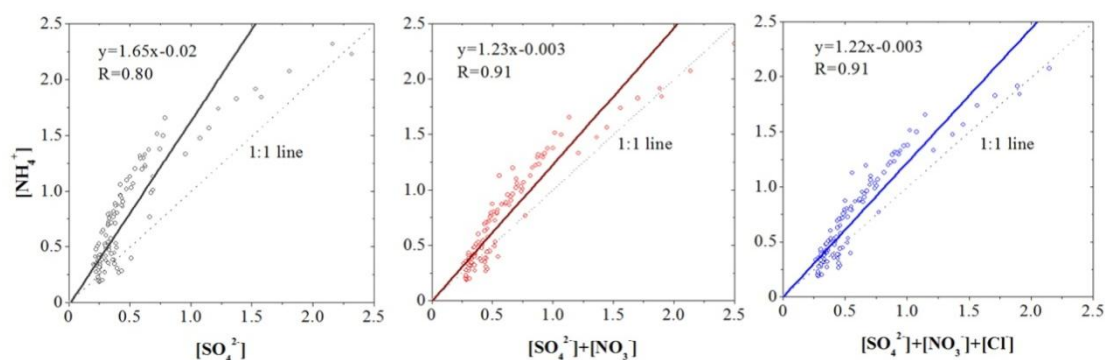


Figure 10. Correlations between  $[\text{NH}_4^+]$  and  $[\text{SO}_4^{2-}]$  (left),  $[\text{NH}_4^+]$  and  $[\text{SO}_4^{2-}]+[\text{NO}_3^-]$  (middle) and  $[\text{NH}_4^+]$  and  $[\text{SO}_4^{2-}]+[\text{NO}_3^-]+[\text{Cl}^-]$  (right) during 7-11 August 2013.

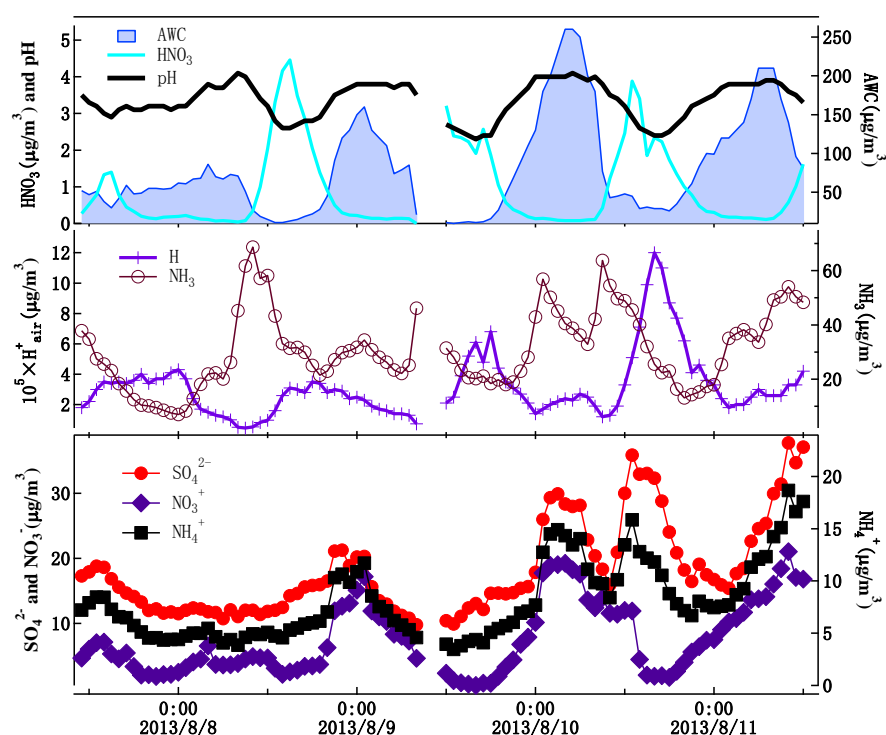


Figure S6. Time series of predicted fine particle pH, predicted particle water mass, predicted  $\text{H}_{\text{air}}^+$  and measured  $\text{NH}_3$  and measured inorganic ions during 7-11 August 2013

### Specific comments

**Page 1, line 29:** please define “transport of air mass from the North China Plain region”, as the site itself is in the middle of NCP.

**Answer:** Yes, the site is located in the middle of NCP. The concentrations of pollutant levels at Gucheng site are not only driven by local sources but also affected by long range transport. We have changed the title of Section 3.5 to "Long range transport and local source of ammonia and ammonium" and revised the text as follows:

"Dependence of the concentrations of  $\text{NH}_3$  on wind direction at Gucheng is studied to get insight into the distribution of local emission sources around the monitoring site. As shown in Fig. 11, during



the sampling period, the prevailing surface winds at Gucheng were northeasterly and southwesterly. High  $\text{NH}_3$  originated from the southwest sector of the measurement site, which may be due to a local unidentified agricultural or industrial source or transport from the Xushui township, which is approximately 15 km away from Gucheng. Lower  $\text{NH}_3$  concentrations were observed under winds from other sectors. Since  $\text{NH}_3$  is either readily converted to  $\text{NH}_4^+$  or subjected to dry deposition, high concentrations are found only close to the surface and near the emission sources. Previous studies have reported an inverse relationship between ground-level concentrations of trace gases, such as ammonia, and wind speed (Robarge et al., 2002; Lin et al., 2011). Thus,  $\text{NH}_3$  concentrations might be generally lower at higher wind speeds because of turbulent diffusion.

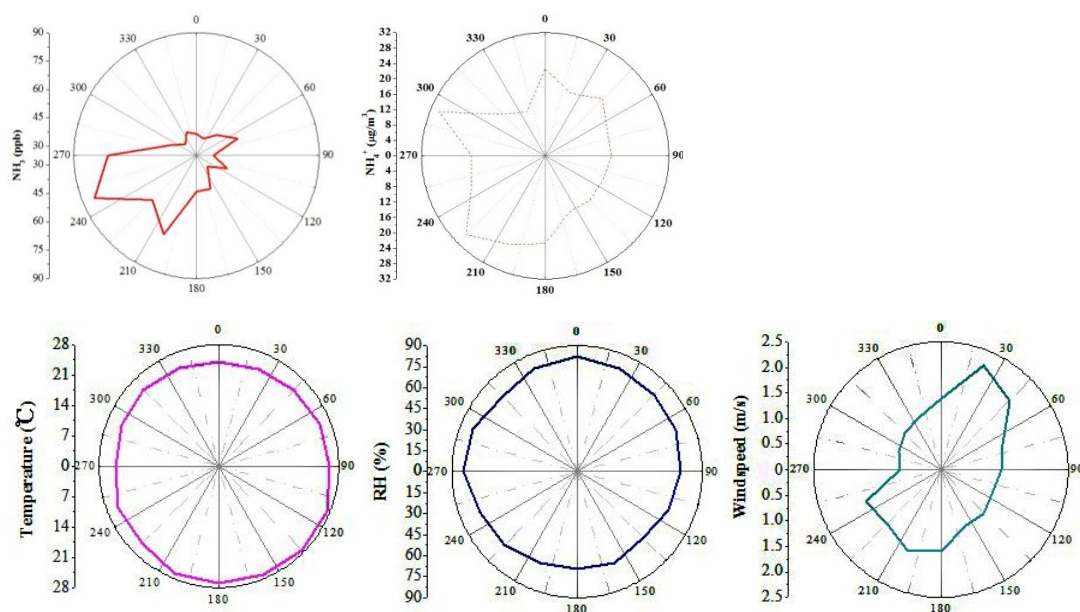


Figure 11. The average  $\text{NH}_3$ ,  $\text{NH}_4^+$  concentrations and meteorological data roses in different wind sectors during summer 2013.”

Lin, W., Xu, X., Ge, B., and Liu, X.: Gaseous pollutants in Beijing urban area during the heating period 2007-2008: variability, sources, meteorological and chemical impacts, *Atmos. Chem. Phys.*, 11, 8157-8170, 2011.

Robarge, W. P., Walker, J. T., McCulloch, R. B., and Murray, G.: Atmospheric concentrations of ammonia and ammonium at an agricultural site in the southeast United States, *Atmos. Environ.*, 36, 16611-1674, 2002.

**Page 3, line 22: how large is the “surrounding area” that impacts the measurements of this site?**

**Answer:** The site is situated in the middle of a large agricultural region with many villages. The information of Gucheng site in details can be found in Lin et al. (2009). According to the maps from Lin et al. (2009) shown below, the Gucheng site is surrounded by farms, dense villages/towns, and the transportation network in the NCP. The accurate size of the surrounding area that really impacts the measurements at Gucheng is not easy to define and varies with meteorological condition, particularly

wind speed. One can do footprint analysis by setting criteria, but this is out of the scope of this paper.

D00G14

LIN ET AL.: GASEOUS POLLUTANTS AT GUCHENG

D00G14

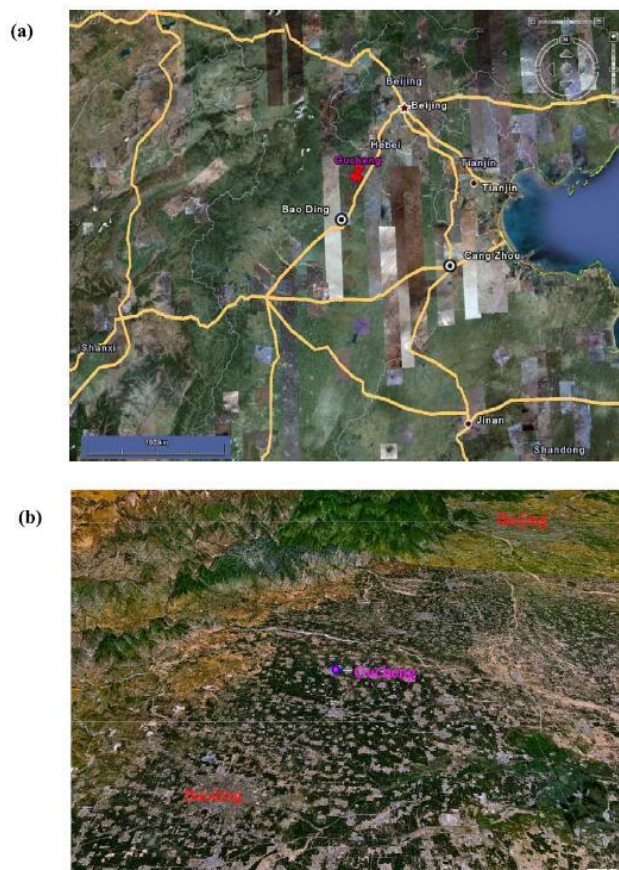


Figure 1. Location of Gucheng site and the topography of the surrounding region (a) from Google Earth imagery (copyright Google Inc., used with permission) and (b) from NASA satellite map (Community Landsat-7 visible color; <http://worldwind.arc.nasa.gov>).

## Section 2.2: what's the response time of the Los Gatos instrument? What is the concentration and accuracy of the calibration gas?

**Answer:** We have added information revised the related text as follows:

"Ambient  $\text{NH}_3$  was measured using an ammonia analyzer (DLT-100, Los Gatos Research, USA), which utilize a unique laser absorption technology called Off-Axis Integrated Cavity Output Spectroscopy (OA-ICOS). The analyzer has a precision of 0.2 ppb at 100 sec average and a maximum drift of 0.2 ppb over 24 hrs. The response time of the analyzer is less than 2 s (with optional external N920 vacuum pump). During the campaign,  $\text{NH}_3$  data were recorded as 100-s average. In principle, the  $\text{NH}_3$  analyzer does not need external calibration, because the measured fractional absorption of light at an ammonia resonant wavelength is an absolute measurement of the ammonia density in the cell (Manual of Economical Ammonia Analyzer - Benchtop Model 908-0016, Los Gatos Research). However, we confirmed the good performance of the  $\text{NH}_3$  analyzer using a reference gas mixture  $\text{NH}_3/\text{N}_2$  (Scottgas, USA) traceable to US National Institute for Standards and Technology (NIST). The reference gas of  $\text{NH}_3$  (25.92 ppm with an accuracy of  $\pm 2\%$ ) was diluted to different concentrations using zero air and supplied to the analyzer and a sequence with 5 points of different  $\text{NH}_3$  concentrations (including zero) were repeated for several times to check the performance of the analyzer. As shown in Fig. S1, the analyzer followed rapidly to changes of the  $\text{NH}_3$  concentration,

produced stable response under stabilized  $\text{NH}_3$  concentrations, and repeated accurately (within the uncertainty) the supplied  $\text{NH}_3$  concentrations. The  $\text{NH}_3$  analyzer contains an internal inlet aerosol filter, which was cleaned before our campaign. Nevertheless, some very fine particles can deposit on the mirrors of the ICOS cell, leading to gradual decline in reflectivity. However, slight mirror contamination does not cause errors in  $\text{NH}_3$  measurements because the mirror reflectivity is continually monitored and the measurement is compensated using the mirror ringdown time. Interferences to  $\text{NH}_3$  measurements can be from the sample inlets, for example, due to water condensation or adsorption/desorption effects (e.g., Schwab, 2008; Norman et al., 2009). Such interferences were not quantified but reduced as possibly as we could. PTFE tubing (4.8 mm ID), which is one of the well suited materials for  $\text{NH}_3$  measurement (Norman et al., 2009), was used to induced ambient air. The length of the tubing was kept as short as possible (about 5 m) to limit the residue time to less than 3 s. The aerosol filter at the inlet was changed every two weeks. Water condensation was avoided. Nevertheless, we cannot exclude the influence from the adsorption and desorption, which can also occur on dry surfaces. However, this influence should be small at our site, where the  $\text{NH}_3$  concentration is very high, and cause mainly a lag in the recorded  $\text{NH}_3$  concentration. "

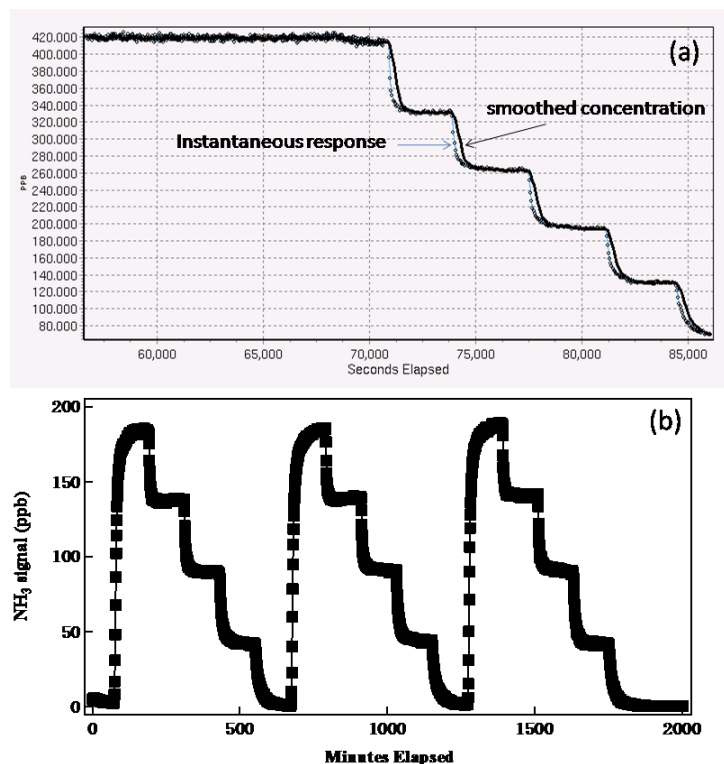


Figure S1 Confirmation of the performance of  $\text{NH}_3$  analyzer using diluted standard gas (mixture  $\text{NH}_3/\text{N}_2$ ). (a) Instrument response to changed  $\text{NH}_3$  concentration and stability; (b) repeated multipoint calibrations.

Norman, M., Spirig, C., Wolff, V., Trebs, I., Flechard, C., Wisthaler, A., Schnitzhofer, R., Hansel, A., and Neftel, A.: Intercomparison of ammonia measurement techniques at an intensively managed grassland site (Oensingen, Switzerland), *Atmos. Chem. Phys.*, 9, 2635–2645, 2009.

Schwab, J.J.: Ambient Gaseous Ammonia: Evaluation of Continuous Measurement Methods Suitable for Routine Deployment, Final Report Prepared for the New York State Energy Research and

Development Authority (NYSERDA), Final Report 08-15, New York, October 2008.

**Page 6, line 3: please define “human activity” as it seems a very broad concept.**

**Answer:** We have changed "human activity" to "human excrement and waste disposal".

**Page 6, line 5: there is no “Zhng et al., 2010” in the reference list.**

**Answer:** This was one of the typos. We have corrected it to “Zhang et al., 2010”.

**Page 6, line 8-9: please clarify how can these results “be used in improving NH<sub>3</sub> emission inventory and making future emission control policies”.**

**Answer:** We have revised our expression as follows:

"In recent year a few publications about China's national and regional emission inventories of NH<sub>3</sub> (e.g., Zhou et al., 2015; Xu et al., 2015, 2016; Kang et al., 2016). However, these inventories are based on bottom-up studies, subject to substantial uncertainties in spatial and temporal variations of NH<sub>3</sub> emissions. Ground based observations of NH<sub>3</sub> have been sparse. Our measurements, together with others, can be used for validating and constraining models that use bottom-up inventories, and hence help to reveal potential bias in NH<sub>3</sub> emission inventory."

Kang, K., Liu, M., Song, Y., Huang, X., Yao, H., Cai, X., Zhang, H., Kang, L., Liu, X., Yan, X., He, H., Zhang, Q., Shao, M., and Zhu, T.: High-resolution ammonia emissions inventories in China from 1980 to 2012, *Atmos. Chem. Phys.*, 16, 2043–2058, 2016.

Xu, P., Zhang, Y., Gong, W., Hou, X., Kroeze, C., Gao, W., and Luan, S.: An inventory of the emission of ammonia from agricultural fertilizer application in China for 2010 and its high-resolution spatial distribution, *Atmos. Environ.*, 115, 141-148, 2015.

Xu, P., Liao, Y. J., Lin, Y. H., Zhao, C. X., Yan, C. H., Cao, M. N., Wang, G. S., and Luan, S. J.: High-resolution inventory of ammonia emissions from agricultural fertilizer in China from 1978 to 2008, *Atmos. Chem. Phys.*, 16, 1207–1218, 2016.

Zhou, Y., Cheng, S., Lang, J., Chen, D., Zhao, B., Liu, C., Xu, R., and Li, T.: A comprehensive ammonia emission inventory with high-resolution and its evaluation in the Beijing-Tianjin-Hebei (BTH) region, China, *Atmos. Environ.*, 106, 305-317, 2015.

**Figure 2: I understand ammonia is shown in log scale because its concentration spanned three orders of magnitude. However I suggest add a sub plot with linear scale so that the variability is comparable at different concentration levels and the individual spikes from pollution episodes are clearer.**

**Answer:** Thank you for your suggestion. We have redrawn Figure 2 as shown below:

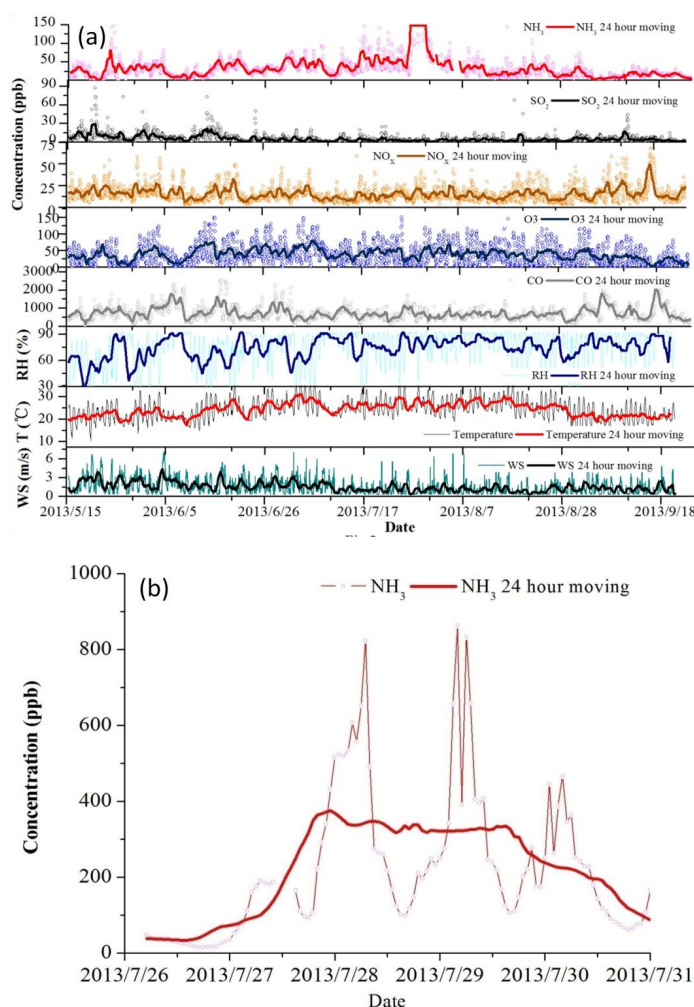


Figure 2. Time series of hourly data of NH<sub>3</sub>, other trace gases and meteorological parameters measured during the sampling period (a) and a blow-up of the period with extremely high NH<sub>3</sub> values during 27–31 July 2013.

**Page 7, line 6: where the urea was applied and how large was the applied area?**

**Answer:** We have added the required information and revised the text as follows:

"The Gucheng station has a farmland of 8.67 hectares. The observation period was in the time of the wheat harvest and corn seeding and growing. Corn was sown and fertilized with about 600 kg of fertilizer per hectare in late June. On 20 July corn was additionally fertilized with 225 to 300 kg of urea per hectare. After this fertilization, there was a raining period. The NH<sub>3</sub> concentration increased rapidly on the seventh day after the urea application on 20 July, peaking during the 27–30 July period (Fig. 2b)."

**Page 7, line 29: what are these "trace gases"?**

**Answer:** We have added "such as NO<sub>x</sub> and CO" at the end of "trace gases" to in our revised version.

**Page 8, lines 14-15 and page 8, lines 30: these two sentences seem contradict each other.**



**Answer:** We have deleted the paragraph there.

**Page 10, line 1: higher NO<sub>3</sub> level than what?**

**Answer:** We have deleted this sentence and changed the sentence before to " On the other hand, NH<sub>3</sub> was more efficient in summer to react with SO<sub>2</sub> to form (NH<sub>4</sub>)<sub>2</sub>SO<sub>4</sub>. The average concentration of NO<sub>3</sub><sup>-</sup> in PM<sub>2.5</sub> was 11.3 ± 9.1 μg m<sup>-3</sup>. The highest value of 109.3 μg m<sup>-3</sup> was observed at 14:00 on 22 June 2013 at the highest RH (93%) and AWC (910 μg m<sup>-3</sup>)".

**Page 10, line 20-25: I suggest add a figure showing the slope and correlations. The SO<sub>4</sub> should be normalized with its number of charge. What is the evidence for the existence of NH<sub>4</sub>HSO<sub>4</sub>?**

**Answer:** We have added a figure to show the correlations as you suggested and revised the text accordingly.

" During 7-11 August 2013, the relationships of the observed NH<sub>4</sub><sup>+</sup> versus those of SO<sub>4</sub><sup>2-</sup>, the sum of SO<sub>4</sub><sup>2-</sup> and NO<sub>3</sub><sup>-</sup> and the sum of SO<sub>4</sub><sup>2-</sup>, NO<sub>3</sub><sup>-</sup> and Cl<sup>-</sup> are presented in Fig. 10. It is known that (NH<sub>4</sub>)<sub>2</sub>SO<sub>4</sub> is preferentially formed and the least volatile, NH<sub>4</sub>NO<sub>3</sub> is relatively volatile, while NH<sub>4</sub>Cl is the most volatile. NH<sub>4</sub><sup>+</sup> is thought to be first associated with SO<sub>4</sub><sup>2-</sup>, afterwards, the excess of NH<sub>4</sub><sup>+</sup> is with nitrate and chloride (Meng et al., 2015). It is noted that the correlation of NH<sub>4</sub><sup>+</sup> with the sum of SO<sub>4</sub><sup>2-</sup> and NO<sub>3</sub><sup>-</sup> (R=0.91, slope=1.23, with P < 0.01) was better than that of NH<sub>4</sub><sup>+</sup> with SO<sub>4</sub><sup>2-</sup> (R=0.80, slope=1.65, with P < 0.01), suggesting that both SO<sub>4</sub><sup>2-</sup> and NO<sub>3</sub><sup>-</sup> were associated with NH<sub>4</sub><sup>+</sup>. As shown in Fig.10, sulfate and nitrate were almost completely neutralized with most of the data above the 1:1 line. A few scattered data below the 1:1 line may be caused by uncertainties in measurements. Little different was found between the regression slopes of NH<sub>4</sub><sup>+</sup> with the sum of SO<sub>4</sub><sup>2-</sup> and NO<sub>3</sub><sup>-</sup> and the sum of SO<sub>4</sub><sup>2-</sup>, NO<sub>3</sub><sup>-</sup> and Cl<sup>-</sup> due to the very low amount of NH<sub>4</sub>Cl. In this study, the level of NH<sub>3</sub> was high enough to neutralize both SO<sub>4</sub><sup>2-</sup> and NO<sub>3</sub><sup>-</sup>, and likely to be form (NH<sub>4</sub>)<sub>2</sub>SO<sub>4</sub> and NH<sub>4</sub>NO<sub>3</sub>. In addition to these substances, it is likely that NH<sub>3</sub> also reacted with oxalic acid and other dicarboxylic acid to form ammonium oxalate and other organic ammonium aerosols, as discussed above."

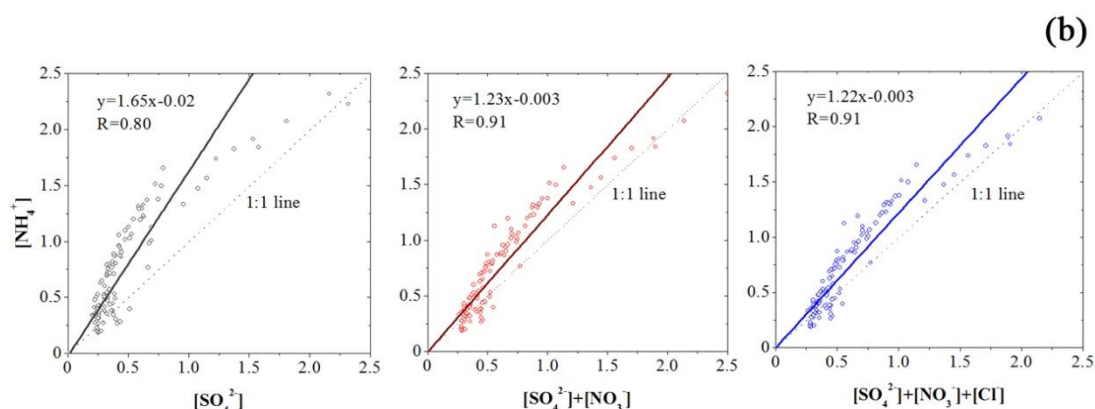


Figure 10. Correlations between  $[NH_4^+]$  and  $[SO_4^{2-}]$  (a),  $[NH_4^+]$  and  $[SO_4^{2-}] + [NO_3^-]$  (b) and  $[NH_4^+]$  and  $[SO_4^{2-}] + [NO_3^-] + [Cl^-]$  (c) during 7-11 August 2013.

Meng, Z. Y., Xie, Y. L., Jia, S. H., Zhang, R., Lin, W. L., Xu, X. B., and Yang W.: The characteristics of atmospheric ammonia at Gucheng, a Rural Site in the North China Plain in summer 2013, J.

applied. meteor. sci., 26, 141-150, 2015. (in Chinese).

**Page 11, line 17: again, it is better to have more evidences showing that NH<sub>3</sub> dry deposition dominates NH<sub>x</sub> deposition.**

**Answer:** This is a speculation. No evidence is available. We have deleted this paragraph.

**Page 12, line 2: where is the reference Meng et al. 2017?**

**Answer:** We have added the reference.

Meng, Z. Y., Lin, W. L., Zhang, R. J., Han, Z. W. and Jiang, X. F.: Summertime ambient ammonia and its effects on ammonium aerosol in urban Beijing, China, Sci. Total Environ., 579, 1521-1530, 2017.

# Role of ambient ammonia in particulate ammonium formation at a rural site in the North China Plain

Zhaoyang Meng<sup>1</sup>, Xiaobin Xu<sup>1</sup>, Weili Lin<sup>2</sup>, [Baozhu Ge](#)<sup>3</sup>, Yulin ~~Xie~~<sup>3</sup>[Xie](#)<sup>4,5</sup>, Bo ~~Song~~<sup>3</sup>[Song](#)<sup>4</sup>, Shihui Jia<sup>1,56</sup>, Rui ~~Zhang~~<sup>6</sup>[Zhang](#)<sup>7,78</sup>, Wei Peng<sup>1</sup>, Ying Wang<sup>1</sup>, Hongbin Cheng<sup>1</sup>, Wen ~~Yang~~<sup>5</sup>[Yang](#)<sup>7</sup>, Huarong Zhao<sup>1</sup>

<sup>1</sup> State Key Laboratory of Severe Weather & Key Laboratory for Atmospheric Chemistry of CMA, Chinese Academy of Meteorological Sciences, Beijing 100081, China

<sup>2</sup> CMA Meteorological Observation Centre, Beijing 100081, China

<sup>3</sup> [State Key Laboratory of Atmospheric Boundary Layer Physics and Atmospheric Chemistry, Institute of Atmospheric Physics, Chinese Academy of Sciences, Beijing 100029, China](#)

<sup>3,4</sup> [University of Science and Technology Beijing, Beijing 100083, China](#)

<sup>4,5</sup> [Baotou Steel Group Mining Research Institute, Baotou 014010, China](#)

<sup>5,6</sup> [South China University of Technology, Guangzhou 510641, China](#)

<sup>6,7</sup> [Chinese Research Academy of Environmental Sciences, Beijing 100012, China](#)

<sup>7,8</sup> [Beijing Municipal Research Institute of Environmental Protection, Beijing 100037, China](#)

Correspondence to: Zhaoyang Meng (mengzy@cma.cma.cn)

**Abstract.** The real-time measurements of NH<sub>3</sub> and trace gases were conducted, in conjunction with semi-continuous measurements of water-soluble ions in PM<sub>2.5</sub> at a rural site in the North China Plain (NCP) from May to September 2013 in order to better understand of chemical characteristics for ammonia, and of the impact on formation of secondary ammonium aerosols in the NCP. Extremely high NH<sub>3</sub> and NH<sub>4</sub><sup>+</sup> concentrations were observed after a precipitation event within 7-10 days following urea application. Elevated NH<sub>3</sub> levels coincided with elevated NH<sub>4</sub><sup>+</sup>, ~~suggesting indicating~~ that NH<sub>3</sub> ~~plays a vital role~~ likely influenced in enhancing particulate ammonium mass. For the sampling period, the average oxidation/conversion ratios for SO<sub>4</sub><sup>2-</sup> (SOR), NO<sub>3</sub><sup>-</sup> (NOR) and NH<sub>4</sub><sup>+</sup> (NHR) were estimated to be 0.64%, 0.24% and 0.30%, respectively. The increased NH<sub>3</sub> concentrations mainly from agricultural activities and regional transport, coincided with the prevailing meteorological conditions ~~could promote the secondary transformation, resulting in higher hourly SOR, NOR and~~ The high NH<sub>3</sub> level and lower NHR indicate that the emission of NH<sub>3</sub> in the NCP is much higher than needed for aerosol acids neutralization. Our observation and modelling results indicate that strong acids in aerosol are completely neutralized. Additional NH<sub>4</sub><sup>+</sup> exists in aerosol, probably a result of presence of substantial amount of oxalic and other diacids. The concentrations of NH<sub>3</sub>, NH<sub>4</sub><sup>+</sup>, and NHR had clear diurnal



~~variations, which could be attributed to their sources, meteorological conditions, and formation mechanisms. There is no evidence in our measurements of aerosol formation driven by NH<sub>3</sub>. Nevertheless, NH<sub>3</sub> plays an important role in the formation of secondary aerosols as a key neutralizer. The back trajectory analysis indicates that the transport of air masses from the North China Plain region contributed to the atmospheric NH<sub>3</sub> variations, and both regional sources and long distance transport from southeast played important roles in the observed ammonium aerosol at rural site in the NCP. The findings of this study are expected to facilitate developing future NH<sub>3</sub> emission control policies for the North China Plain.~~

**Keywords:** Ambient ammonia; ammonium in PM<sub>2.5</sub>; the conversion ratio of NH<sub>4</sub><sup>+</sup>; [thermodynamic equilibrium](#); agricultural activity; North China Plain.

## 1 Introduction

Ammonia (NH<sub>3</sub>) is a very important alkaline constituent in the atmosphere, plays an important role in atmospheric chemistry and is closely related to ecosystems. NH<sub>3</sub> has both direct and indirect impacts on critical environmental issues, including regional fine particles, acid rain, and eutrophication (Roelle and Aneja, 2002; Krupa, 2003; Reche et al., 2012). In addition, NH<sub>3</sub> is a key species for neutralising H<sub>2</sub>SO<sub>4</sub> and HNO<sub>3</sub> in the atmosphere and forming (NH<sub>4</sub>)<sub>2</sub>SO<sub>4</sub>, NH<sub>4</sub>HSO<sub>4</sub>, and NH<sub>4</sub>NO<sub>3</sub> (Erisman and Schaap, 2004; Walker et al., 2004), which are major [inorganic](#) components of fine particulate matters and contribute to regional haze (Ye et al., 2011; Meng et al., 2014; Wei et al., 2015). Global ammonia emission has more than doubled since pre-industrial times, mainly because of agricultural intensification (Galloway et al., 2015). The total ammonia emission in China in 2006 was estimated to be 16.07 million tons (Mt) (Dong et al., 2015). Such high emission makes NH<sub>3</sub> one of the key species related to atmospheric environmental problems. ~~Many~~ [Some](#) studies have indicated that [reducing NH<sub>3</sub> concentrations could be an effective method for alleviating secondary inorganic PM<sub>2.5</sub> pollution in China](#) ~~ammonia is a crucial precursor in the formation of fine particles~~ (Cao et al., 2009; ~~Wu et al., 2009; Meng et al., 2011; Shen et al., 2011;~~ Park et al., 2014; Wang et al., 2015; [Xu et al., 2017](#)).

As global food production requirements increase, agriculture plays an increasingly important role in local, regional, and global air quality (Walker et al., 2006). The North China Plain (NCP) is a highly

populated region with intensive agricultural production as well as heavy industry. The region has been affected by severe haze and photochemical pollution in recent years (Guo et al., 2010; Wang et al., 2010; Luo et al., 2013). Covering only 3.3% of the national area, the NCP region provides 40% and 25% of China's wheat and corn production. To sustain such high agricultural productivity, chemical fertilisers have been intensively applied. Less than 30% efficiency in N application causes approximately 40% N loss through various routes including the leaching of  $\text{NO}_3^-$  and emission of  $\text{NH}_3$ ,  $\text{N}_2\text{O}$ , and  $\text{N}_2$  (Zhang et al., 2010). So far, only a few limited studies have paid attentions to impacts of  $\text{NH}_3$  on air pollution in the NCP region. According to some studies (Dong et al., 2010; Ianniello et al., 2010; Meng et al., 2011; Shen et al., 2011; Meng et al., 2015), the high  $\text{NH}_3$  emission intensities observed in the NCP have been caused by high fertiliser application rates and numerous intensive livestock farms. However there were few simultaneous high time resolution measurements of  $\text{NH}_3$  and  $\text{NH}_4^+$  in  $\text{PM}_{2.5}$ , and investigating the role in fine particulate formation in China. These studies are necessary to improve our understanding of ammonia pollution on regional air quality, and of the impact on formation of secondary ammonium aerosols in the NCP.

During May–September 2013, the intensive field measurements of  $\text{NH}_3$  and other trace gases, water-soluble ions in  $\text{PM}_{2.5}$ , and meteorological parameters took place at a rural site in the NCP. In this article, we report the results on  $\text{NH}_3$ , trace gases and major water-soluble ions in  $\text{PM}_{2.5}$ . We discuss temporal variations and diurnal patterns of  $\text{NH}_3$  and  $\text{NH}_4^+$ , ~~and examine their sources and chemical conversion mechanism.~~ In this study, we also show results from thermodynamic equilibrium simulations and compared them with observations predicted fine particle acidity during pollution episodes in summer 2013 by using hourly measured particulate water soluble ions and precursor gases. Our results would provide insight into secondary aerosol formation associated with aerosol acidity.

## 2 Description of Experiment

### 2.1 Measurement site

The measurements were performed from May to September 2013 at Gucheng (39°08'N, 115°40'E, 15.2 m a.s.l.), a rural site in the NCP, which is an Integrated Ecological Meteorological Observation and Experiment Station of the Chinese Academy of Meteorological Sciences. In Fig. 1, the location of the site is shown on the NCP map with the  $\text{NH}_3$  emission distribution for the year 2012 from the multi-resolution emission inventory of China (<http://meicmodel.org/index.html>). The measurement

site chosen is situated for monitoring regional background concentrations of air pollutants in the North China Plain, has good regional representativeness (Lin et al., 2009). The site is approximately 110 km southwest of Beijing, 130 km west of Tianjin, and 160 km northeast of Shijiazhuang City in Hebei Province. The site is surrounded by farms, dense villages/towns, and the transportation networks s in the NCP. The main crops in the area surrounding the site are wheat (winter and spring) and corn (summer and fall). The site is influenced by high  $\text{NH}_3$  emissions from fertiliser use and animal husbandry in the surrounding area. Being in the warm temperate zone, the site has a typical temperate continental monsoon climate. Precipitation occurs mainly between May to August.

## 2.2 Sampling and analysis

Ambient  $\text{NH}_3$  was measured using an ammonia analyser (DLT-100, Los Gatos Research, USA), which utilize a unique laser absorption technology called Off-Axis Integrated Cavity Output Spectroscopy (OA-ICOS). The analyzer has a precision of 0.2 ppb at 100 sec average and a maximum drift of 0.2 ppb over 24 hrs. The response time of the analyzer is less than 2 s (with optional external N920 vacuum pump). During the campaign,  $\text{NH}_3$  data were recorded as 50100-s average. A set of commercial instruments from Thermo Environmental Instruments, Inc. was used to measure  $\text{O}_3$  (TE 49C),  $\text{NO}/\text{NO}_2/\text{NO}_x$  (TE 42CTL),  $\text{CO}$  (TE 48C), and  $\text{SO}_2$  (TE 43CTL). All instruments were housed in an air-conditioned room in the observation building at the Gucheng site. Two parallel inlet tubes (Teflon, 4.8 mm ID×8 m length) were shared by the analyzers. The height of the inlets was 1.8 m above the roof of the building and about 8m above the ground. The inlet residence time was estimated to be less than 5 s.

In principle, the  $\text{NH}_3$  analyzer does not need external calibration, because the measured fractional absorption of light at an ammonia resonant wavelength is an absolute measurement of the ammonia density in the cell (Manual of Economical Ammonia Analyzer - Benchtop Model 908-0016, Los Gatos Research). However, we confirmed the good performance of calibrated the  $\text{NH}_3$  analyzer using a reference gas mixture  $\text{NH}_3/\text{N}_2$  (Scottgas, USA) traceable to US National Institute for Standards and Technology (NIST). The reference gas of  $\text{NH}_3$  (25.92 ppm with an accuracy of  $\pm 2\%$ ) was diluted to different concentrations using zero air and supplied to the analyzer. During calibration, and a sequence with 5 points of different  $\text{NH}_3$  concentrations (including zero) were repeated for several times overnight to check the performance of the analyzer. As shown in Fig. S1, the analyzer followed rapidly to changes of the  $\text{NH}_3$  concentration, produced stable response under stabilized  $\text{NH}_3$

concentrations, and repeated accurately (within the uncertainty) the supplied  $\text{NH}_3$  concentrations. Because of its absorbability, the duration time of each point was set to 3 hr for a fully stabilizations. The  $\text{NH}_3$  analyzer contains an internal inlet aerosol filter, which was cleaned before our campaign. Nevertheless, some very fine particles can deposit on the mirrors of the ICOS cell, leading to gradual decline in reflectivity. However, slight mirror contamination does not cause errors in  $\text{NH}_3$  measurements because the mirror reflectivity is continually monitored and the measurement is compensated using the mirror ringdown time. Interferences to  $\text{NH}_3$  measurements can be from the sample inlets, for example, due to water condensation or adsorption/desorption effects (e.g., Schwab, 2008; Norman et al., 2009). Such interferences ~~to~~ were not quantified but reduced as possibly as we could. PTFE tubing (4.8 mm ID), which is one of the well suited materials for  $\text{NH}_3$  measurement (Norman et al., 2009), was used to induced ambient air. The length of the tubing was kept as short as possible (about 5 m) to limit the residue time to less than 3 s. The aerosol filter at the inlet was changed every two weeks. Water condensation was avoided. Nevertheless, we cannot exclude the influence from the adsorption and desorption, which can also occur on dry surfaces. However, this influence should be small at our site, where the  $\text{NH}_3$  concentration is very high, and cause mainly a lag in the recorded  $\text{NH}_3$  concentration.

A set of commercial instruments from Thermo Environmental Instruments, Inc. were used to measure  $\text{O}_3$  (TE 49C),  $\text{NO}/\text{NO}_2/\text{NO}_x$  (TE 42CTL), CO (TE 48C), and  $\text{SO}_2$  (TE 43CTL). All instruments were housed in an air-conditioned room in the observation building at the site. Two parallel inlet tubes (Teflon, 4.8 mm ID×8 m length) were shared by the analyzers. The height of the inlets was 1.8 m above the roof of the building and about 8m above the ground. The inlet residence time was estimated to be less than 5 s (Lin et al., 2009). Zero and span checks ~~of other trace gases~~ were performed weekly on the analyzers of these trace gases to identify possible analyser malfunctions and zero drifts. Multipoint calibrations of  $\text{SO}_2$ ,  $\text{NO}_x$ , CO and  $\text{O}_3$  analysers were performed on the instruments at approximately 1-month intervals. Measurement records were saved as 1-min averages After the correction of data on the basis of the multipoint calibrations, hourly average data were calculated and used for the analysis.

An Ambient Ion Monitor (AIM) (URG 9000D Series, USA) was deployed at the site to measure

hourly concentrations of water-soluble inorganic components in PM<sub>2.5</sub> during 15 June–11 August, 2013.

A detailed description of performance evaluation of AIM-IC system is reported by Han et al., (2016). Briefly, ambient air was introduced in to the AIM with a 2 meter Teflon coated aluminum pipe and particles larger than 2.5  $\mu\text{m}$  were removed by a cyclone at a flow rate of 3 L/min. A liquid diffusion denuder was used to remove the interfering acidic and basic gases, in combination with a Steam-Jet Aerosol Collector followed by an Aerosol Sample Collector, until the particles can be injected into the Ion Chromatograph (Hu et al., 2014). The detection limit of  $\text{NH}_4^+$ ,  $\text{SO}_4^{2-}$  and  $\text{NO}_3^-$  were  $0.05 \mu\text{g m}^{-3}$ ,  $0.04 \mu\text{g m}^{-3}$  and  $0.05 \mu\text{g m}^{-3}$ , respectively. The AIM is  $0.1 \mu\text{g m}^{-3}$  for various ionic components. For the AIM, multipoint calibrations were performed weekly by using calibration standard solutions. Acceptable linearity of ions was obtained with an  $R^2$  of  $\geq 0.999$ . The flow rate of the AIM was checked weekly at the sample inlet with a certified flow meter. The flow rate of the AIM was maintained at  $3 \text{ L min}^{-1}$  and checked weekly at the sample inlet. The flow rate of the AIM was kept at  $3 \text{ L/min}$  with standard derivation of  $<1\%$ . Hourly data were obtained for the concentrations of water-soluble inorganic ions in summer 2013.

Meteorological parameters were measured at the site. Air temperature, and relative humidity were monitored using a humidity and temperature probe (HMP155, Vaisala, Finland); wind speed and direction were measured using an anemometer (ZQZ-TFD12, Jiangsu Radio Scientific Institute Co., Ltd, China); rainfall was measured using a tilting rain gauge (SL2-1, Tianjin Meteorological Instrument Factory, China). Global radiation observation was made at the site but showed a drift by the end of July, 2013. Instead we use the photolysis rate  $j\text{NO}_2$  observed using a 2-pi-actinic-flux spectrograph (CCD type, Meteorologie Consult GmbH, Germany) to indicate radiation condition for photochemistry. Hourly meteorological data were calculated from obtained from the site the in-situ measurements and used in this paper, with a resolution of 1 hour. Planetary boundary layer height at 14:00– values at 14:00 were derived from the ERA-Interim data using the Bulk Ricardson number method (Guo et al., 2016; Miao et al., 2017).

## 2.3 Data analysis

### 2.3.1 Chemical conversions of species

Sulfate and nitrate oxidation ratios (SOR and NOR) are defined as the molar ratio of  $\text{SO}_4^{2-}$  and  $\text{NO}_3^-$  in PM<sub>2.5</sub> to the total oxidized S and N, respectively (Zhang et al., 2011).

$$\text{SOR} = \frac{\text{SO}_4^{2-}}{\text{SO}_4^{2-} + \text{SO}_2} \quad (1)$$

$$\text{NOR} = \frac{\text{NO}_3^-}{\text{NO}_3^- + \text{NO}_x} \quad (2)$$

Similarly, the conversion ratio of ammonium (NHR) is expressed in terms of the ratio of ammonium to total ammonia ( $\text{NH}_x$ ), which could be a measure of the extent of transformation from  $\text{NH}_3$  to  $\text{NH}_4^+$  in areas with major local  $\text{NH}_3$  sources (Hu et al., 2014).

$$\text{NHR} = \frac{\text{NH}_4^+}{\text{NH}_4^+ + \text{NH}_3} \quad (3)$$

### 2.3.2 Thermodynamic equilibrium

Thermodynamic gas-aerosol equilibrium characteristics during summer 2013 were examined using ISORROPIA II model (Fountoukis and Nenes, 2007). ISORROPIA II is a thermodynamic equilibrium model for inorganic gases and aerosols in the atmosphere (available at [http://isorroopia.eas.gatech.edu/index.php?title=Main\\_Page](http://isorroopia.eas.gatech.edu/index.php?title=Main_Page)~~http://isorroopia.eas.gatech.edu~~). To obtain the best available predictions of aerosol pH, ISORROPIA II<sub>7</sub> was run in the forward mode with metastable aerosol state salts precipitate once the aqueous phase becomes saturated with respect to salts, which often showed better performance than the stable state solution (solid + liquid) and was commonly applied in previous pH predictions (Guo et al., 2015; Guo et al., 2015; Bougiatioti et al., 2016; Liu et al., 2017). The concentrations of the measured  $\text{NH}_3$  and water-soluble ions in  $\text{PM}_{2.5}$  were input into the model as total (gas + aerosol) concentrations, along with simultaneously measured relative humidity and temperature data. In this study, the aerosol properties as acidity and the water content of the aerosol are needed to investigate the aerosol acidity characteristics and role of heterogeneous chemistry in nitrate formation. The bulk particle pH of aerosol water was calculated using the following equation:

$$\text{pH} = -\log_{10} \frac{1000H_{\text{air}}^+}{\text{AWC}} \quad (4)$$

where  $H_{\text{air}}^+$  ( $\mu\text{g m}^{-3}$ ) is the ion concentration of equilibrium particle hydronium ion concentration per volume air and AWC ( $\mu\text{g m}^{-3}$ ) is the aerosol water content output from the ISORROPIA-II simulation. The evaluation of AWC prediction has been evaluated in previous studies and showed a good

performance compared with observed particle water-measurements (Bian et al., 2014; Guo et al., 2015).

### **2.3.2.3 Trajectory calculation**

The 72-h backward trajectories were calculated using the HYSPLIT 4.9 model (<http://www.arl.noaa.gov/ready/hysplit4.html>). The trajectories terminated ~~on at a~~ at the height of 100 m above the ground. The trajectory calculations were done for four times (00:00, 06:00, 12:00, and 18:00 UTC) per day in summer 2013. Individual ~~The various~~ back trajectories were grouped into five clusters. The number of clusters is identified according to the changes of total spatial variance (TSV). Five is chosen as the final number of clusters considering optimum separation of trajectories (larger number of clusters) and simplicity of display (lower number of cluster). The corresponding concentrations of trace gases and water soluble ions were averaged over the period of 3 h ahead and after the arrival time for each backward trajectory for further analysis.

## **3 Results and discussion**

### **3.1 Overview of concentration levels of measured species**

During 15 May–25 September 2013, the average concentrations (ranges) of NH<sub>3</sub>, SO<sub>2</sub> and NO<sub>x</sub> were 36.2 ~~±56.4~~ (0-862.9), 5.0 ~~±6.5~~ (0-86.8) and 15.4 ~~±9.3~~ (2.7-67.7) ppb, respectively. As listed in Table 1, the concentration of NH<sub>3</sub> at the NCP rural site was lower than those reported in Asian and Africa urban sites such as Lahore (Pakistan) (Biswas et al., 2009), Colonelganj (India) (Behera et al., 2010) and Cairo (Egypt) (Hassan et al., 2013), but higher than those from other areas in China, Europe and North American (Plessow et al., 2005; Yao et al., 2006; Lin et al., 2006; Walker et al., 2006; Hu et al., 2008; Meng et al., 2011; Shen et al., 2011; Schaap et al., 2011; Makkonen et al., 2012; Behera et al., 2013; Gong et al., 2013; Meng et al., 2014; Li et al., 2014). For example, the NH<sub>3</sub> at the NCP rural site was higher than those found at Shangdianzi regional background station in the NCP (Meng et al., 2011), Lin'an regional background station in the Yangtze River Delta (YRD) in Eastern China (Meng et al., 2014) and the rural site in Beijing (Shen et al., 2011). The relatively high concentrations of NH<sub>3</sub> observed in this study were attributed to agricultural activities involving fertiliser use, vegetation, and livestock, as well as human excrement and waste disposal ~~human activity~~ in the surrounding region.

According to an inventory study (Zhang et al., 2010), the total agricultural NH<sub>3</sub>-N emission in 2004 in the NCP was 3071 kt yr<sup>-1</sup>, accounting for 27% of the total emissions in China with the 1620 kt yr<sup>-1</sup> of

NH<sub>3</sub>-N emissions caused by fertiliser applications, which is the largest emission source accounting for more than half of the total agricultural emissions. [In recent year a few publications about China's national and regional emission inventories of NH<sub>3</sub> \(e.g., Zhou et al., 2015; Xu et al., 2015, 2016; Kang et al., 2016\). However, these inventories are based on bottom-up studies, subject to There are substantial uncertainties in spatial and temporal variations of NH<sub>3</sub> emissions. due to the scarcity of Ground based observations of NH<sub>3</sub> have been sparse. Our results—measurements, together with others, are expected to can be used for validating and constraining models that use bottom-up inventories, and hence help to reveal potential bias in improving NH<sub>3</sub> emission inventory—and making future emission control policies in the NCP.](#)

The observed concentration of SO<sub>2</sub> at the NCP rural site was markedly lower than those reported for the same period in 2006–2007 (Lin et al., 2009). Because of a series of emission reduction measures implemented in recent years, SO<sub>2</sub> levels have decreased markedly in the NCP (Lin et al., 2011). The average concentration of NO<sub>x</sub> was higher than those at Shangdianzi (Meng et al., 2011) and Lin'an (Meng et al., 2014) regional background stations in the NCP and YRD region of China, which might be due to emission from agricultural activities and motor vehicle sources (Liu et al., 2013; Lei and Wuebbles, 2013) in the NCP, but was lower than those at urban sites in India (Behera et al., 2010) and Egypt (Hassan et al., 2013).

The average concentrations of NH<sub>4</sub><sup>+</sup>, SO<sub>4</sub><sup>2-</sup>, and NO<sub>3</sub><sup>-</sup> in PM<sub>2.5</sub> were 19.8 ± 33.2, 20.5 ± 13.6 and 11.3 ± 9.1 μg m<sup>-3</sup>, respectively, at the NCP rural site during 15 June–11 August 2013. The average concentration of NH<sub>4</sub><sup>+</sup> in PM<sub>2.5</sub> was higher than those observed at the rural or urban sites in the NCP (Meng et al., 2011), YRD (Meng et al., 2014), Beijing (Shen et al., 2011), Guangzhou (Hu et al., 2008), and Hong Kong (Yao et al., 2006) in China, and comparable to that at urban site in India (Behera et al., 2010). The average concentration of SO<sub>4</sub><sup>2-</sup> in PM<sub>2.5</sub> was higher than those at rural sites in the NCP (Meng et al., 2011) and YRD (Meng et al., 2014) in China, but was lower than that observed at rural sites in Guangzhou (Hu et al., 2008) in China, as well as urban sites in India (Behera et al., 2010) and Egypt (Hassan et al., 2013). The average concentration of NO<sub>3</sub><sup>-</sup> in PM<sub>2.5</sub> was higher than those observed at the rural sites in the YRD and Guangzhou (Hu et al., 2008) in China, and lower than those at urban sites in India (Behera et al., 2010) and Pakistan (Biswas et al., 2008). The elevated NH<sub>3</sub> and NH<sub>4</sub><sup>+</sup> in PM<sub>2.5</sub> concentrations at the NCP rural site demonstrate severe ammonia and fine particulate ammonium pollution in this area.



## 3.2 Ambient ammonia

### 3.2.1 Temporal variation of NH<sub>3</sub>

The time series of hourly averages of NH<sub>3</sub> and other trace gases together with meteorological parameters during 15 May–25 September 2013 at Gucheng are shown in Fig. 2. NH<sub>3</sub> concentrations varied considerably during the observation period, ranging from 0.12 to 862.9 ppb. The Gucheng station has a farmland of 8.67 hectares. The observation period was in the time of the wheat harvest and corn seeding and growing. Corn was sown and fertilized, with about 600 kg of fertilizer per hectare in late June. On 20 July corn was additionally fertilized applied to corn, with 225 to 300 kg of urea per hectare on 20 July. After applying this fertilization, there was a raining period. The NH<sub>3</sub> concentration increased rapidly on the seventh day after the urea application on 20 July, peaking during the 27–30 July period (Fig. 2b). The highest hourly value of NH<sub>3</sub> (862.9 ppb) was observed at 04:00 local time on 29 July 2013, with the second highest concentration observed at 06:00 on the same day. The extremely high NH<sub>3</sub> concentrations were probably caused by intensified soil emissions after rainfall on 26 July, which enhanced the soil moisture. Precipitation and the resulting soil water dynamics are known to strongly affect urea hydrolysis and subsequent NH<sub>3</sub> emissions (Reynold and Wolf, 1987; Aranibar et al., 2004). The general increase in NH<sub>3</sub> emissions was observed when soils with high moisture content began to dry because of increased diffusion (Burch et al., 1989). In addition, high temperatures in summer promote NH<sub>3</sub> volatilisation from urea and ammonium dibasic phosphate applied to crops.

The monthly concentration of NH<sub>3</sub> depends on its source and meteorological conditions. The monthly average values of NH<sub>3</sub> were 28.4, 73.9, 26.4, and 13.5 ppb in June, July, August, and September 2013, respectively. In summer, high temperature promotes the emission of NH<sub>3</sub> from natural and fertilised soils, as well as vegetation. The concentration of NH<sub>3</sub> in July was approximately five times higher than that in September, which was influenced by higher temperature and increased emission rates of local agricultural NH<sub>3</sub> sources in July.

SO<sub>2</sub> and NO<sub>x</sub> are the main precursors of sulfate and nitrate aerosols, and O<sub>3</sub> play an important role in atmospheric chemistry because they act as sources of OH radicals through photolysis. The maximum hourly average concentrations of SO<sub>2</sub> and NO<sub>x</sub> were 86.8 ppb at 00:00 on 21 May and 67.7 ppb at 10:00 on 17 September, respectively. O<sub>3</sub> monthly levels were high in June (44.3 ppb) and July (43.7 ppb), with a maximum hourly average value of 149.9 ppb at 15:00 on 25 July 2013.

In contrast to  $\text{NH}_3$ , the highest monthly levels of  $\text{SO}_2$  (7.0 ppb) and CO (885 ppb) were observed in June, which could be due to the open burning of agricultural waste (straw, cornstalk, and other crops) after harvest in the surrounding area. Previous studies have shown that the burning of crop residues is a crucial source of trace gases such as  $\text{NO}_x$  and CO in the NCP during summer (Meng et al., 2009; Lin et al., 2011). The obvious impact of biomass burning was observed during 16-19 June 2013 period. As CO is mainly emitted from anthropogenic sources such as the burning of biomass, the elevated CO concentrations (2529 ppb at 22:00 on 16 and 2488 ppb at 22:00 on 17 June) were observed. During this pollution episode, the average concentrations of  $\text{NH}_3$ ,  $\text{SO}_2$ ,  $\text{NO}_x$ ,  $\text{O}_3$  and CO were 42.6, 7.69, 18.8, 44.0 and 1092 ppb, respectively, which were about 1.2-1.5 times than the average values for the whole study period. The monthly concentrations of  $\text{SO}_2$ ,  $\text{NO}_x$  and CO in July and August decreased compared to those in June. In addition to less influences from biomass burning, meteorological conditions were also in favor of lowering the concentrations of these gases. Figure S2 shows the monthly average diurnal variations of  $\text{jNO}_2$  and the time-series of hourly rainfall during June-August 2013. As can be seen, the average  $\text{jNO}_2$  increased from June to August, indicating better because conditions for of rapid photochemical reduction, in July and August. and There was also a slight increase in rainfall from June to August, which may promote additional removal by rainfall of the pollutants, and excellent vertical mixing. For the secondary pollutant  $\text{O}_3$ , the highest concentration was observed in June. This is consistent with previous results from Gucheng (Lin et al., 2009) and should be related with the annual maximum of background  $\text{O}_3$  in the NCP, which occurs in June (Lin et al., 2008; Ding et al., 2008). ~~peak was observed in the rural site in the NCP~~ highest monthly value was observed in June 2013, which was subject to strong influences from photochemical production of  $\text{O}_3$  as already discussed above.  $\text{K}^+$  in  $\text{PM}_{2.5}$  is the indicator for biomass burning emission, having the highest monthly concentration in June 2013. It has been shown that regional transport from neighbouring Tianjin, Shijiazhuang, and Shanxi can have a significant impact on background site air quality in the NCP (Meng et al., 2009; Lin et al., 2009). Similarly, Ding et al. (2008) analyzed satellite and meteorological data and reported that the  $\text{O}_3$  maximum in June in Beijing located in the NCP was a result of strong photochemical production, transport of regional pollution, and more intense burnings of biomass in Central Eastern China, intense burning of biomass, and transport of regional pollution.

### 3.2.2 Diurnal variations of $\text{NH}_3$

The average diurnal variations of  $\text{NH}_3$  during June to September 2013 are shown in Fig. 3. As indicated

in Fig. 3a,  $\text{NH}_3$  concentration maxima and minima were observed during 08:00–13:00 and 19:00–23:00, respectively. As for July,  $\text{NH}_3$  concentrations showed a considerably more pronounced diurnal pattern with a maximum of 59.5 ppb at 08:00. The concentration of  $\text{NH}_3$  gradually increased during 00:00–03:00, remained relatively constant during 04:00–06:00, and then rapidly increased from 06:00 (beginning just after sunrise). After peaking at approximately 08:00, a decrease was observed until it reached the minimum of 29.8 ppb at 19:00.

The morning peak of  $\text{NH}_3$  was also observed elsewhere and could be resulted from emissions from fertilised soils and plant stomata, evaporation of dew, and human sources, as well as mixing down of ammonia from the residual layer (Trebs et al., 2004; Norman et al., 2009; Bash et al., 2010; Ellis et al., 2011). Figure 4b–3b reveals that the relative humidity (90%–89%) and temperature (21.5–22.1°C) remained relatively constant before 06:00, but increased later in the morning. The increasing temperature can heat the earth's surface and vegetation leaves sufficiently and reduce the RH, potentially leading to promote emissions from evaporation of  $\text{NH}_3$  morning dew and from the soil and plant stomatas and volatilization of ammonium aerosol (Trebs et al., 2004; Norman et al., 2009; Ellis et al., 2011), which may increase  $\text{NH}_3$  concentrations in the morning. When the emission was occurring into a shallow ~~nocturnal~~ boundary layer,  $\text{NH}_3$  increase would be more prominent (~~Bash et al. 2010~~). In addition, the morning rise ~~may might~~ also be due to the break-up of the nocturnal boundary layer. It was supposed by Ellis et al. (2011) When the vertical mixing begins that, the downward mixing of air containing higher  $\text{NH}_3$  from the residual layer containing relatively higher  $\text{NH}_3$  concentrations could lead to an increase of surface  $\text{NH}_3$  in after the breakup of the nocturnal boundary layersurface (Ellis et al., 2011).

~~$\text{NH}_3$  concentrations began to decrease in the afternoon as the daytime mixed layer further developed with the high wind speed. The decreasing of  $\text{NH}_3$  level from midnight to early morning might be related to the relatively small amount of night time emissions under low temperature and the enhanced participation of  $\text{NH}_3$  in particulate formation. Another simultaneous flux measurements and modeling studies are necessary for more robust explanation to the observed diurnal variations of  $\text{NH}_3$ .~~

From Fig. 3a, it can be seen that in July the higher the  $\text{NH}_3$  maximum level is was the highest and, the peaked earlier str it appears such as in July. One reason for this might be the increased emissions of local agricultural  $\text{NH}_3$  sources in July compared with those in June, August, and September. On the

average, the level  $\text{NH}_3$  in July had a maximum nighttime increase (20.0 ppb from 20:00 to 06:00), which is much larger than those in June (5.2 ppb), August (9.9 ppb) and September (1.8 ppb). The early morning increase of  $\text{NH}_3$  in July started from a much higher level than in other months, the resulting a earliest  $\text{NH}_3$  peak in July ~~occurred earlier than it did in the other months, particularly in September.~~

There is no direct evidence of increased agricultural  $\text{NH}_3$  emission in July. However, the Gucheng site is an experiment station for agrometeorological studies. Corn is the main crop in the station area and nearly all the agricultural areas in the surrounding. According to the climate in the NCP, corn is planted around the middle of June and grows rapidly in July. Therefore, July is the key period for the application of nitrogen fertilisers like urea. As mentioned above, the urea application in the station on 20 July 2013 and a precipitation process afterwards caused huge  $\text{NH}_3$  spikes during the end of July (Fig. 2b). In addition, the highest nighttime temperature in July (Fig. 3b) could promote the soil emission of  $\text{NH}_3$ , and the relatively lower wind speed (Fig. 3b) and lowest PBLH (Fig. S3) in July was in favor of the accumulation of  $\text{NH}_3$  in surface air.

In summary, ~~ambient the diurnal variation of~~  $\text{NH}_3$  ~~was at~~ Gucheng showed interesting diurnal cycles, which look significantly different in different summer months. We believe the interplay of some processes, such as ~~notably affected by the local emissions from~~ agricultural sources, ~~and the synoptic meteorological conditions or more specifically by the combined effects of~~ (temperature, relative humidity, wind speed, and PBLH height, etc.) as well as chemical conversion, are important in the determination of levels and diurnal patterns of  $\text{NH}_3$  at the site at the rural site in the NCP. Whether or not these processes are all important in the morning variation of  $\text{NH}_3$ ? How important are they? And what makes the difference in the peaking time and concentration of  $\text{NH}_3$  in different months? These are questions to be answered in the future. ~~Another possible cause for the earlier peak in August than in June involves meteorological factors such as the higher temperature, RH, and the lower wind speed in August. For instance, the air temperature increased from 07:00 reaching maximum value (30.9°C) at 15:00 in August, which was about of 3.3°C higher than that in June, meanwhile the highest wind speed (2.73 m s<sup>-1</sup>) at 13:00 in June was about of 1.0 m s<sup>-1</sup> higher than that in August.~~

~~Ambient  $\text{NH}_3$  concentrations in an area of intensive crop production correlate positively with the air temperature. The maximum monthly value of  $\text{NH}_3$  concentrations was consistent with the highest~~

ambient temperature in July 2013. Predictably, the highest average diurnal amplitude of  $\text{NH}_3$  (30.4 ppb) was observed in July, with the lowest average diurnal amplitude of  $\text{NH}_3$  (8.4 ppb) observed in September 2013.

### 3.3 Ambient ammonium aerosol

Secondary inorganic aerosols form from gas-phase precursors, which are mostly from anthropogenic activities such as industrial, agricultural, and motor vehicle emissions. Therefore, the major precursors ( $\text{NH}_3$ ,  $\text{SO}_2$  and  $\text{NO}_x$ ) are responsible for the formation of particulate ammonium, sulphate, and nitrate.

The hourly  $\text{NH}_4^+$  concentrations during 15 June–11 August 2013 ranged from 1.07 to 340.6  $\mu\text{g m}^{-3}$ , with an average concentration of  $19.8 \pm 33.2 \mu\text{g m}^{-3}$ . The highest monthly level of  $\text{NH}_4^+$  appeared in July and lowest level appeared in June 2013. Similar to  $\text{NH}_3$ , the concentration of  $\text{NH}_4^+$  also increased sharply after urea fertilisation, with the highest value (360.6  $\mu\text{g m}^{-3}$ ) observed at 09:00 on 28 July 2013.

~~The highest monthly level of  $\text{NH}_4^+$  appeared in July and lowest level appeared in June 2013.~~

The highest hourly  $\text{SO}_4^{2-}$  concentration (116.9  $\mu\text{g m}^{-3}$ ) was observed at 10:00 on 9 July and the second highest value was 111.4  $\mu\text{g m}^{-3}$  at 18:00 on 6 August, 2013, with the average concentration of  $20.5 \pm 13.6 \mu\text{g m}^{-3}$ . Despite the lower concentrations of  $\text{SO}_2$ , higher  $\text{SO}_4^{2-}$  concentrations in summer were attributed to the higher temperature,  $\text{O}_3$  concentration and solar radiation, which increase the photochemical activities, the atmospheric oxidation and markedly faster conversion of  $\text{SO}_2$  to  $\text{SO}_4^{2-}$ .

The average concentration of  $\text{NO}_3^-$  in  $\text{PM}_{2.5}$  was  $11.3 \pm 9.1 \mu\text{g m}^{-3}$ . ~~with the highest value of 109.3  $\mu\text{g m}^{-3}$  observed at 15:14:00 on 22 June, 2013, with at the highest RH of (93%) and the highest aerosol water content (AWC) of (910  $\mu\text{g m}^{-3}$ ).~~

Figure 4 shows correlations of observed  $\text{NH}_4^+$  with the sum of observed with observed  $\text{SO}_4^{2-}$ ,  $\text{SO}_4^{2-} + \text{NO}_3^-$  and  $\text{SO}_4^{2-} + \text{NO}_3^- + \text{Cl}^-$ . Although all the correlations are significant, the slopes of the regression lines are far from unit. This cannot be due bias in measurements. The major ion balance shows ratio of 1.05:1 for cation:anion. The slope is 0.56 when all three strong acid are considered, suggesting that the neutralization of the strong acids explain 56% of the observed  $\text{NH}_4^+$ . In other words, nearly 44% of the observed  $\text{NH}_4^+$  was due to the presence of other acids in aerosol particles.

### 3.4 Results from thermodynamic equilibrium simulation

We have used the thermodynamic equilibrium model ISORROPIA II to investigate gas-aerosol partitioning characteristics.  $\text{NO}_3^-$ ,  $\text{SO}_4^{2-}$  and  $\text{NH}_4^+$ . The model outputs include equilibrium  $\text{NO}_3^-$ ,  $\text{SO}_4^{2-}$ ,  $\text{NH}_4^+$ ,  $\text{H}^+$ ,  $\text{HNO}_3$ ,  $\text{NH}_3$ , AWC, etc. As shown in Fig. 5, the modelled  $\text{NO}_3^-$ ,  $\text{SO}_4^{2-}$ ,  $\text{NH}_3$  show excellent

correlations with the corresponding measurements, but modelled  $\text{NH}_4^+$  is much worse correlated with the measured one. Modelled  $\text{NO}_3^-$ ,  $\text{SO}_4^{2-}$ , and  $\text{NH}_3$  values agree well with the measurements, while the modelled  $\text{NH}_4^+$  largely underestimate the measurements. Considering the unbalance between observed  $\text{NH}_4^+$  and the sum of observed  $\text{SO}_4^{2-} + \text{NO}_3^- + \text{Cl}^-$ , we can confirm that other acids in aerosol particles are important in the conversion of  $\text{NH}_3$  to  $\text{NH}_4^+$ . These other acids may be oxalic acid and other dicarboxylic acids. Although we did not measure organic acids in aerosol, the presence of oxalic acid and other low molecular weight dicarboxylic acids in aerosols is often reported (e.g., Hsieh et al., 2007; Kawamura et al., 2010, 2013; Sauerwein and Chan, 2017). There is no doubt about the presence of significant amount of dicarboxylic acids over the North China Plain particularly during summer (Kawamura et al., 2013). Therefore, it is highly possible that neutralizing dicarboxylic acids in aerosol particles contributed significantly to the conversion of ammonia to ammonium.

The simulated  $\text{HNO}_3$  concentrations was  $0.9 \pm 1.1 \mu\text{g m}^{-3}$ , showing a maximum value of  $7.41 \mu\text{g m}^{-3}$  at 11:00 on 19 June 2013. The average diurnal variations of  $\text{HNO}_3$  and  $\text{H}^+_{\text{air}}$  are shown in Fig. S4. The fine particles were moderately acidic in summer, with an average pH values of 3.5. The pH values of aerosol water, estimated based on the simulated results using equation (4), are mostly in the range of 2.5-4.5, with an average of 3.5. On average, pH is over 3.5 during nighttime and below 3.5 during daytime (Fig. 6). Under the medium acidic conditions and high  $\text{NH}_3$  concentrations, organic acid like diacids are able to reaction with ammonia to form ammonium. Because we used ISORROPIA-II for inorganic aerosol composition and no organic acids measurements are available, we cannot analyze in detail the role of organic acids though the model performed quite well (Fig. S5).

On several days during the study period, very high  $\text{NH}_3$  and inorganic  $\text{PM}_{2.5}$  concentrations were observed. As shown in Fig. 6a, the peak  $\text{NH}_3$  value of 76.3 ppb at 09:00 on 10 August was observed, with  $\text{SO}_2$  and  $\text{NO}_x$  concentrations of 3.33 ppb and 14.72 ppb, respectively. A few hours later, the concentration of  $\text{SO}_4^{2-}$  increased by a factor of 2.0 from 18.3 to 35.9  $\mu\text{g m}^{-3}$  and  $\text{NH}_4^+$  concentration rose by a factor of 1.6 from 15.9 to 24.8  $\mu\text{g m}^{-3}$ , with  $\text{NO}_3^-$  concentration from 14.3 to 15.7  $\mu\text{g m}^{-3}$  at 13:00 on 10 August. High  $\text{NH}_3$  concentration was accompanied by the large increase in concentrations of  $\text{SO}_4^{2-}$ ,  $\text{NO}_3^-$  and  $\text{NH}_4^+$  during this period. Several pollution episodes of precursor gases,  $\text{SO}_4^{2-}$ ,  $\text{NO}_3^-$  and  $\text{NH}_4^+$  in  $\text{PM}_{2.5}$  were observed during the study period. As shown in Fig. 46a, the peak values of  $\text{NH}_3$ ,  $\text{SO}_2$  and  $\text{NO}_x$  (76.3 ppb at 09:00, 14.9 ppb at 14:00 on and 42.2 ppb at 00:00 on 10 August, respectively) were observed, which were accompanied by the large increase in concentrations of  $\text{SO}_4^{2-}$ ,

$\text{NO}_3^-$  and  $\text{NH}_4^+$  during 7–11 August 2013. This suggests that  $\text{NH}_3$  played an important role in PM mass formation and that gas–particle conversion occurred when  $\text{NH}_3$  was available, though  $\text{SO}_4^{2-}$  partitions to the aerosol phase regard less of  $\text{NH}_3$  level (Gong et al., 2013). Due to the atmospheric conditions favoring the accumulation of pollutants, the concentrations of  $\text{NH}_4^+$ ,  $\text{SO}_4^{2-}$  and  $\text{NO}_3^-$  (24.8, 35.9 and  $15.7 \mu\text{g m}^{-3}$ , respectively) at 13:00 on 10 August were detected and higher compared with the average concentrations during 7–11 August 2013 by around 127%, 81% and 83%, respectively. These secondary ions concentrations had similar temporal distributions with slow accumulation and relatively rapid clearing under favourable meteorological conditions. There were good correlation between  $\text{NH}_3$  with  $\text{NH}_4^+$ ,  $\text{SO}_4^{2-}$  and  $\text{NO}_3^-$  ( $R=0.33$ ,  $0.27$  and  $0.49$ , respectively, with  $P < 0.01$ ). Our study and other research reveal that reducing  $\text{NH}_3$  concentrations could be an effective method for alleviating secondary inorganic  $\text{PM}_{2.5}$  pollution in the NCP, besides the reduction of primary  $\text{SO}_2$ ,  $\text{NO}_x$  and aerosol emissions. This observation emphasizes the important role of  $\text{NH}_3$  in the formation of secondary  $\text{SO}_4^{2-}$ ,  $\text{NO}_3^-$  and  $\text{NH}_4^+$  aerosols, which should be further explored to solve the current air pollution problems in NCP and other regions of the world.

During 7–11 August 2013, the relationships of the observed  $\text{NH}_4^+$  versus those of  $\text{SO}_4^{2-}$ , the sum of  $\text{SO}_4^{2-}$  and  $\text{NO}_3^-$  and the sum of  $\text{SO}_4^{2-}$ ,  $\text{NO}_3^-$  and  $\text{Cl}^-$  are presented in Fig. 4b also analyzed. It is known that  $(\text{NH}_4)_2\text{SO}_4$  is preferentially formed and the least volatile,  $\text{NH}_4\text{NO}_3$  is relatively volatile, while  $\text{NH}_4\text{Cl}$  is the most volatile.  $\text{NH}_4^+$  is thought to be first associated with  $\text{SO}_4^{2-}$ , afterwards, the excess of  $\text{NH}_4^+$  is with nitrate and chloride (Meng et al., 2015). It is noted that the correlation of  $\text{NH}_4^+$  with the sum of  $\text{SO}_4^{2-}$  and  $\text{NO}_3^-$  ( $R=0.91$ , slope=1.23, with  $P < 0.01$ ) was better than that of  $\text{NH}_4^+$  with  $\text{SO}_4^{2-}$  ( $R=0.80$ , slope=1.65, with  $P < 0.01$ ), suggesting that both  $\text{SO}_4^{2-}$  and  $\text{NO}_3^-$  were associated with  $\text{NH}_4^+$ . As shown in Fig. 4b, sulfate and nitrate were almost completely neutralized with most of the data above the 1:1 line. A few scattered data below the 1:1 line. Little different was found between the regression slopes of  $\text{NH}_4^+$  with the sum of  $\text{SO}_4^{2-}$  and  $\text{NO}_3^-$  and the sum of  $\text{SO}_4^{2-}$ ,  $\text{NO}_3^-$  and  $\text{Cl}^-$  due to the very low amount of  $\text{NH}_4\text{Cl}$ . In this study,  $\text{NH}_4^+$  was enough to neutralize both  $\text{SO}_4^{2-}$  and  $\text{NO}_3^-$ , and likely to be in the form of  $(\text{NH}_4)_2\text{SO}_4$ ,  $\text{NH}_4\text{HSO}_4$  and  $\text{NH}_4\text{NO}_3$ .

The analysis of water soluble ions in  $\text{PM}_{2.5}$  at NCP rural site also indicated that biomass burning was a crucial source of aerosol species. This attribution is supported by the concentrations of  $\text{K}^+$  in  $\text{PM}_{2.5}$ , an excellent indicator for biomass burning emission. The monthly concentrations of  $\text{K}^+$  in  $\text{PM}_{2.5}$  were 2.17, 1.62 and  $0.98 \mu\text{g m}^{-3}$  in June, July and August, respectively, with the highest concentration in

June 2013. During the period of 16–19 June, 2013, elevated concentrations of  $K^+$  ( $33.28 \mu\text{g m}^{-3}$  at 08:00 on 16 June),  $\text{NH}_4^+$  ( $33.28 \mu\text{g m}^{-3}$ ),  $\text{SO}_4^{2-}$  ( $24.53 \mu\text{g m}^{-3}$ ), and  $\text{NO}_3^-$  ( $29.79 \mu\text{g m}^{-3}$ ) were observed, which is consistent with the increase of  $\text{CO}$ ,  $\text{SO}_2$ ,  $\text{NO}_x$  and  $\text{NH}_3$  at the same time.

The comparison of the model and measurement results of the partitioning between  $\text{NH}_3$  and inorganic ions in  $\text{PM}_{2.5}$  was shown in Fig. 5. The model predictions and measurements were in reasonable agreement, and the agreement on  $\text{NH}_3$  was better than the  $\text{NO}_3^-$ ,  $\text{SO}_4^{2-}$  and  $\text{NH}_4^+$ . According to Fig. 5, the simulated  $\text{NH}_3$  was in good agreement with observation with an  $R^2=0.94$  and normalized mean bias (NMB) of 26.9% for all the data, implying a good performance of ISORROPIA II. However, in most cases the model tended to under-predict aerosols species, especially for  $\text{NH}_4^+$  in summer.

During sampling period, aerosols water content (AWC), ranged between 2.3 and  $910 \mu\text{g m}^{-3}$ , with an average concentration of  $78.7 \pm 74.3 \mu\text{g m}^{-3}$ , which was primarily due to both high RH and denser fine particles in the atmospheric boundary layer (Bian et al., 2014).

### 3.4.5 Relationship between ammonia and ammonium aerosol

The gas-to-particle conversion between  $\text{NH}_3$  and  $\text{NH}_4^+$  has been reported to be strongly affected by temperature, RH, radiation conditions, the concentration of primary acid gas, and other factors. In this study,  $\text{NH}_4^+$  concentrations correlated significantly and positively with  $\text{NH}_3$  concentrations with a correlation coefficient of 0.78 and a slope of 1.48 (Fig. 7a,  $R=0.78$ ,  $n=915$ ,  $P < 0.01$ ), suggesting that  $\text{NH}_3$  played an important precursor role in  $\text{NH}_4^+$  in  $\text{PM}_{2.5}$  formation.

The ratio of  $\text{NH}_3$  to  $\text{NH}_x$  ( $\text{NH}_3 + \text{NH}_4^+$ ) has been used to identify the source of  $\text{NH}_x$  and the relative contribution of  $\text{NH}_3$  to  $\text{NH}_x$  deposition (Lefer et al., 1999; Walker et al., 2004). A value higher than 0.5 signifies that  $\text{NH}_x$  is mainly from local  $\text{NH}_3$  sources and that the dry deposition of  $\text{NH}_3$  dominates the  $\text{NH}_x$  deposition. Robarge et al. (2002) reported that more than 70% of  $\text{NH}_x$  was in the form of  $\text{NH}_3$  at an agricultural site in the South-eastern United States, and concluded that given a larger deposition velocity of ammonia compared with that of ammonium, a considerable fraction of  $\text{NH}_x$  could be deposited locally rather than be transported out of the region. According to hourly average concentrations, the ratio of  $\text{NH}_3/\text{NH}_x$  varied from 0.22 to 0.97, with a mean ratio of  $0.69 \pm 0.14$ , suggesting that  $\text{NH}_3$  remained predominantly in the gas phase rather than the aerosol phase in summer 2013 at Gucheng.

The diurnal changes in gaseous precursors and aerosol species are controlled by emission and



deposition processes, horizontal and vertical transport and gas-particle partitioning. To investigate gas-particle conversion further, diurnal variation of  $\text{NH}_x$  was showed in Fig. 7b. Between 08:00–18:00, a decrease in  $\text{NH}_3$  would result in an increase in  $\text{NH}_4^+$ , which coincided with higher sulfate concentrations (discussed in Sect. 3.4). The decrease in gas phase ammonia is likely the result of uptake onto aerosols to form  $(\text{NH}_4)_2\text{SO}_4$ . The diurnal variability of  $\text{NH}_x$  may be controlled by transport and vertical exchange. Between the hours of 08:00–18:00,  $\text{NH}_3$  decreased by 43% while  $\text{NH}_x$  decreased by 49%, suggested that  $\text{NH}_3$  remained predominantly in the gas phase. Between 19:00 and 07:00,  $\text{NH}_3$  increased by 42% and  $\text{NH}_x$  increased by 51%, indicating that gas-particle partitioning contributes significantly to the decrease in gas phase ammonia during this time.

According to hourly average concentrations, the ratio of  $\text{NH}_3/\text{NH}_x$  varied from 0.22 to 0.97, with a mean ratio of  $0.69 \pm 0.14$ , suggesting that  $\text{NH}_x$  was mainly influenced by local sources in summer 2013. It can also be inferred that  $\text{NH}_3$  dry deposition could dominate  $\text{NH}_x$  deposition, while  $\text{NH}_4^+$  was contributed to by both long range transport and local formation.

#### 3.4.5.1 Gas- to-particle conversion ratio of $\text{NH}_3$

Sulphate and nitrate oxidation ratios (SOR and NOR) are defined in literature to investigate  $\text{SO}_4^{2-}$  and  $\text{NO}_3^-$  formation and gas-particle transformation (Zhang et al., 2011). The average values of SOR and NOR were estimated to be 0.64% and 0.24% during the observation period at Gucheng, with SOR and NOR being higher than previous measurements (Zhou et al., 2009; Du et al., 2011; Zhang et al., 2011). Yao et al.(2002) pointed out an SOR lower than 0.10% under conditions of primary source emissions and higher than 0.10% when sulphate was mainly produced through the secondary transformation of  $\text{SO}_2$  oxidation. The value of SOR reached to 0.70% in August 2013, indicating that the secondary transformation was very significant during which may due to the enhanced atmospheric oxidant levels, sufficient ammonia for neutralization, and higher RH in summer at Gucheng (Tang et al., 2016).

To gain further insights into the transformation of  $\text{NH}_3$  to  $\text{NH}_4^+$ , the conversion ratio of ammonium (NHR) was investigated. NHR is a measure of the extent of transformation from  $\text{NH}_3$  to  $\text{NH}_4^+$  in areas with significant local  $\text{NH}_3$  sources, although it encompasses both transformation and local equilibrium, the latter dominating further downwind from the source major local  $\text{NH}_3$  sources. In this study, the average hourly values of NHR ranged from 0.03% to 0.77%, with an average of 0.30% during summer 2013. The average NHR level in this study was higher than that observed at an urban site in Beijing (Meng et al., 2017), indicating that high  $\text{NH}_3$  concentrations resulting from agricultural

activities had a marked influence on the formation of ammonium. After applying fertilizer such as urea,  $\text{NH}_3$  volatilization achieved the peak values, especially after the rainfall, which was in favour of the formation of  $\text{NH}_4^+$ . To specifically explore the behaviour and chemical transformation, we analyzed in detail the episode during which the highest hourly  $\text{NH}_3$  and  $\text{NH}_4^+$  were observed.

Figure 5-98 illustrates the time series of the concentrations of air pollutants related to  $\text{NH}_4^+$  formation and meteorological data on 27 to 31 July, 2013.  $\text{NH}_3$  concentrations increased gradually from the afternoon of 27 July, and the obvious formation of  $\text{NH}_4^+$  was also observed. In addition, during the night time (20:00 on 27-07:00 on 28 July), the average RH was 92% and the wind speed was  $0.4 \text{ m s}^{-1}$ , respectively, which may enhance the conversion of ammonia to ammonium via aqueous phase processes. As the rapid increase of solar radiation, the highest hourly value of  $\text{NH}_4^+$  was observed at 09:00 on 28 July, and the corresponding NHR peaked (0.63%) at the same time.

$\text{NH}_3$  exhibited a maximum average concentration at 04:00 on 29 July, while  $\text{NH}_4^+$  concentrations increased rapidly and remained high levels in the morning, with the NHR value rising to 0.53% at 09:00 on 29 July. Elevated  $\text{NH}_3$  levels coincided with elevated  $\text{NH}_4^+$ , indicating that  $\text{NH}_3$  was the main factor promoting  $\text{NH}_4^+$  formation.

Furthermore, on 30 July, the higher  $\text{NH}_4^+$  concentration and NHR occurred around noon after  $\text{NH}_3$  decreased, which is consistent with increasing solar radiation and  $\text{O}_3$  concentration. This suggests that strong solar radiation intensity accelerated the photochemical formation of sulphuric acid or nitric acid, which subsequently reacted with  $\text{NH}_3$  to form  $\text{NH}_4^+$ . The increases in NHR coincided with those of  $\text{NH}_3$  and  $\text{O}_3$  concentrations and strong solar radiation intensity.

### 3.54.2 Diurnal patterns of NHR, SOR and NOR

Fig. 6-109 presents the diurnal patterns of NHR, SOR, NOR, gaseous precursors, and major water soluble ions, and meteorological factors. As a key species contributing to the oxidation capacity of the atmosphere,  $\text{O}_3$  can promote  $\text{HNO}_3$  formation, affecting the conversion ratio of  $\text{NH}_3$ .  $\text{O}_3$  exhibited low levels in the morning and enhanced levels in the late afternoon. The lower morning concentrations may be due to the depositional loss of  $\text{O}_3$  under stable atmospheric conditions in early morning hours, and the higher levels in the afternoon could be due to the photochemical production of  $\text{O}_3$ . The  $\text{NH}_4^+$  concentration started to increase at noon, reaching the maximum value ( $15.8 \mu\text{g m}^{-3}$ ) at 18:00, with a diurnal difference of  $3.6 \mu\text{g m}^{-3}$ . This diurnal pattern may be due to a combination of high  $\text{NH}_3$  concentrations, the intense solar radiation at noon, and the high oxidation capacity of the

atmosphere in the afternoon. A clear diurnal cycle of NHR existed, with an amplitude of 8.2% and a peak of 0.48%34.8% was observed at 19:00, which is consistent with the higher  $\text{NH}_4^+$  and  $\text{SO}_4^{2-}$  concentrations SOR and RH.

The  $\text{SO}_2$  concentration showed a maximum at 09:00, with a secondary peak at 22:00. The concentration of  $\text{SO}_4^{2-}$  showed small peak at 13:00, 16:00, and 19:00, respectively, but no strong diurnal variation. SOR displayed a diurnal cycle with the highest value of 0.53%73.8% observed at 19:00 and the second highest level of 0.51% exhibited at 04:00. The higher daytime maximum value of  $\text{SO}_4^{2-}$  coincide to  $\text{O}_3$  and SOR, which may due to the intense solar radiation and the high oxidization degree of the atmosphere. It is noted that the SOR was lower during daytime when photochemical reaction is intense. Higher SOR during nighttime suggests importance of dark reactions.  $\text{SO}_2$  is highly soluble and can easily absorbed by wet aerosol particles. The much RH during night may promoted this process.

As for the diurnal cycle of  $\text{NO}_x$ , a peak was observed at 06:00 when the mixing layer was stable, and a broad valley was observed in the daytime, which was likely due to reflecting the influences of a higher mixing layer and stronger photochemical conversion. During the night,  $\text{NO}_x$  concentrations increased again, resulting in the second maximum at 23:00.  $\text{NO}_3^-$  concentrations did not show profound diurnal variations, but slightly higher values during the night time, probably because of the hydrolysis of dinitrogenpentoxide ( $\text{N}_2\text{O}_5$ ) and the condensation of  $\text{HNO}_3$  under the relatively low temperature.

Nighttime formation, aerosol uptake and hydrolysis of  $\text{N}_2\text{O}_5$  are highly uncertain as has been pointed out (e.g., Xue et al. 2014). The  $\text{NO}_x$  concentration during nighttime was higher than during daytime, while the  $\text{NO}_3^-$  level during nighttime was only slightly higher than that during daytime. By assuming high aerosol surface to mass ratio ( $33.7 \text{ m}^2/\text{g}$ , Okuda, 2013) and a high uptake coefficient (0.1, Seinfeld and Pandis, 2006), we estimate the nighttime  $\text{N}_2\text{O}_5$  under the conditions over our site to be in the range of about 3-10 ppb, corresponding to a  $\text{HNO}_3$  production rate of about 1-3 ppb/hr (or  $2.6\text{-}7.7 \text{ }\mu\text{g}/\text{m}^3$ ). This rate of  $\text{HNO}_3$  production would cause an obvious night production of  $\text{NH}_4^+$ . Indeed we can see increases in the  $\text{NH}_4^+$  concentration and NHR during night (Fig. 8). However, a more or less accurate estimate of the relative contribution of the night  $\text{N}_2\text{O}_5$  chemistry to  $\text{NH}_3$  conversion needs to be made in the future.

### 3.6 A case study of a pollution period

On several days during the study period, very high  $\text{NH}_3$  and inorganic  $\text{PM}_{2.5}$  concentrations were observed. Here make a case study of a pollution period during 7-11 August 2013. Data of gases, major aerosol ions and some key meteorological parameters are presented in Fig. 9. Some other measure and calculated parameters during this period are given in Fig. S6. As shown in Figs. 9 and S6, there was a sharp increase of  $\text{NO}_x$  during the night and early morning of 10 August, followed by that of  $\text{NH}_3$  (peak value 64 ppb at 03:00. In the meantime, a large peak of AWC occurred and gaseous  $\text{HNO}_3$  decreased to nearly zero (Fig. S6), suggesting rapid uptake of wet aerosol. This event caused the first largest peak of  $[\text{SO}_4^{2-}] + [\text{NO}_3^-] + [\text{NH}_4^+]$ . After this event  $\text{NH}_3$  rose again and reached a even higher peak (76.3) shortly before noon of 10 August. This peak of  $\text{NH}_3$  coincided with a valley of  $\text{NO}_x$ , but the  $\text{HNO}_3$  level increased and pH value decreased was observed in parallel. A few hours later  $\text{SO}_2$  showed a large peak and the second largest peak of  $[\text{SO}_4^{2-}] + [\text{NO}_3^-] + [\text{NH}_4^+]$  occurred. These data show that high  $\text{NH}_3$  concentration was accompanied by the large increase in concentrations of  $\text{SO}_4^{2-}$ ,  $\text{NO}_3^-$  and  $\text{NH}_4^+$ , confirming that  $\text{NH}_3$  play an important role in PM mass formation and that gas-particle conversion occurred when  $\text{NH}_3$  was available, though  $\text{SO}_4^{2-}$  partitions to the aerosol phase regard less of  $\text{NH}_3$  level (Gong et al., 2013). The secondary ions concentrations had similar temporal distributions with slow accumulation and relatively rapid clearing under favourable meteorological conditions. There were good correlation between  $\text{NH}_3$  with  $\text{NH}_4^+$ ,  $\text{SO}_4^{2-}$  and  $\text{NO}_3^-$  ( $R=0.33$ ,  $0.27$  and  $0.49$ , respectively, with  $P < 0.01$ ). However, there was also situation when high  $\text{NH}_3$  did not associate with high  $[\text{SO}_4^{2-}] + [\text{NO}_3^-] + [\text{NH}_4^+]$ , as indicated by the data around noon of 8 August (Fig. 9). During this case, AWC was extremely low and RH was around 40%. These conditions do not favor heterogeneous reactions.

During 7-11 August 2013, the relationships of the observed  $\text{NH}_4^+$  versus those of  $\text{SO}_4^{2-}$ , the sum of  $\text{SO}_4^{2-}$  and  $\text{NO}_3^-$  and the sum of  $\text{SO}_4^{2-}$ ,  $\text{NO}_3^-$  and  $\text{Cl}^-$  are presented in Fig. 10. It is known that  $(\text{NH}_4)_2\text{SO}_4$  is preferentially formed and the least volatile,  $\text{NH}_4\text{NO}_3$  is relatively volatile, while  $\text{NH}_4\text{Cl}$  is the most volatile.  $\text{NH}_4^+$  is thought to be first associated with  $\text{SO}_4^{2-}$ , afterwards, the excess of  $\text{NH}_4^+$  is with nitrate and chloride (Meng et al., 2015). It is noted that the correlation of  $\text{NH}_4^+$  with the sum of  $\text{SO}_4^{2-}$  and  $\text{NO}_3^-$  ( $R=0.91$ , slope=1.23, with  $P < 0.01$ ) was better than that of  $\text{NH}_4^+$  with  $\text{SO}_4^{2-}$  ( $R=0.80$ , slope=1.65, with  $P < 0.01$ ), suggesting that both  $\text{SO}_4^{2-}$  and  $\text{NO}_3^-$  were associated with  $\text{NH}_4^+$ . As shown in Fig.10, sulfate and nitrate were almost completely neutralized with most of the data above the 1:1 line. A few scattered data below the 1:1 line may be caused by uncertainties in measurements. Little different was found

between the regression slopes of  $\text{NH}_4^+$  with the sum of  $\text{SO}_4^{2-}$  and  $\text{NO}_3^-$  and the sum of  $\text{SO}_4^{2-}$ ,  $\text{NO}_3^-$  and  $\text{Cl}^-$  due to the very low amount of  $\text{NH}_4\text{Cl}$ . In this study, the level of  $\text{NH}_3$  was high enough to neutralize both  $\text{SO}_4^{2-}$  and  $\text{NO}_3^-$ , and likely to be form  $(\text{NH}_4)_2\text{SO}_4$  and  $\text{NH}_4\text{NO}_3$ . In addition to these substances, it is likely that  $\text{NH}_3$  also reacted with oxalic acid and other dicarboxylic acid to form ammonium oxalate and other organic ammonium aerosols, as discussed above.

NOR displayed a diurnal pattern with a maximum of 0.34% at 14:00, which was likely related to photochemical reactions under the conditions of high  $\text{O}_3$  concentrations and solar radiation.

### **3.5.7 The impact of air masses Long range transport on the and local surface ammonia and ammonium**

Dependence of the concentrations of  $\text{NH}_3$  on wind direction at Gucheng is studied to get insight into the distribution of local emission sources around the monitoring site. As shown in Fig. 11, during the sampling period, the prevailing surface winds at Gucheng were northeasterly and southwesterly. High  $\text{NH}_3$  originated from the southwest sector of the measurement site, which may be due to a local unidentified agricultural or industrial source or transport from the Xushui township, which is approximately 15 km away from Gucheng. Lower  $\text{NH}_3$  concentrations were observed under winds from other sectors. Since  $\text{NH}_3$  is either readily converted to  $\text{NH}_4^+$  or subjected to dry deposition, high concentrations are found only close to the surface and near the emission sources. Previous studies have reported an inverse relationship between ground-level concentrations of trace gases, such as ammonia, and wind speed (Robarge et al., 2002; Lin et al., 2011). Thus,  $\text{NH}_3$  concentrations might be generally lower at higher wind speeds because of turbulent diffusion.

To identify the impact of long-range air transport on the surface air pollutants levels and secondary ions at Gucheng, the 72-h backward trajectories were calculated using the HYSPLIT 4.9 model.

As can be seen in Fig. 712, the Clusters 1, 2 and 3 represent relatively low and slow moving air parcels, with cluster 2 coming from northwest areas at the lowest transport height among the five clusters. The Cluster 4 and 5 represent air parcels mainly from the far northwest.

The trajectories in Clusters 2 ~~come~~ came from the local areas around Gucheng, and it was the most important cluster to the Gucheng site, contributing 56% ~~of to the~~ air masses. Based on the statistics, the number of trajectories in Cluster 1, 2 and 3 accounts to 88% of the all trajectories. As more than 80% air masses originated from or passing over the North China Plain region can influence the surface measurements at Gucheng, the observation results at Gucheng can well represent the regional ~~changes~~ situation of atmospheric components in the North China Plain region.

Since the emission sources of pollutants are unevenly distributed in the areas surrounding the Gucheng site, air masses from different directions containing different levels of pollutants. The corresponding mean concentrations of  $\text{NH}_3$ ,  $\text{SO}_2$ ,  $\text{NO}_x$ ,  $\text{NH}_4^+$ ,  $\text{SO}_4^{2-}$  and  $\text{NO}_3^-$  in  $\text{PM}_{2.5}$  in different clusters of backward trajectories are also included in Table 2 in order to characterize the dependences of the pollutants concentrations on air masses.

Large differences in the concentrations of  $\text{NH}_3$ ,  $\text{SO}_2$ ,  $\text{NO}_x$ ,  $\text{NH}_4^+$ ,  $\text{SO}_4^{2-}$  and  $\text{NO}_3^-$  in  $\text{PM}_{2.5}$  existed among the different clusters, with cluster 2 corresponding to the highest  $\text{NH}_3$  (48.9 ppb) and second highest  $\text{NO}_x$ ,  $\text{NH}_4^+$  and  $\text{SO}_4^{2-}$  (14.4 ppb, 17.5  $\mu\text{g m}^{-3}$  and 22.1  $\mu\text{g m}^{-3}$ , respectively). The cluster 1 corresponds to highest  $\text{SO}_2$ ,  $\text{NH}_4^+$ ,  $\text{SO}_4^{2-}$  and  $\text{NO}_3^-$  (7.9 ppb, 22.3  $\mu\text{g m}^{-3}$ , 22.6  $\mu\text{g m}^{-3}$  and 17.7  $\mu\text{g m}^{-3}$ , respectively), the second highest  $\text{NH}_3$  level (32.8 ppb). The cluster 3 had the highest  $\text{NO}_x$  level (15.1 ppb), the second highest  $\text{SO}_2$  and  $\text{NO}_3^-$  (4.8 ppb and 11.8  $\mu\text{g m}^{-3}$ , respectively), and had the third highest concentration of  $\text{NH}_3$ ,  $\text{NH}_4^+$  and  $\text{SO}_4^{2-}$  levels (28.5 ppb, 14.6  $\mu\text{g m}^{-3}$ , and 20.2  $\mu\text{g m}^{-3}$ , respectively). Based on table 2, the lowest  $\text{NH}_3$ ,  $\text{SO}_2$ ,  $\text{NO}_x$ ,  $\text{NH}_4^+$ ,  $\text{SO}_4^{2-}$  and  $\text{NO}_3^-$  levels were corresponding to clusters 5, which was expected to bring cleaner air masses into surface. As demonstrated by backward trajectory, more than half of the air masses during the sampling period from North China Plain region contributed to the atmospheric  $\text{NH}_3$  variations, and both regional sources and long-distance transport from southeast played important roles in the observed ammonium aerosol at the rural site in the NCP.

#### 4 Conclusions

Online measurements of  $\text{NH}_3$ , trace gases, and water-soluble ions in  $\text{PM}_{2.5}$  were conducted during May–September 2013 at a rural site in the NCP, where a large amount of ammonia was emitted because of agricultural activities. The average concentrations of  $\text{NH}_3$  and  $\text{NH}_4^+$  in  $\text{PM}_{2.5}$  were  $36.2 \pm 56.4$  ppb during 15 May–25 September, 2013, and  $18.9 \pm 33.2$   $\mu\text{g m}^{-3}$  during 15 June–11 August, 2013, respectively; these are considerably higher than those reported at other sites in China, Europe and North American. Extremely high  $\text{NH}_3$  and  $\text{NH}_4^+$  concentrations were observed, which was attributed to high soil moisture level due to rainfall on these days following the urea application. Elevated  $\text{NH}_3$  levels coincided with elevated  $\text{NH}_4^+$ , indicating the contribution of atmospheric  $\text{NH}_3$  to secondary inorganic aerosols during periods of agricultural activity.  $\text{NH}_3$  contributed 69% to the total  $\text{NH}_3+\text{NH}_4^+$  in summer, suggesting that  $\text{NH}_x$  was influenced by local sources and that  $\text{NH}_3$  dry deposition could contribute a large part of the  $\text{NH}_x$  deposition.

The average conversion/oxidation ratio for  $\text{NH}_4^+$  (NHR),  $\text{SO}_4^{2-}$  (SOR), and  $\text{NO}_3^-$  (NOR) were estimated to be 30%, 64%, and 24% in summer 2013, respectively. Results reveal that the concentrations of  $\text{NH}_3$ ,  $\text{NH}_4^+$ , and NHR had clear diurnal variations during the observation period. High  $\text{NH}_3$  and  $\text{NH}_4^+$  were observed during late night and early morning period. NHR also showed higher values during night, suggesting the importance of heterogeneous reactions driven by high nighttime RH. Our measurement and modelling results indicate that the strong acids in aerosol particles over the rural site were well neutralized by  $\text{NH}_3$ . Nearly a half of the ammonium was ~~The increased  $\text{NH}_3$  concentrations mainly from fertilization, coincided with the prevailing meteorological conditions, including high relative humidity, degree of oxidisation, and low wind could promote the secondary transformation, resulting in higher hourly SOR, NOR and NHR. not associated with strong acids but probably with oxalic acid and other diacids, which may present under the medium aerosol acidity (pH around 3.5).~~

The back trajectory analysis indicates that the transport from the North China Plain region contributed for 56% of air mass with high  $\text{NH}_3$  levels, meanwhile the long-distance transport from southeast accounted for 32% of air mass with high  $\text{NH}_4^+$ ,  $\text{SO}_4^{2-}$  and  $\text{NO}_3^-$  at the rural site in the NCP.

$\text{NH}_3$  is currently not included in China's emission control policies of air pollution precursors though people have been discussing the necessity for years. ~~Although we have not seen any evidence of  $\text{NH}_3$  driving the formation of secondary aerosol,~~ our findings highlight the important role of  $\text{NH}_3$  in the participation of secondary inorganic and organic aerosol formation. As the emission and concentration of  $\text{NH}_3$  in the NCP are much higher than needed for aerosol acids neutralization, we speculate that a substantial amount of reduction in  $\text{NH}_3$  emission is required to see its effect on the alleviation of  $\text{PM}_{2.5}$  pollution in the NCP. If such effect is realized, aerosol particles may be very acidic. Therefore, further strong reduction of the emissions of primary aerosol,  $\text{SO}_2$ ,  $\text{NO}_x$ , and VOCs is suggested.

~~and are expected to facilitate developing future  $\text{NH}_3$  emission control policies for the North China Plain.~~

## References

Aranibar, J. N. , Otter, L., Macko, S. A., Feral, C. J. W., Epstein, H. E., Dowty, P. R., Eckardt, F., Shugart, H. H., and Swap, R. J.: Nitrogen cycling in the soil plant system along a precipitation gradient in the

Kalahari sands, Glob. Chang. Biol., 10, 359-373, 2004.

Bash, J. O., Walker, J. T., Katul, G. G., Jones, M. R., Nemitz, E., and Robarg, W. P.: Estimation of In-Canopy Ammonia Sources and Sinks in a Fertilized Zea mays Field, Environ. Sci. Tech., 44, 1683-1689, 2010.

Behera, S. N., Betha, R., and Balasubramanian, R.: Insight into chemical coupling among acidic gases, ammonia and secondary inorganic aerosols, Aerosol Air Qual. Res., 13, 1282-1296, 2013.

Behera, S. N. and Sharma, M.: Investigating the potential role of ammonia in ion chemistry of fine particulate matter formation for an urban environment, Sci. Total Environ., 408, 3569-3575, 2010.

[Bian, Y. X., Zhao, C. S., Ma, N., Chen, J., and Xu, W. Y.: A study of aerosol liquid water content based on hygroscopicity measurements at high relative humidity in the North China Plain, Atmos. Chem. Phys., 14, 6417-6426, <https://doi.org/10.5194/acp-14-6417-2014>, 2014.](#)

[Bougiatioti, A., Nikolaou, P., Stavroulas, I., Kouvarakis, G., Weber, R., Nenes, A., Kanakidou, M., and Mihalopoulos, N.: Particle water and pH in the eastern Mediterranean: Source variability and implications for nutrient availability, Atmos. Chem. Phys., 16, 4579–4591, 2016.](#)

Biswas, K.F., Ghauri, B. M. and Husain, L.: Gaseous and aerosol pollutants during fog and clear episodes in South Asian urban atmosphere, Atmos. Environ., 42, 7775-7785, 2008.

Burch, J. A. and Fox, R. H.: The effect of temperature and initial soil moisture content on the volatilization of ammonia from surface applied urea, Soil Sci., 147, 311-318, 1989.

Cao, J. J., Zhang, T., Chow, J. C., Watson, J. G., Wu, F., and Li, H.: Characterization of Atmospheric Ammonia over Xi'an, China, Aerosol Air Qual. Res., 9, 277-289, 2009.

[Ding, A. J., Wang, T., Thouret, V., Cammas, J.-P., and Nédélec, P.: Tropospheric ozone climatology over Beijing: analysis of aircraft data from the MOZAIC program, Atmos. Chem. Phys., 8, 1-13, <https://doi.org/10.5194/acp-8-1-2008>, 2008.](#)

Dong, W., Xing, J. and Wang, S.: Temporal and spatial distribution of anthropogenic ammonia emissions in China: 1994-2006, Environ. Sci., 31, 1457-1463, 2010. (in Chinese).

Du, H. H., Kong, L. D., Cheng, T. T., Chen, J. M., Du, J. F., Li, L., Xia, X. G., Leng, C. P., and Huang, G. H.: Insights into summertime haze pollution events over Shanghai based on online water soluble ionic composition of aerosols, Atmos. Environ., 45, 5131–5137, 2011.

Ellis, R. A., Murphy, J. G., Markovic, M. Z., VandenBoer, T. C., Makar, P. A., Brook, J., and Mihele, C.: The influence of gas-particle partitioning and surface-atmosphere exchange on ammonia during



BAQS-Met, Atmos. Chem. Phys., 11, 133-145, 2011.

Erisman, J. W. and Schaap, M.: The need for ammonia abatement with respect to secondary PM reductions in Europe, Environ. Pollut., 129, 159-163, 2004.

[Fountoukis, C. and Nenes, A.: ISORROPIA II: a computationally efficient thermodynamic equilibrium model for  \$K^+\$ - \$Ca^{2+}\$ - \$Mg^{2+}\$ - \$NH\_4^+\$ - \$Na^+\$ - \$SO\_4^{2-}\$ - \$NO\_3^-\$ - \$Cl^-\$ - \$H\_2O\$  aerosols, Atmos. Chem. Phys., 7, 4639–4659, doi:10.5194/acp-7-4639-2007, 2007.](#)

[Fountoukis, C., Nenes, A., Sullivan, A., Weber, R., Van Reken, T., Fischer, M., Matias, E., Moya, M., Farmer, D., and Cohen, R. C.: Thermodynamic characterization of Mexico City aerosol during MILAGRO 2006, Atmos. Chem. Phys., 9, 2141–2156, doi:10.5194/acp-9-2141-2009, 2009.](#)

Galloway, J. N., Aber, J. D., Erisman, J. W., Seitzinger, S. P., Howarth, R. W., Cowling, E. B., and Cosby, B. J.: The nitrogen cascade, BioScience, 53, 341-353, 2003.

Gong, L. W., Lewicki, R., Griffin, R. J., Tittel, F. K., Lonsdale, C. R., Stevens, R. G., Pierce, J. R., Malloy, Q. G.J., Travis, S. A., Bobmanuel, L. M., Lefer, B. L., and Flynn, J. H.: Role of atmospheric ammonia in particulate matter formation in Houston during summertime, Atmos. Environ., 77, 893-900, 2013.

[Guo, H., Xu, L., Bougiatioti, A., Cerully, K. M., Capps, S. L., Hite Jr., J. R., Carlton, A. G., Lee, S.-H., Bergin, M. H., Ng, N. L., Nenes, A., and Weber, R. J.: Fine-particle water and pH in the southeastern United States, Atmos. Chem. Phys., 15, 5211-5228, 2015.](#)

[Guo, J., Miao, Y., Zhang, Y., Liu, H., Li, Z., Zhang, W., He, J., Lou, M., Yan, Y., Bian, L., and Zhai, P.: The climatology of planetary boundary layer height in China derived from radiosonde and reanalysis data, Atmos. Chem. Phys., 16, 13309-13319, <https://doi.org/10.5194/acp-16-13309-2016>, 2016.](#)

Guo, S., Hu, M., Wang, Z. B., and Zhao, Y. L.: Size-resolved aerosol water-soluble ionic compositions in the summer of Beijing: implication of regional secondary formation, Atmos. Chem. Phys., 10, 947-959, 2010.

[Han, B., Zhang, R., Yang, W., Bai, Z., Ma, Z., and Zhang, W.: Heavy haze episodes in Beijing during January 2013: inorganic ion chemistry and source analysis using highly time-resolved measurements from an urban site, Sci. Total Environ., 544, 319-329, 2016.](#)

[Hassan, S. K., El-Abssawy, A. A., and Khoder, M. I.: Characteristics of gas-phase nitric acid and ammonium-nitrate-sulfate aerosol, and their gas-phase precursors in a suburban area in Cairo, Egypt, Atmos. Pollut. Res., 4, 117-129, 2013.](#)

- Hu, M., Wu, Z.J., Slanina, J., Lin, P., Liu, S., and Zeng, L. M.: Acidic gases, ammonia and water-soluble ions in PM<sub>2.5</sub> at a coastal site in the Pearl River Delta, China, *Atmos. Environ.*, 42, 6310-6320, 2008.
- Hu, G. Y., Zhang, Y. M., Sun, J. Y., Zhang, L. M., Shen, X. J., Lin, W. L., and Yang, Y.: Variability, formation and acidity of water-soluble ions in PM<sub>2.5</sub> in Beijing based on the semi-continuous observations, *Atmos. Res.*, 145-146: 1-11, 2014.
- Ianniello, A., Spataro, F., Esposito, G., Allegrini, I., Rantica, E., Ancora, M. P., Hu, M., and Zhu, T.: Occurrence of gas phase ammonia in the area of Beijing (China), *Atmos. Chem. Phys.*, 10, 9487-9503, 2010.
- Kang, K., Liu, M., Song, Y., Huang, X., Yao, H., Cai, X., Zhang, H., Kang, L., Liu, X., Yan, X., He, H., Zhang, Q., Shao, M., and Zhu, T.: High-resolution ammonia emissions inventories in China from 1980 to 2012, *Atmos. Chem. Phys.*, 16, 2043–2058, 2016.
- Krupa, S. V.: Effects of atmospheric ammonia (NH<sub>3</sub>) on terrestrial vegetation: A review. *Environ. Pollut.*, 124, 179-221, 2003.
- [Lefer, B., Talbot, R., and Munger, J.: Nitric acid and ammonia at a rural northeastern US site. \*J. Geophys. Res.\* 104, 1645-1661, 1999.](#)
- Lei, H. and Wuebbles, D.J.: Chemical competition in nitrate and sulfate formations and its effect on air quality, *Atmos. Environ.*, 80, 472-477, 2013.
- Li, Y., Schwandner, F. M., Sewell, H. J., Zivkovich, A., Tigges, M., Raja, S., Holcomb, S., Molenaar, J.V., Sherman, L., Archuleta, C., Lee, T., and Collett, J. L.: Observations of ammonia, nitric acid, and fine particles in a rural gas production region, *Atmos. Environ.*, 83, 80-89, 2014.
- Lin, Y. C., Cheng, M. T., Ting, W. Y., and Yeh, C. R.: Characteristics of gaseous HNO<sub>2</sub>, HNO<sub>3</sub>, NH<sub>3</sub> and particulate ammonium nitrate in an urban city of central Taiwan, *Atmos. Environ.*, 40, 4725-4733, 2006.
- [Lin, W., Xu, X., Zhang, X., and Tang, J.: Contributions of pollutants from North China Plain to surface ozone at the Shangdianzi GAW Station, \*Atmos. Chem. Phys.\*, 8, 5889–5898, 2008.](#)
- Lin, W., Xu, X., and Zhang, X.: Characteristics of gaseous pollutants at Gucheng, a rural site southwest of Beijing, *J. Geophys. Res.*, 114, 10339, 2009.
- Lin, W., Xu, X., Ge, B., and Liu, X.: Gaseous pollutants in Beijing urban area during the heating period 2007-2008: variability, sources, meteorological and chemical impacts, *Atmos. Chem. Phys.*, 11, 8157-8170, 2011.

Liu, M., Song, Y., Zhou, T., Xu, Z., Yan, C., Zheng, M., Wu, Z., Hu, M., Wu, Y., and Zhu, T.: Fine particle pH during severe haze episodes in northern China, *Geophys. Res. Lett.*, 44, doi:10.1002/2017GL073210, 2017.

Liu, X. J., Zhang, Y., Han, W.X., Tang, A. H., Shen, J. L., Cui, Z. L., Peter, V., Jan, W. E., Keith, G., Peter, C., Andreas, F., and Zhang, F. S.: Enhanced nitrogen deposition over China, *Nature*, 28, 459-463, 2013.

Luo, X. S., Liu, P., Tang, A. H., Liu, J. Y., Zong, X. Y., Zhang, Q., Kou, C. L., Zhang, L. J., Fowler, D., Fangmeier, A., Christie, P., Zhang, F. S., and Liu, X. J.: An evaluation of atmospheric Nr pollution and deposition in North China after the Beijing Olympics, *Atmos. Environ.*, 74, 209-216, 2013.

Makkonen, U., Virkkula, A., Mäntykinen, J., Hakola, H., Keronen, P., Vakkari, V., and Aalto, P. P.: Semi-continuous gas and inorganic aerosol measurements at a Finnish urban site: comparisons with filters, nitrogen in aerosol and gas phases, and aerosol acidity, *Atmos. Chem. Phys.*, 12, 5617-5631, 2012.

Meng, Z. Y., Lin, W. L., Jiang, X. M., Yan, P., Wang, Y., Zhang, Y. M., Jia, X. F., and Yu, X. L.: Characteristics of atmospheric ammonia over Beijing, China, *Atmos. Chem. Phys.*, 11, 6139-6151, 2011.

Meng, Z. Y., Lin, W. L., Zhang, R. J., Han, Z. W. and Jiang, X. F.: Summertime ambient ammonia and its effects on ammonium aerosol in urban Beijing, China, *Sci. Total Environ.*, ~~578~~579, ~~2185~~1521-22011530, ~~2016~~2017.

Meng, Z. Y., Xie, Y. L., Jia, S. H., Zhang, R., Lin, W. L., Xu, X. B., and Yang W.: The characteristics of atmospheric ammonia at Gucheng, a Rural Site in the North China Plain in summer 2013, *J. applied. meteor. sci.*, 26, 141-150, 2015. (in Chinese).

Meng, Z. Y., Xu, X. B., Yan, P., Ding, G. A., Tang, J., Lin, W. L., Xu, X. D., and Wang, S. F.: Characteristics of trace gaseous pollutants at a regional background station in Northern China, *Atmos. Chem. Phys.*, 9, 927-936, 2009.

Meng, Z. Y., Zhang, R. J., Lin, W. L., Jia, X. F., Yu, X. M., Yu, X. L., and Wang, G. H.: Seasonal variation of ammonia and ammonium aerosol at a background station in the Yangtze River Delta Region, China, *Aerosol Air Qual. Res.*, 3, 756-766, 2014.

Miao, Y., Guo, J., Liu, S., Liu, H., Li, Z., Zhang, W., and Zhai, P.: Classification of summertime synoptic patterns in Beijing and their associations with boundary layer structure affecting aerosol pollution, *Atmos. Chem. Phys.*, 17, 3097-3110, <https://doi.org/10.5194/acp-17-3097-2017>, 2017.

[Fountoukis, C. and Nenes, A.: ISORROPIA II: a computationally efficient thermodynamic equilibrium model for K<sup>+</sup>-Ca<sup>2+</sup>-Mg<sup>2+</sup>-NH<sub>4</sub><sup>+</sup>-Na<sup>+</sup>-SO<sub>4</sub><sup>2-</sup>-NO<sub>3</sub><sup>-</sup>-Cl<sup>-</sup>-H<sub>2</sub>O aerosols, Atmos. Chem. Phys., 7, 4639–4659, doi:10.5194/acp-7-4639-2007, 2007.](#)

[Norman, M., Spirig, C., Wolff, V., Trebs, I., Flechard, C., Wisthaler, A., Schnitzhofer, R., Hansel, A., and Neftel, A.: Intercomparison of ammonia measurement techniques at an intensively managed grassland site \(Oensingen, Switzerland\), Atmos. Chem. Phys., 9, 2635–2645, 2009.](#)

Park, R. S., Lee, S., Shin, S. K. and Song, C. H.: Contribution of ammonium nitrate to aerosol optical depth and direct radiative forcing by aerosols over East Asia, Atmos. Chem. Phys., 14, 2185–2201, 2014.

[Pathak, R. K., Wu, W. S., and Wang, T.: Summertime PM<sub>2.5</sub> ionic species in four major cities of China: nitrate formation in an ammonia-deficient atmosphere, Atmos. Chem. Phys., 9, 1711–1722, <https://doi.org/10.5194/acp-9-1711-2009>, 2009.](#)

Plessow, K., Spindler, G., Zimmermann, F. and Matschullat, J.: Seasonal variations and interactions of N-containing gases and particles over a coniferous forest, Saxony, Germany, Atmos. Environ., 39, 6995–7007, 2005.

Reche, C., Viana, M., Karanasiou, A., Cusack, M., Alastuey, A., Artiñano, B., Revuelta, M., López-Mahía, P., Blanco-Heras, G., Rodríguez, S., Sánchez de la Campa, A., Fernández-Camacho, R., González-Castanedo, Y., Mantilla, E., Tang, S., and Querol, X.: Urban NH<sub>3</sub> levels and sources in six major Spanish cities, Chemosphere, 119, 769–777, 2015.

Reynold, C.M. and Wolf, D.: Effect of soil moisture and air relative humidity on ammonia volatilization from surface-applied urea, Soil Sci., 143, 144–152, 1987.

Robarge, W. P., Walker, J. T., McCulloch, R. B., and Murray, G.: Atmospheric concentrations of ammonia and ammonium at an agricultural site in the southeast United States, Atmos. Environ., 36, 16611–1674, 2002.

Roelle, P. A. and Aneja, V. P.: Characterization of ammonia emissions from soils in the upper coastal plain, North Carolina, Atmos. Environ. 36, 1087–1097, 2002.

Schaap, M., Otjes, R. P. and Weijers, E. P.: Illustrating the benefit of using hourly monitoring data on secondary inorganic aerosol and its precursors for model evaluation, Atmos. Chem. Phys., 11, 11041–11053, 2011.

[Schwab, J.J.: Ambient Gaseous Ammonia: Evaluation of Continuous Measurement Methods Suitable](#)

[for Routine Deployment, Final Report Prepared for the New York State Energy Research and Development Authority \(NYSERDA\), Final Report 08-15, New York, October 2008.](#)

Shen, J. L., Liu, X. J., Zhang, Y., Fangmeier, A., Goulding, K., and Zhang, F. S.: Atmospheric ammonia and particulate ammonium from agricultural sources in the North China Plain, *Atmos. Environ.*, 45, 5033-5041, 2011.

[Sudheer, A. K., and Rengarajan, R.: Time-resolved inorganic chemical composition of fine aerosol and associated precursor gases over an urban environment in western India: Gas-aerosol equilibrium characteristics, \*Atmos. Environ.\*, 109:217-227, 2015.](#)

[Tang, X., Zhang, X.S., Ci, Z.J., Guo, J and Wang, J. Q.: Speciation of the major inorganic salts in atmospheric aerosols of Beijing, China: Measurements and comparison with model. \*Atmos. Environ.\*, 133:123-134, 2016.](#)

Walker, J. T., Robarge, W. P., Shendrikar, A., and Kimball, H.: Inorganic PM<sub>2.5</sub> at a U.S. agricultural site, *Environ. Pollut.*, 139, 258-271, 2006.

Walker, J. T., Whittall, D. R., Robarge, W., and Paerl, H. W.: Ambient ammonia and ammonium aerosol across a region of variable ammonia emission density, *Atmos. Environ.*, 38, 1235-1246, 2004.

Wang, S. S., Nan, J.L., Shi, C. Z., Fu, Q. Y., Gao, S., Wang, D. F., Cui, H. X., Alfonso, S. L., and Zhou, B.: Atmospheric ammonia and its impacts on regional air quality over the megacity of Shanghai, China. *Sci. Rep.*, 5, 15842, 2015.

Wang, T., Nie, W., Gao, J., Xue, L. K., Gao, X. M., Wang, X. F., Qiu1, J., Poon, C. N., Meinardi, S., Blake, D., Wang, S. L., Ding, A. J., Chai, F. H., Zhang, Q. Z., and Wang, W. X.: Air quality during the 2008 Beijing Olympics: secondary pollutants and regional impact, *Atmos. Chem. Phys.*, 10, 7603-7615, 2010.

Wei, L. F., Duan, J. C., Tan, J. H., Ma, Y. L., He, K. B., Wang, S. X., Huang, X. F., and Zhang, Y. X.: Gas-to-particle conversion of atmospheric ammonia and sampling artifacts of ammonia in spring of Beijing, *Sci. China Earth Sci.*, 58, 345-355, 2015.

[Wen, L., Chen, J., Yang, L., Wang, X., Xu, C., & Sui, X., et al.: Enhanced formation of fine particulate nitrate at a rural site on the north china plain in summer: the important roles of ammonia and ozone. \*Atmos. Environ.\*, 101, 294-302, 2015.](#)

[Wu, W. S. and Wang, T.: On the performance of a semi-continuous PM<sub>2.5</sub> sulphate and nitrate instrument under high loadings of particulate and sulphur dioxide. \*Atmos. Environ.\* 41, 5442-5451, 2007.](#)

Xu, P., Zhang, Y., Gong, W., Hou, X., Kroeze, C., Gao, W., and Luan, S.: An inventory of the emission of ammonia from agricultural fertilizer application in China for 2010 and its high-resolution spatial distribution, *Atmos. Environ.*, 115, 141-148, 2015.

[Xu, P., Liao, Y. J., Lin, Y. H., Zhao, C. X., Yan, C. H., Cao, M. N., Wang, G. S., and Luan, S. J.: High-resolution inventory of ammonia emissions from agricultural fertilizer in China from 1978 to 2008, \*Atmos. Chem. Phys.\*, 16, 1207–1218, 2016.](#)

[Xu, W., Song, W., Zhang, Y., Liu, X., Zhang, L., Zhao, Y., Liu, D., Tang, A., Yang, D., Wang, D., Wen, Z., Pan, Y., Fowler, D., Collett Jr., J. L., Erisman, J. W., Goulding, K., Li, Y., and Zhang, F.: Air quality improvement in a megacity: implications from 2015 Beijing Parade Blue pollution control actions, \*Atmos. Chem. Phys.\*, 17, 31-46, <https://doi.org/10.5194/acp-17-31-2017>, 2017.](#)

Yao, X. H., Ling, T. Y., Fang, M. and Chan, C. K.: Comparison of thermodynamic predictions for in situ pH in PM<sub>2.5</sub>, *Atmos. Environ.* 40, 2835-2844, 2006.

Yao, X.H., Chak, K.C., Fang, M., Cadle, S., Chan, T., Mulawa, P., He, K.B., and Ye, B.M.: The water-soluble ionic composition of PM<sub>2.5</sub> in Shanghai and Beijing. China, *Atmos. Environ.* 36, 4223-4234, 2002.

Ye, X. N., Ma, Z., Zhang, J.C., Du, H. H., Chen, J. M., Chen, H., Yang, X., Gao, W., and Geng, F. H.: Important role of ammonia on haze formation in Shanghai, *Environ. Res. Lett.*, 6, 024019, 2011.

Zhang, Y., Dore, A. J., Ma, L., Liu, X. J., Ma, W. Q., Cape, J. N., and Zhang, F. S.: Agricultural ammonia emissions inventory and spatial distribution in the North China Plain, *Environ. Pollut.*, 158, 490-501, 2010.

Zhang, T., Cao, J., Tie, X., Shen, Z., Liu, S., Ding, H., Han, Y., Wang, G., Ho, K., Qiang, J., and Li, W.: Water-soluble ions in atmospheric aerosols measured in Xi'an, China: Seasonal variations and sources, *Atmos. Res.* 102, 110-119, 2011.

[Zhao, M., Wang, S., Tan, J., Hua, Y., Wu, D., and Hao, J.: Variation of Urban Atmospheric Ammonia Pollution and its Relation with PM<sub>2.5</sub> Chemical Property in Winter of Beijing, China. \*Sci. Total Environ.\*, 16\(6\) , 1378-1389, 2016.](#)

Zhou, Y., Wang, T., Gao, X. M., . Xue, L. K., Wang, X. F., Wang, Z., Gao, J., Zhang, Q. Z., and Wang, W. X.: Continuous observations of water-soluble ions in PM<sub>2.5</sub> at Mount Tai (1534 m a.s.l.) in central-eastern China, *J. Atmos. Chem.* 64, 107-127, 2009.

Zhou, Y., Cheng, S., Lang, J., Chen, D., Zhao, B., Liu, C., Xu, R., and Li, T.: A comprehensive ammonia emission inventory with high-resolution and its evaluation in the Beijing-Tianjin-Hebei (BTH)

region, China, Atmos. Environ., 106, 305-317, 2015.

### **Acknowledgements**

This work was supported by the National Natural Science Foundation of China (2137716, [and 41330422](#) [and 21777191](#)), the Environmental Protection Public Welfare Scientific Research Project, Ministry of Environmental Protection of the People's Republic of China (grant No. 201509001, 201509002-04 and 201309009), and the China Special Fund for Meteorological Research in the Public Interest (GYHY201206015). The authors would like to thank Professor Xiangde Xu and Yu Song for their helpful support and suggestions. The authors would like Professor Yaqiang Wang for providing NH<sub>3</sub> emission data and the plotting helps of Chao He.

## Table Captions

Table 1. The comparisons of the concentration of trace gases (ppb) and water-soluble ions in PM<sub>2.5</sub> (μg m<sup>-3</sup>) at Gucheng with other researches.

Table 2. Occurrence frequency and mean values of NH<sub>3</sub>, other trace gases and water-soluble ions in PM<sub>2.5</sub> for each type of air masses arriving at Gucheng during summer 2013.

## Figure Captions

[Figure 1. Sampling location in the North China Plain with emission distributions of NH<sub>3</sub> for the year 2012 from the multi-resolution emission inventory of China \(<http://meicmodel.org/index.html>\).](#)

[Figure 2. Time series of hourly data of NH<sub>3</sub>, other trace gases and meteorological parameters measured during the sampling period \(a\) and a blow-up of the period with extremely high NH<sub>3</sub> values during 27-31 July 2013.](#)

[Figure 3. Diurnal variation \(a\) NH<sub>3</sub> and \(b\) meteorological parameters during the sampling period.](#)

[Figure 4. Correlation of observed NH<sub>4</sub><sup>+</sup> with observed SO<sub>4</sub><sup>2-</sup>, SO<sub>4</sub><sup>2-</sup>+NO<sub>3</sub><sup>-</sup> and SO<sub>4</sub><sup>2-</sup>+NO<sub>3</sub><sup>-</sup>+Cl<sup>-</sup>.](#)

[Figure 5. Observed and modelled concentrations of NH<sub>3</sub>, NH<sub>4</sub><sup>+</sup>, SO<sub>4</sub><sup>2-</sup> and NO<sub>3</sub><sup>-</sup> in summer 2013.](#)

[Figure 6. Calculated diurnal variation of pH value of aerosol water.](#)

[Figure 7. Relationship between NH<sub>3</sub> and NH<sub>4</sub><sup>+</sup> \(a\) and diurnal variation of NH<sub>x</sub> \(b\) in summer 2013.](#)

[Figure 8. Diurnal variation of NHR, SOR, NOR, gaseous precursors, major water soluble ions, and meteorological factors in summer 2013.](#)

[Figure 9. Hourly concentrations of precursor gas and ionic species measured in the pollution episode](#)

[\(a\) temporal variations and \(b\) correlations of \[NH<sub>4</sub><sup>+</sup>\] versus \[SO<sub>4</sub><sup>2-</sup>\], \[SO<sub>4</sub><sup>2-</sup>\]+\[NO<sub>3</sub><sup>-</sup>\] and](#)

[\[SO<sub>4</sub><sup>2-</sup>\]+\[NO<sub>3</sub><sup>-</sup>\]+\[Cl<sup>-</sup>\] during 7 –11 August 2013](#)

[Figure 10. Correlations between \[NH<sub>4</sub><sup>+</sup>\] and \[SO<sub>4</sub><sup>2-</sup>\] \(left\), \[NH<sub>4</sub><sup>+</sup>\] and \[SO<sub>4</sub><sup>2-</sup>\]+\[NO<sub>3</sub><sup>-</sup>\] \(middle\) and \[NH<sub>4</sub><sup>+</sup>\] and \[SO<sub>4</sub><sup>2-</sup>\]+\[NO<sub>3</sub><sup>-</sup>\]+\[Cl<sup>-</sup>\] \(right\) during 7-11 August 2013.](#)

[Figure 11. The average NH<sub>3</sub>, NH<sub>4</sub><sup>+</sup> and meteorological data roses in different wind sectors during summer 2013.](#)

[Figure 12. 72-h backward trajectories for 100 m above ground level at Gucheng during sampling period 2013.](#)

[Figure S1. Confirmation of the performance of NH<sub>3</sub> analyzer using diluted standard gas \(mixture NH<sub>3</sub>/N<sub>2</sub>\). \(a\) Instrument response to changed NH<sub>3</sub> concentration and stability; \(b\) repeated multipoint calibrations.](#)

[Figure S2. The hourly amount of precipitation in summer 2013 \(a\) and monthly diurnal variations of photolysis rate coefficient of NO<sub>2</sub> \(/NO<sub>2</sub>\) during the sampling period \(b\).](#)



Figure S3. The monthly planetary boundary layer heights at 14:00 during 2013 at Gucheng.

Figure S4. Simulated  $\text{HNO}_3$  and  $\text{H}^+$ <sub>air</sub>.

Figure S5 Correlation of modelled  $\text{NH}_4^+$  with modelled  $\text{SO}_4^{2-}$ ,  $\text{SO}_4^{2-} + \text{NO}_3^-$  and  $\text{SO}_4^{2-} + \text{NO}_3^- + \text{Cl}^-$ .

Figure S6. Time series of predicted fine particle pH, predicted particle water mass, predicted  $\text{H}^+$ <sub>air</sub> and measured  $\text{NH}_3$  and measured inorganic ions during 7-11 August 2013.

Figure 1. Sampling location in the North China Plain with emission distributions of  $\text{NH}_3$  for the year 2012 from the multi-resolution emission inventory of China (<http://meicmodel.org/index.html>).

Figure 2. Time series of hourly data of  $\text{NH}_3$ , other trace gases and meteorological parameters measured during the sampling period.

Figure 3. The hourly amount of precipitation in summer 2013 (a) and monthly boundary layer heights at 14:00 during the sampling period (b).

Figure 34. Diurnal variation (a)  $\text{NH}_3$  and (b) meteorological parameters during the sampling period.

Figure 45. Hourly concentrations of precursor gas and ionic species measured in the pollution episode (a) temporal variations and (b) correlations of  $[\text{NH}_4^+]$  versus  $[\text{SO}_4^{2-}]$ ,  $[\text{SO}_4^{2-}] + [\text{NO}_3^-]$  and  $[\text{SO}_4^{2-}] + [\text{NO}_3^-] + [\text{Cl}^-]$  during 7-11 August 2013.

Figure 6. Observed and modelled concentrations of  $\text{NH}_3$ ,  $\text{NH}_4^+$ ,  $\text{SO}_4^{2-}$  and  $\text{NO}_3^-$  in summer 2013.

Figure 7. Time series of predicted fine particle pH, particle water mass,  $\text{H}^+$ <sub>air</sub> and  $\text{NH}_3$  during 7-11 August 2013.

Figure 8. Relationship between  $\text{NH}_3$  and  $\text{NH}_4^+$  (a) and diurnal variation of  $\text{NH}_3$  (b) in summer 2013.

Figure 59. Time series of the concentrations of air pollutants related to  $\text{NH}_4^+$  formation and meteorological data on 27 to 31 July, 2013.

Figure 610. Diurnal variation of NHR, SOR, NOR, gaseous precursors, major water soluble ions, and meteorological factors in summer 2013.

Figure 11. The average  $\text{NH}_3$ ,  $\text{NH}_4^+$  and meteorological data roses in different wind sectors during summer 2013.

Figure 712. 72 h backward trajectories for 100 m above ground level at Gucheng during sampling period 2013.

Table 1. The comparisons of the concentration of trace gases (ppb) and water-soluble ions in PM<sub>2.5</sub> (μg m<sup>-3</sup>) at Gucheng with other researches.

Location	Type	Period	NH <sub>3</sub>	SO <sub>2</sub>	NO <sub>x</sub>	NH <sub>4</sub> <sup>+</sup>	SO <sub>4</sub> <sup>2-</sup>	NO <sub>3</sub> <sup>-</sup>	Reference
Gucheng, China	Rural	May.-Sept. 2013	36.2±56.4	5.0±6.5	15.4±9.3	19.8±33.2	20.5±13.6	11.3±9.1	This study
Shangdianzi, China	Rural	Jun.2008-Dec.2009	10.4±8.1	5.9±4.6	12.0±6.8	7.03±7.76	15.0±15.7	11.6±11.4	Meng et al. 2011 <sup>14</sup>
Beijing, China	Rural	Aug.2006-Jul.2007	21.1±10.5	—	37.8±11.6	8.8±6.7	22.4±16.2	15.1±11.4	Shen et al. 2011
Lin'an, China	Rural	Sept.2009-Dec.2010	16.5±11.2	6.4±4.2	10.8±5.2	4.3±3.5	9.6±6.1	7.3±7.5	Meng et al. 2014
Guangzhou, China	Rural	Oct.-Nov. 2004	10.5	21.2	—	9.2	24.1	7.2	Hu et al, 2008
Hong Kong, China	Urban	Autumn 2000	3	—	—	2.4	9	1	Yao et al. 2006
Taichung, Taiwan	Urban	Jan.-Dec. 2002	12.2±4.31	—	—	4.6±2.0	15±8.7	6.0±4.0	Lin et al. 2006
Lahore, Pakistan	Urban	Dec.2005-Feb.2006	72.1	7.4	—	16.1	19.2	18.9	Biswas et al, 2008
Colonelganj, India	Urban	Summer 2007	41.3±10.5	6.95±1.99	33.8±8.56	18.4±4.7	27.8±7.6	29.2±7.5	Behera et al. 2010
Singapore	Urban	Sep.-Nov. 2011	3.6	8.3	—	1.76	4.41	1.29	Behera et al. 2013
Oberbärenburg, Germany	Forest	Oct.2001-Apr.2003	0.69	2.24	—	1.55	3.07	2.22	Plessow et al, 2005
Netherlands	Rural	Aug. 2007 and 2008	12.9	0.5	—	2.4	3.1	5.9	Schaap et al. 2011
Helsinki, Finnish	Urban	Spring 2010	0.40±0.59	0.29±0.38	—	0.46±0.50	1.64±1.08	1.40±2.04	Makkonen et al. 2012
Cairo, Egypt	Suburban	Summer 2009	64.7	5.59	28.7	7.5	28	4.2	Hassan et al. 2013
Clinton, USA	Agricultural	Jan.1999-Dec.2000	8	1.5	—	1.76	4.22	2.05	Walker et al. 2006
Houston, USA	Urban	Aug. 2010	3.0±2.5	—	—	0.5±1.0	4.5±4.3	0.3±0.2	Gong et al, 2013
Wyoming, USA	Rural	Dec.2006-Dec.2011	0.24	—	—	0.26	0.48	0.32	Li et al. 2014

Table 2. Occurrence frequency and mean values of  $\text{NH}_3$ , other trace gases (ppb) and ionic species in  $\text{PM}_{2.5}$  ( $\mu\text{g m}^{-3}$ ) for each type of air masses arriving at Gucheng in summer 2013.

Air mass	Ratio(%)	$\text{NH}_3$	$\text{SO}_2$	$\text{NO}_x$	$\text{NH}_4^+$	$\text{SO}_4^{2-}$	$\text{NO}_3^-$
Clusters 1	15	32.8	7.9	14.0	22.3	22.6	17.7
Clusters 2	56	48.9	3.7	14.4	17.5	22.1	10.3
Clusters 3	17	28.5	4.8	15.1	14.6	20.2	11.8
Clusters 4	10	23.4	2.4	12.8	12.9	15.3	7.2
Clusters 5	3	16.3	0.6	9.4	7.5	8.1	5.0

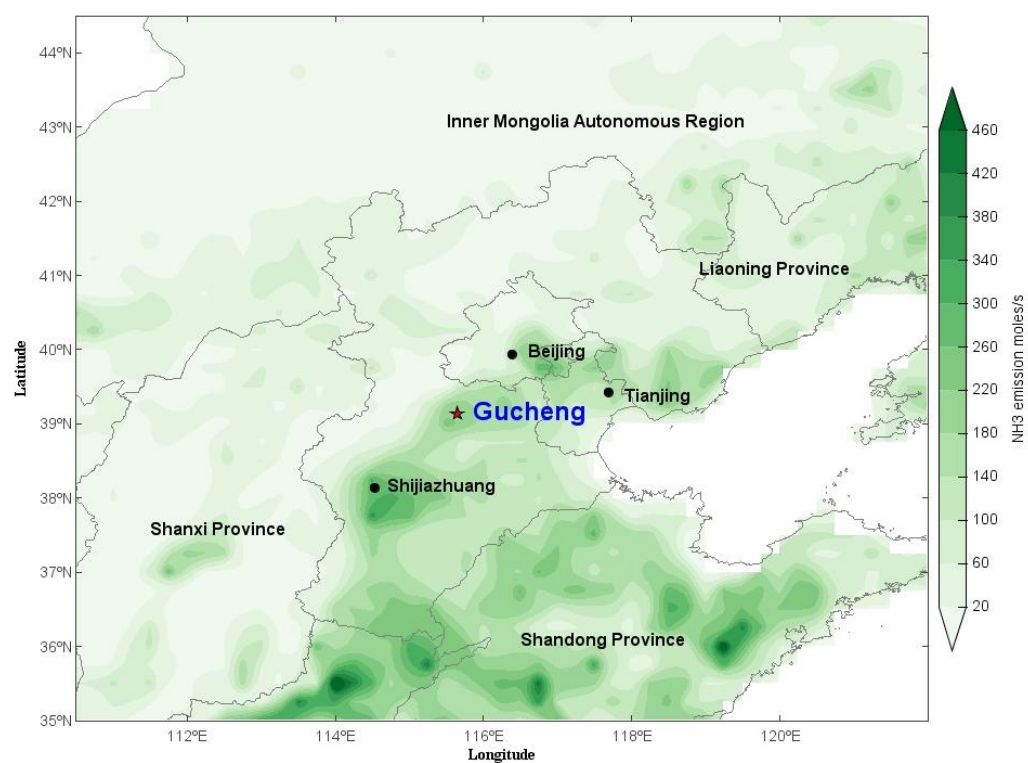


Figure 1. Sampling location in the North China Plain with emission distributions of NH<sub>3</sub> for the year 2012 from the multi-resolution emission inventory of China (<http://meicmodel.org/index.html>).

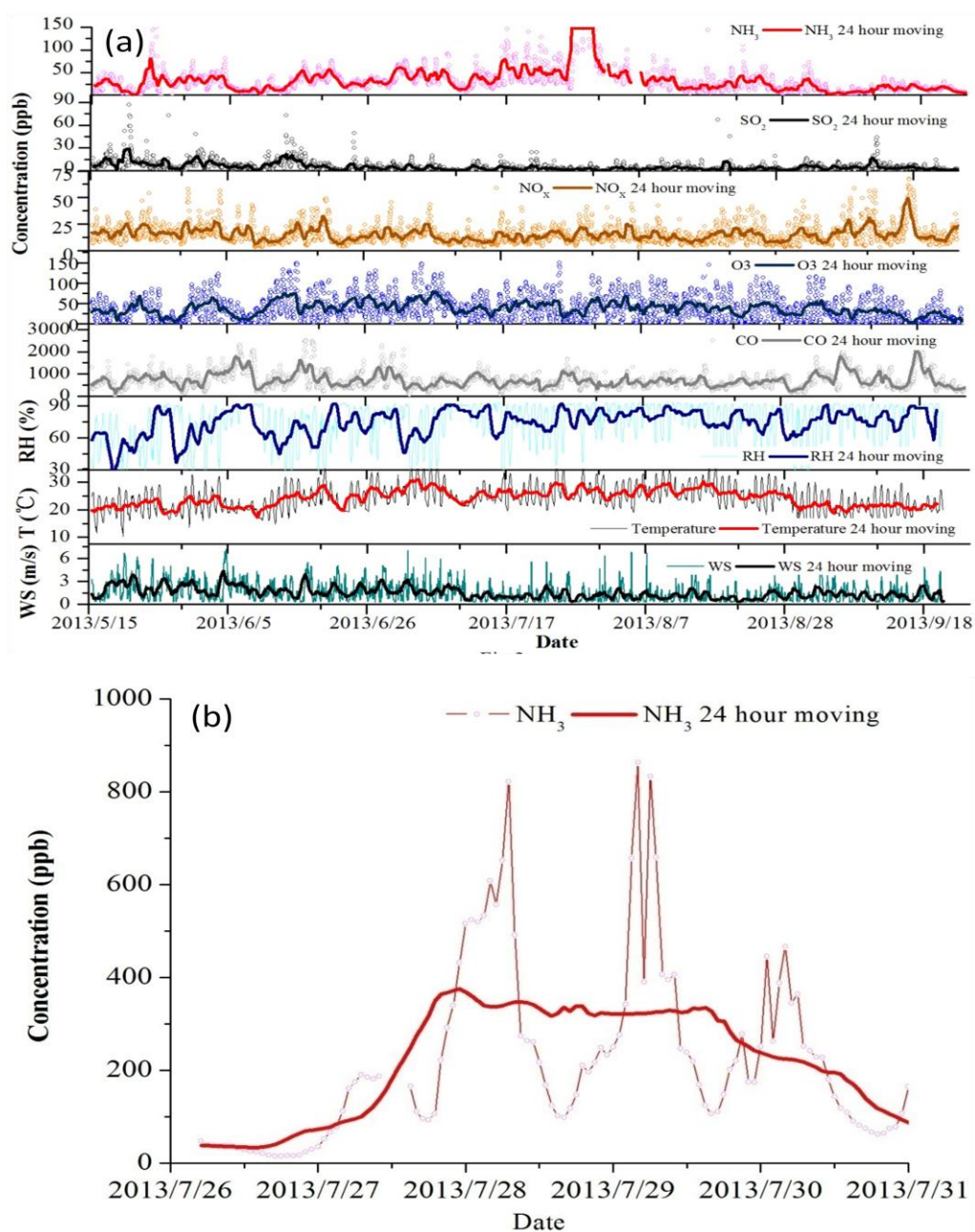


Figure 2. Time series of hourly data of NH<sub>3</sub>, other trace gases and meteorological parameters measured during the sampling period (a) and a blow-up of the period with extremely high NH<sub>3</sub> values during 27-31 July 2013.

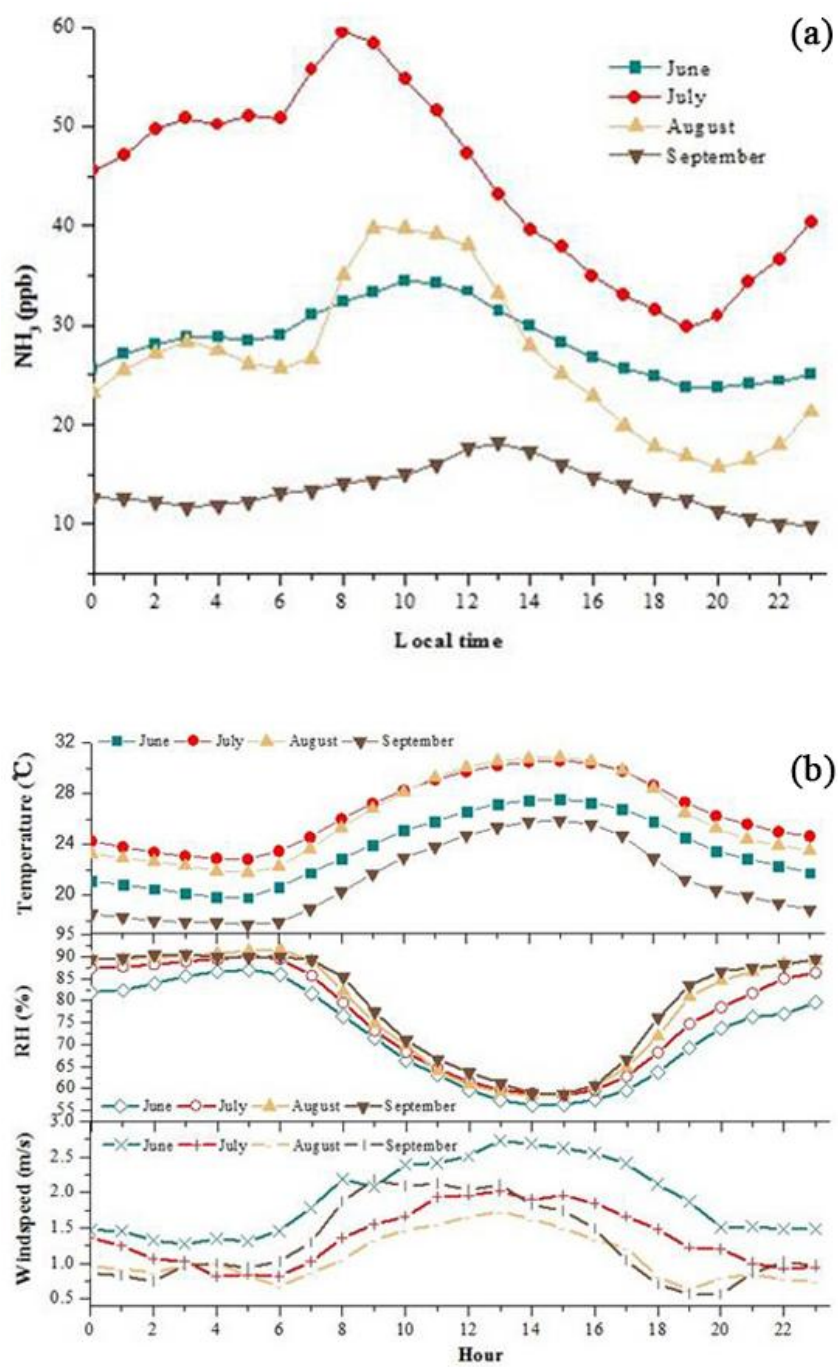


Figure 3. Diurnal variation (a) NH<sub>3</sub> and (b) meteorological parameters during the sampling period.

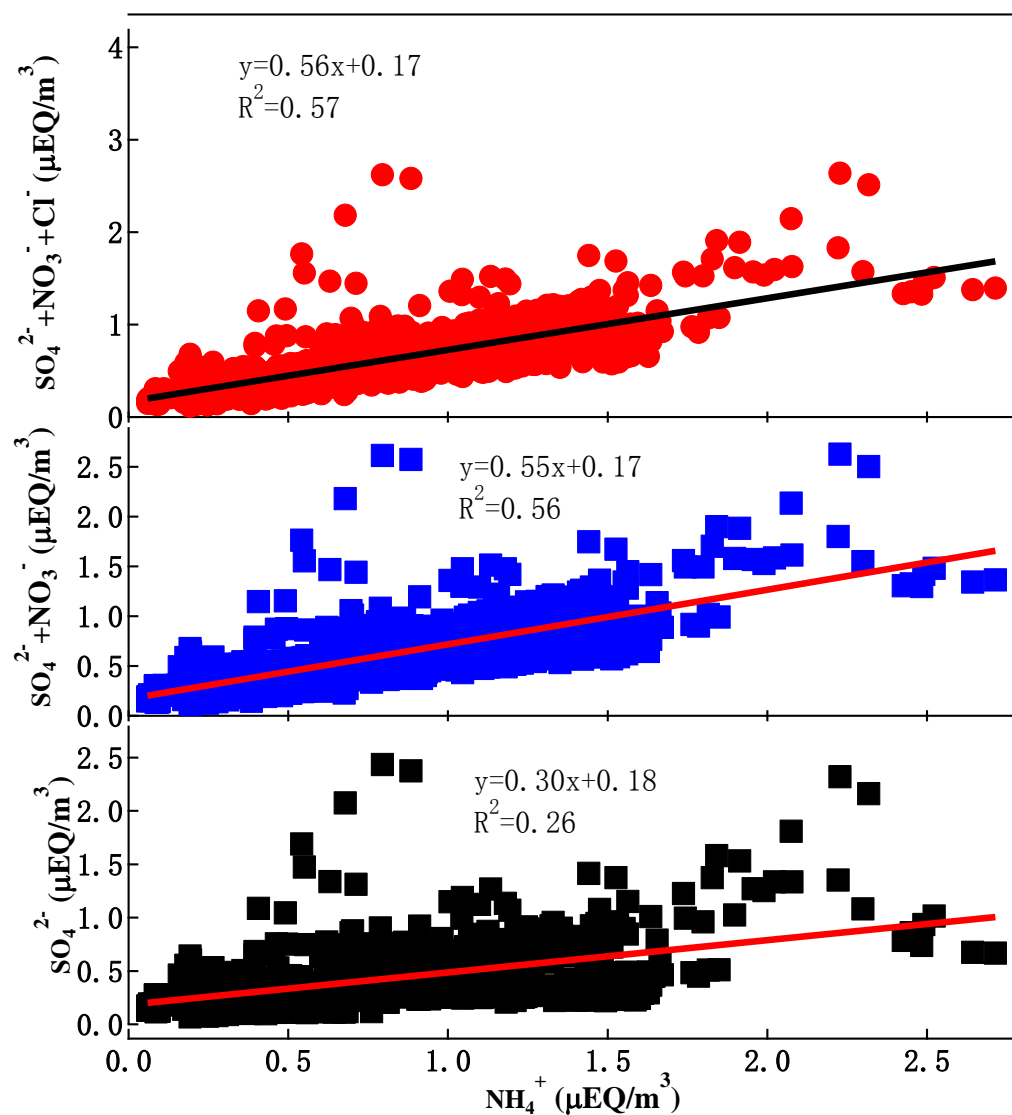


Figure 4. Correlation of observed  $\text{NH}_4^+$  with observed  $\text{SO}_4^{2-}$ ,  $\text{SO}_4^{2-} + \text{NO}_3^-$  and  $\text{SO}_4^{2-} + \text{NO}_3^- + \text{Cl}^-$ .

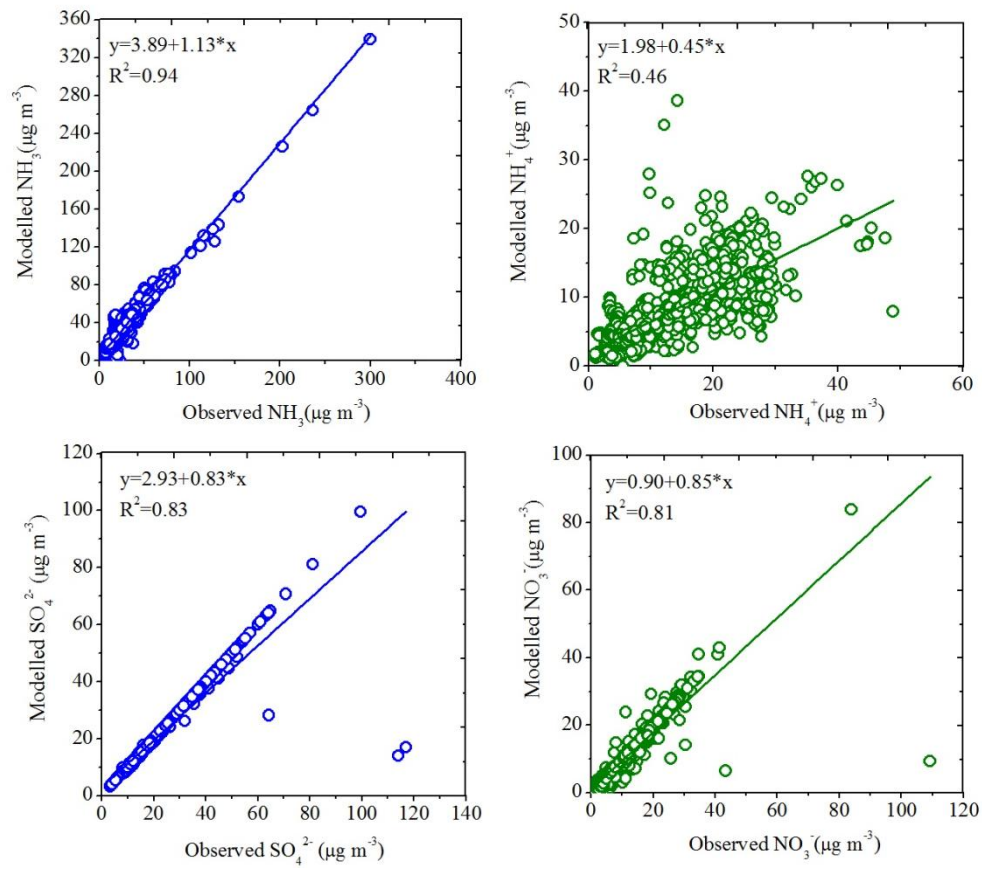


Figure 5. Observed and modelled concentrations of  $\text{NH}_3$ ,  $\text{NH}_4^+$ ,  $\text{SO}_4^{2-}$  and  $\text{NO}_3^-$  in summer 2013.



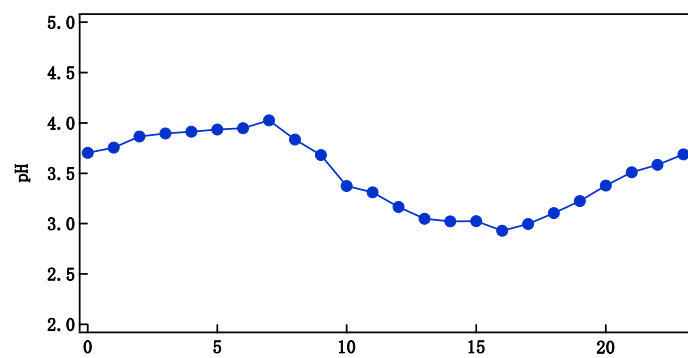


Figure 6. Calculated diurnal variation of pH value of aerosol water.

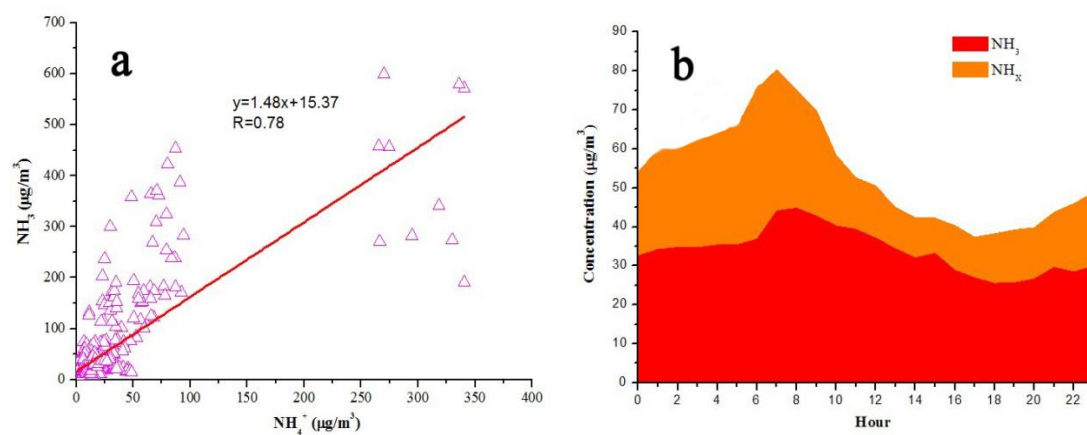


Figure 7. Relationship between  $\text{NH}_3$  and  $\text{NH}_4^+$  (a) and diurnal variation of  $\text{NH}_x$  (b) in summer 2013.

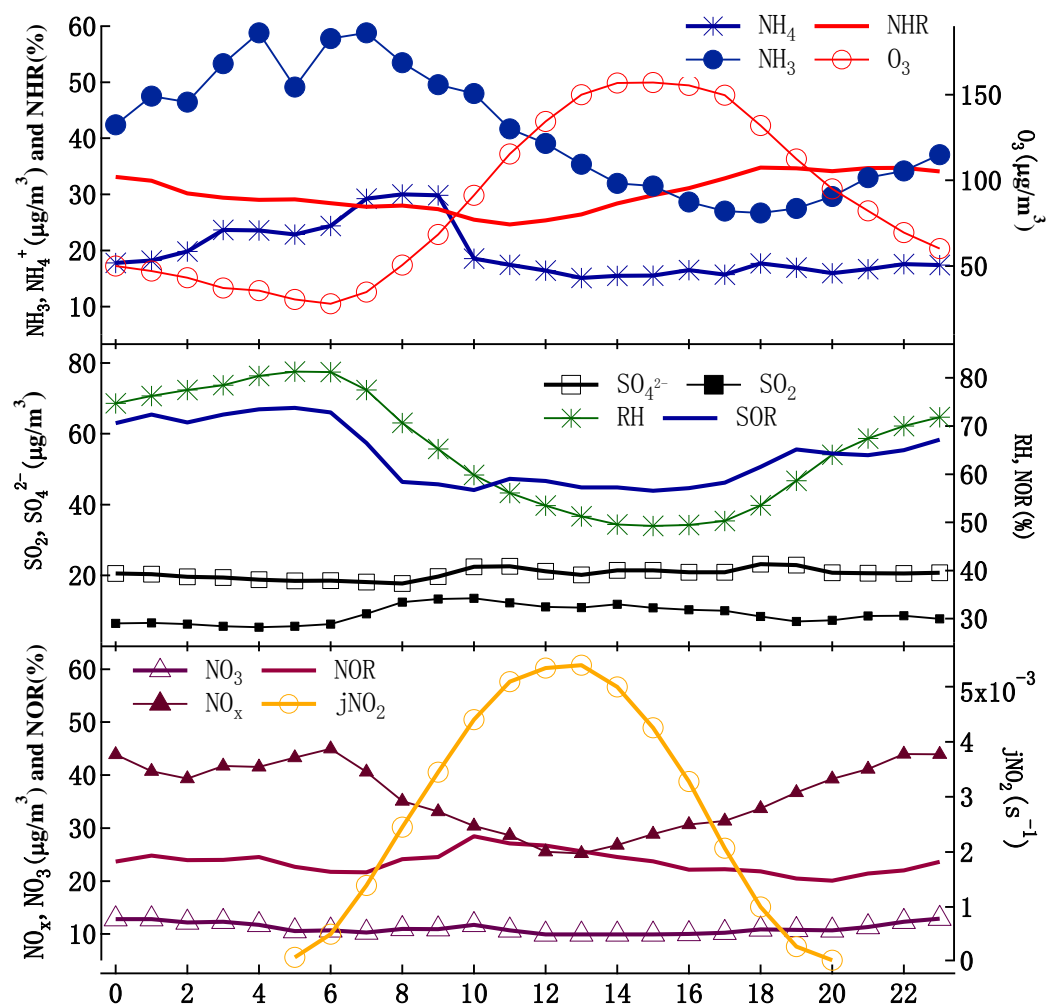


Figure 8. Diurnal variation of NHR, SOR, NOR, gaseous precursors, major water soluble ions, and meteorological factors in summer 2013.

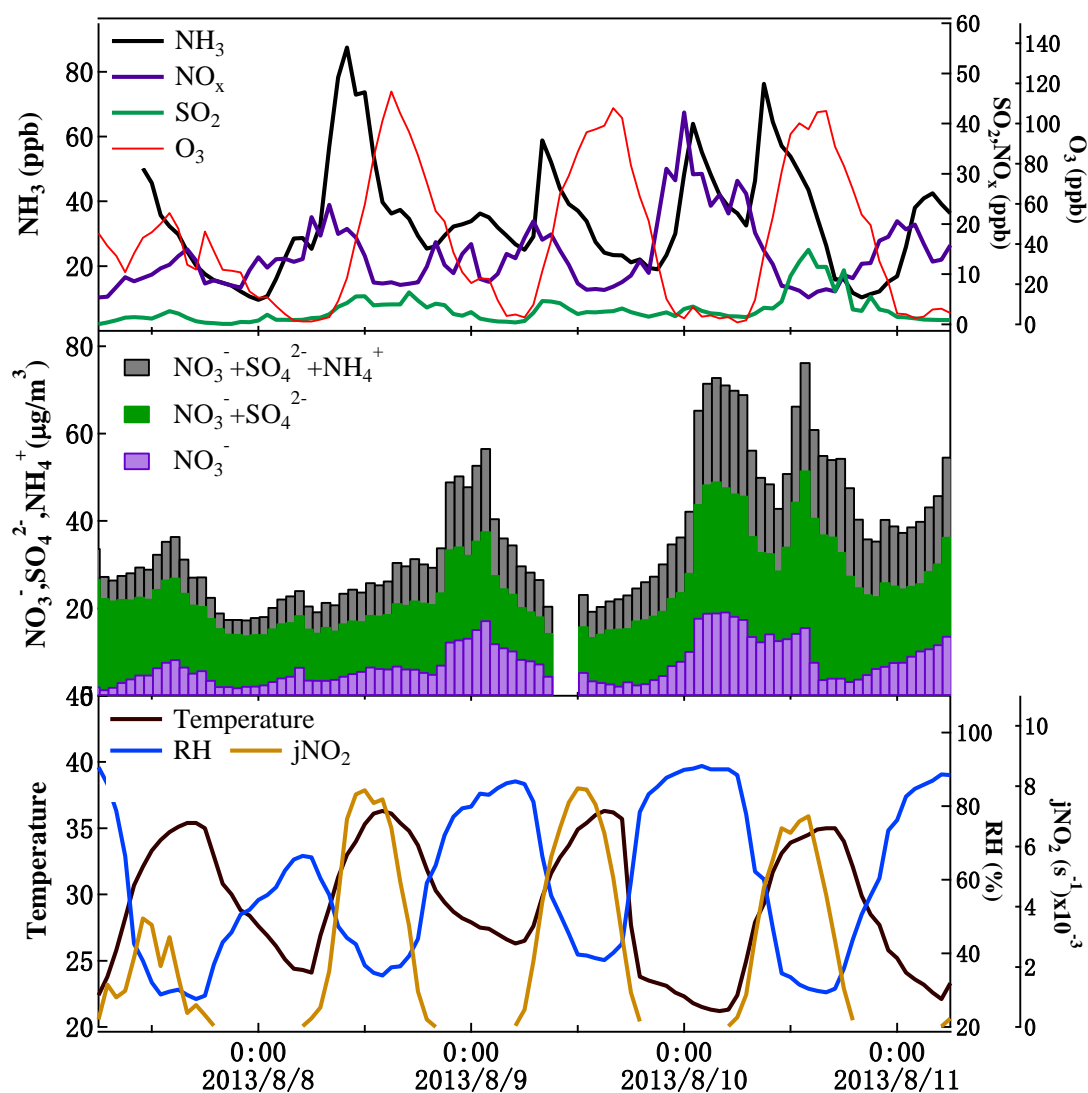


Figure 9. Hourly concentrations of precursor gas and ionic species measured in the pollution episode (a) temporal variations and (b) correlations of  $[\text{NH}_4^+]$  versus  $[\text{SO}_4^{2-}]$ ,  $[\text{SO}_4^{2-}] + [\text{NO}_3^-]$  and  $[\text{SO}_4^{2-}] + [\text{NO}_3^-] + [\text{Cl}^-]$  during 7–11 August 2013.

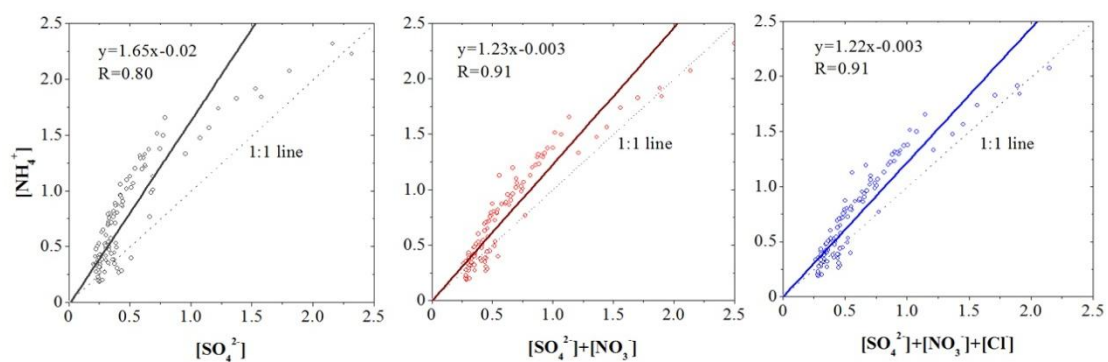


Figure 10. Correlations between  $[\text{NH}_4^+]$  and  $[\text{SO}_4^{2-}]$  (left),  $[\text{NH}_4^+]$  and  $[\text{SO}_4^{2-}] + [\text{NO}_3^-]$  (middle) and  $[\text{NH}_4^+]$  and  $[\text{SO}_4^{2-}] + [\text{NO}_3^-] + [\text{Cl}^-]$  (right) during 7-11 August 2013.

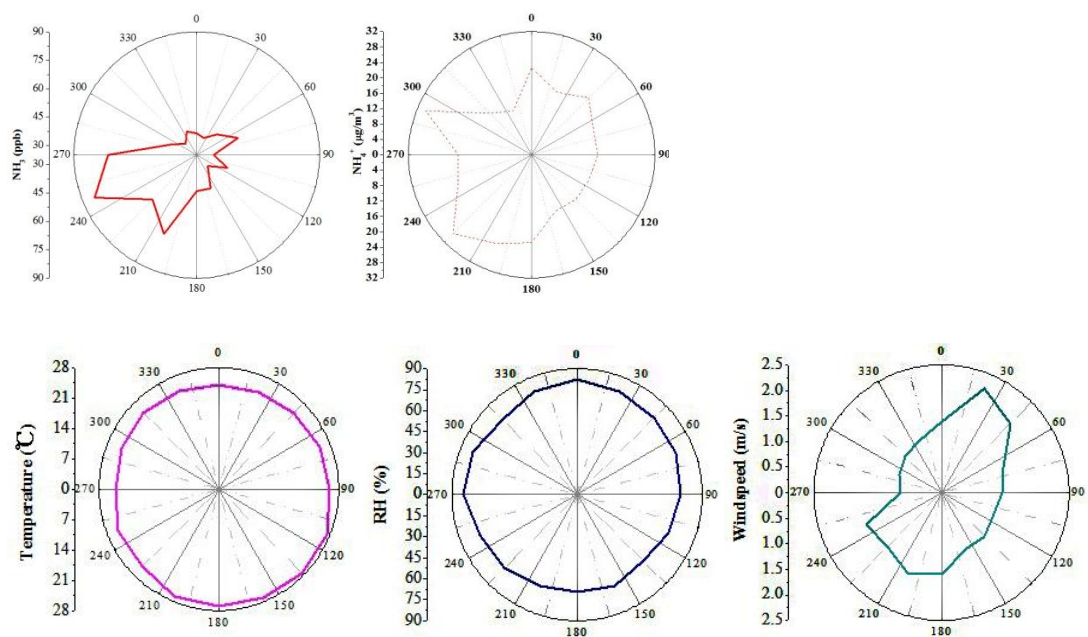


Figure 11. The average  $\text{NH}_3$ ,  $\text{NH}_4^+$  and meteorological data roses in different wind sectors during summer 2013.

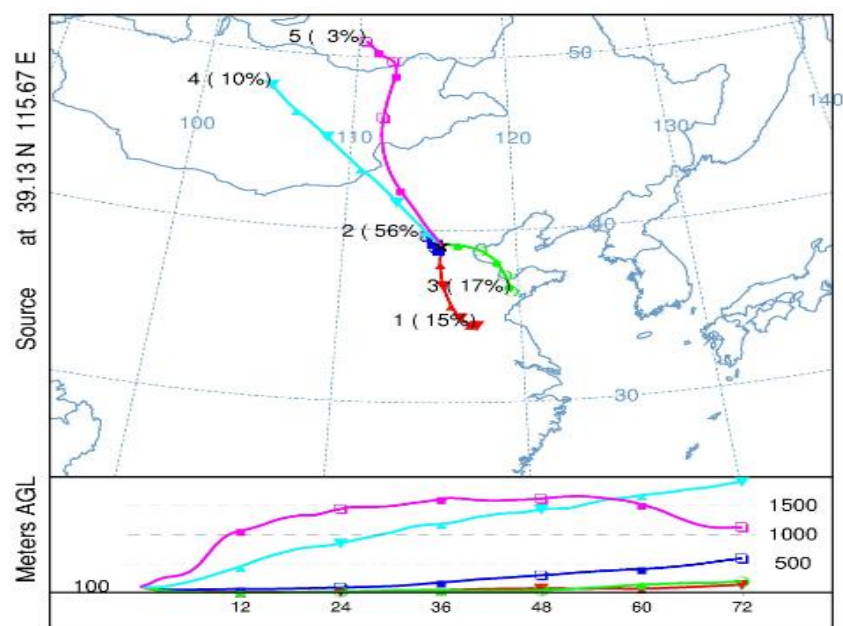


Figure 12. 72-h backward trajectories for 100 m above ground level at Gucheng during sampling period 2013.

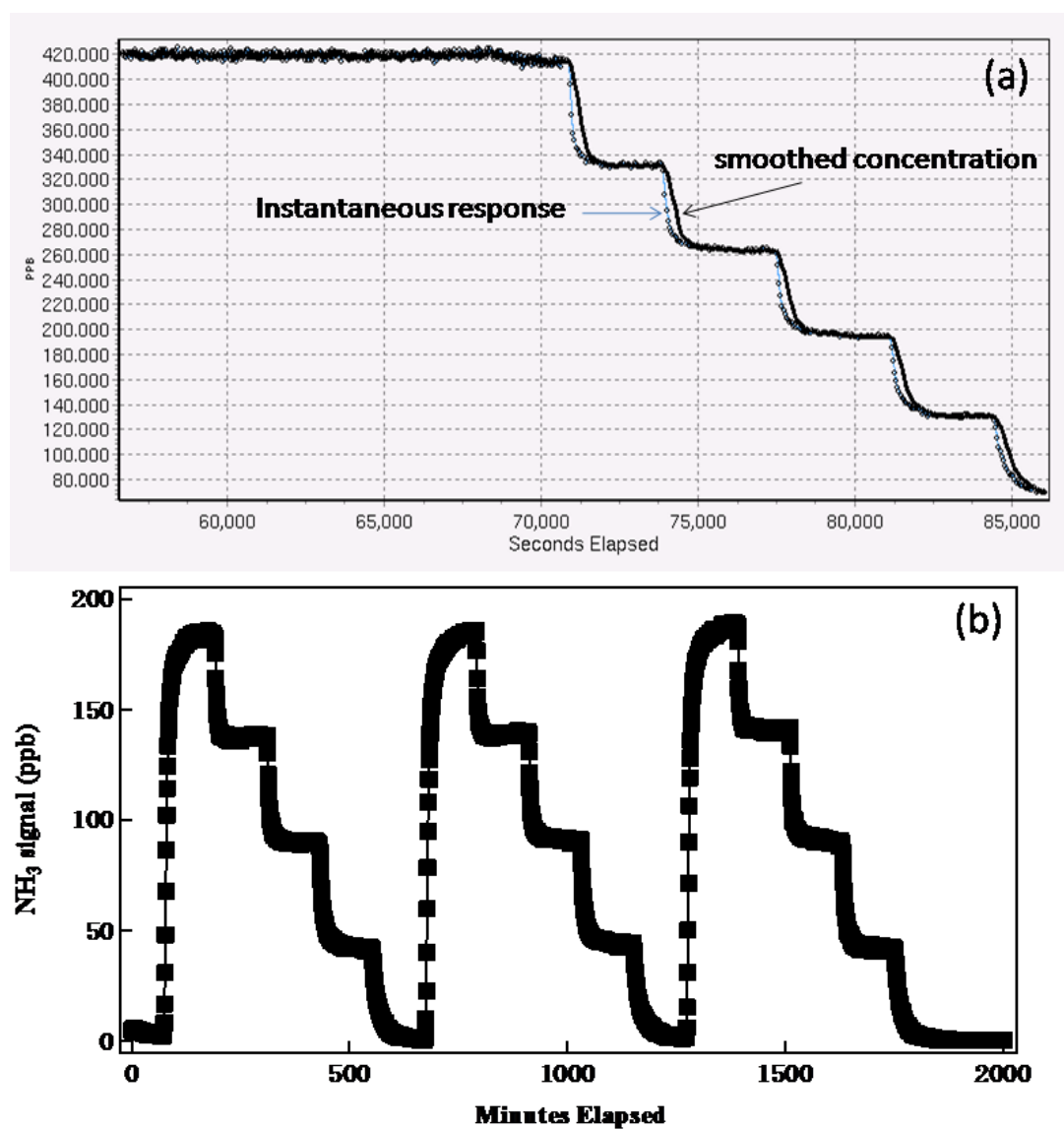


Figure S1. Confirmation of the performance of  $\text{NH}_3$  analyzer using diluted standard gas (mixture  $\text{NH}_3/\text{N}_2$ ). (a) Instrument response to changed  $\text{NH}_3$  concentration and stability; (b) repeated multipoint calibrations.



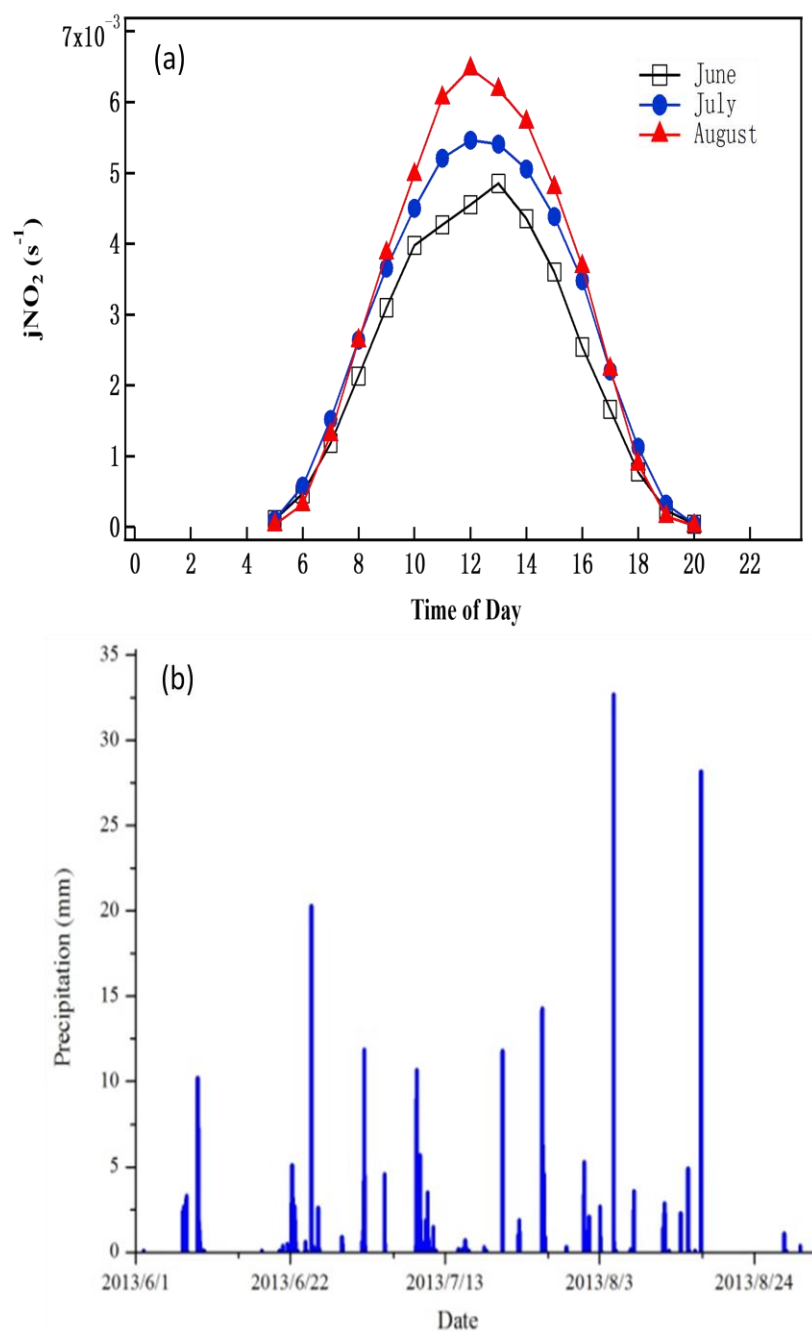


Figure S2. The hourly amount of precipitation in summer 2013 (a) and monthly diurnal variations of photolysis rate coefficient of  $\text{NO}_2$  ( $j\text{NO}_2$ ) during the sampling period (b).

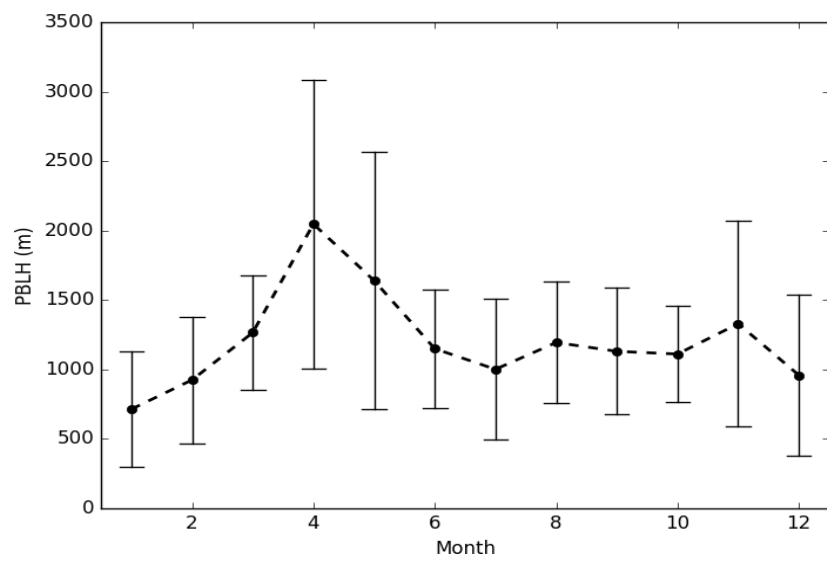


Figure S3. The monthly planetary boundary layer heights at 14:00 during 2013 at Gucheng.

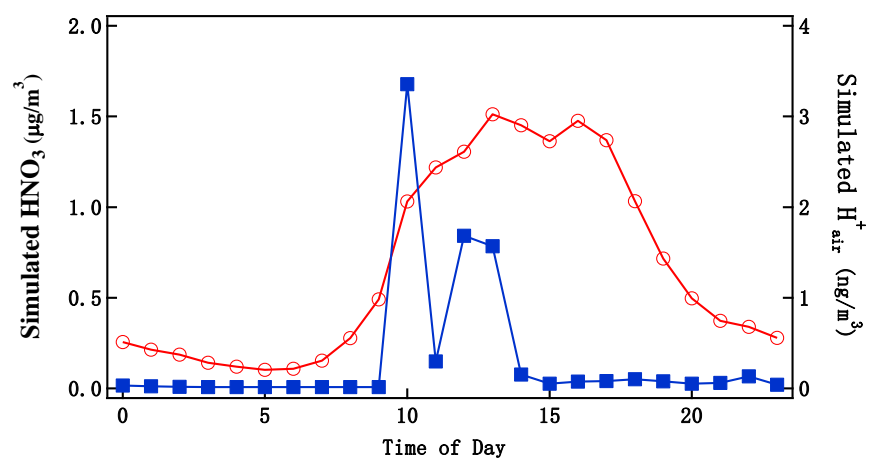


Figure S4. Simulated HNO<sub>3</sub> and H<sup>+</sup><sub>air</sub>.

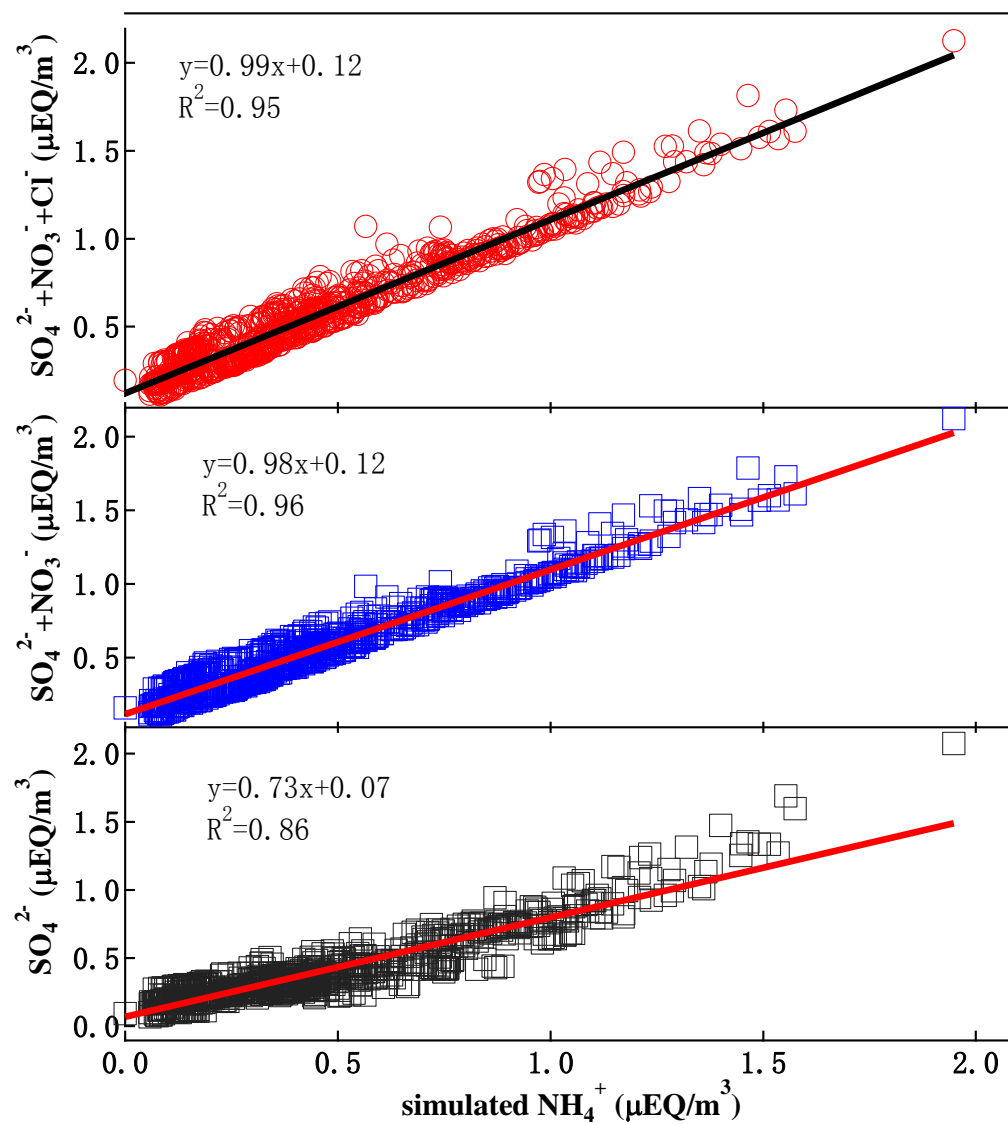


Figure S5 Correlation of modelled  $\text{NH}_4^+$  with modelled  $\text{SO}_4^{2-}$ ,  $\text{SO}_4^{2-} + \text{NO}_3^-$  and  $\text{SO}_4^{2-} + \text{NO}_3^- + \text{Cl}^-$ .

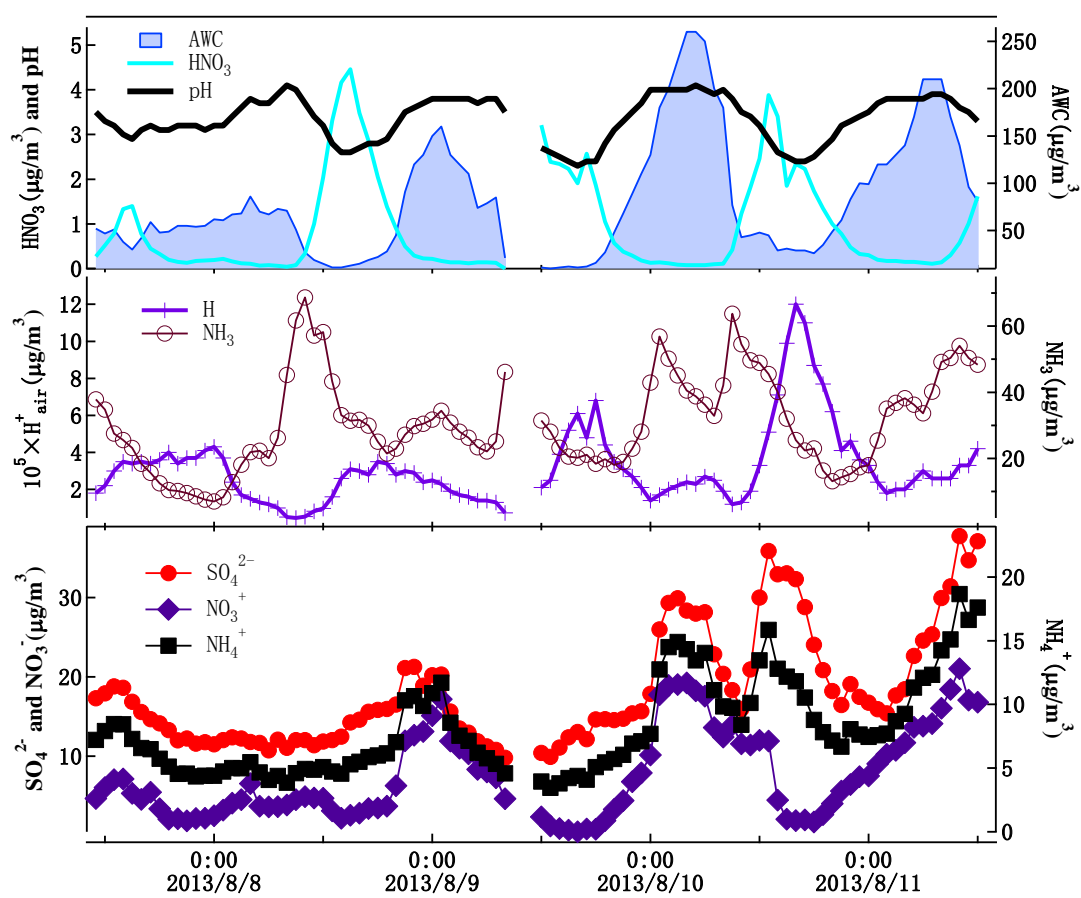


Figure S6. Time series of predicted fine particle pH, predicted particle water mass, predicted  $\text{H}^+_{\text{air}}$  and measured  $\text{NH}_3$  and measured inorganic ions during 7-11 August 2013.